Time-lapse Inverse Theory

with applications in seismic imaging and geomechanics

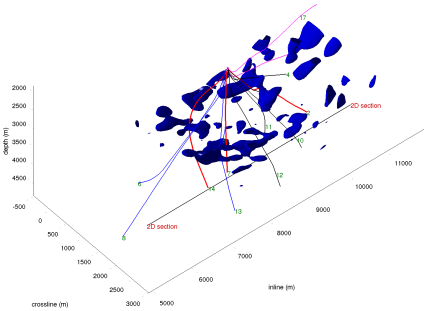

Musa Maharramov

Stanford Exploration Project

February 09, 2016

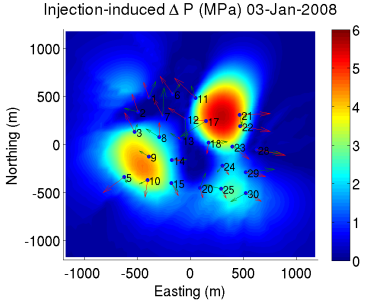

Time-lapse seismic analysis

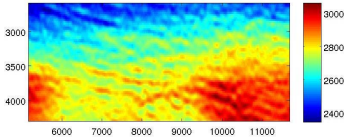

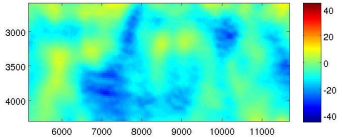

Motivation: improved reservoir monitoring

- Current methods: conversion of time shifts $\Rightarrow$ impedance changes
- More automated tomographic methods exist
- Goal: design a robust 4D FWI less sensitive to repeatability issues

Production effects: USGS http://pubs.usgs.gov/fs/fs091-01/

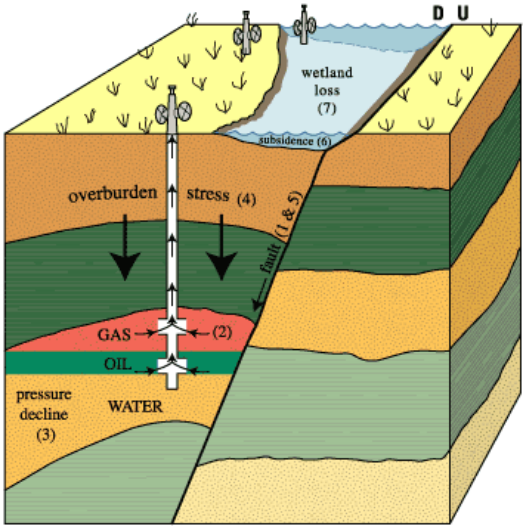

Full-waveform inversion

Find a model $\mathbf{m}$ that minimizes misfit between the true $\mathbf{d}$ and predicted $\mathbf{u}(\mathbf{m})$ data (Lailly, 1983; Tarantola, 1984)

$$\text{Misfit} \;=\; \|\mathbf{W}_d\left[\mathbf{d}-\mathbf{u}(\mathbf{m})\right]\|^2 \;\rightarrow\; \min, \tag{1}$$

with optional model regularization

$$\beta\|\mathbf{R}\mathbf{W}_m\left[\mathbf{m}-\mathbf{m}^{\text{prior}}\right]\|^2, \tag{2}$$

where $\mathbf{m}$ is a subsurface velocity model, $\mathbf{W}_d$ and $\mathbf{W}_m$ are data residual and model weighting operators, $\mathbf{R}$ is a model regularization operator, and $\mathbf{m}^{\text{prior}}$ is a model prior.

Existing model-space 4D FWI methods

- *Parallel Difference* FWI

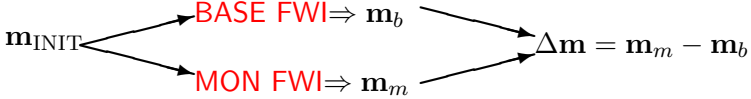

- *Sequential Difference* FWI

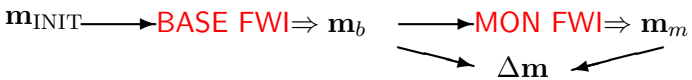

Joint 4D FWI: simultaneous inversion and cross-updating

- NEW: *Simultaneous FWI* of baseline and monitor with *difference regularization*:

$$\text{Baseline Misfit} \; + \; \text{Monitor Misfit} \; + \tag{3}$$

$$\alpha \| \mathbf{R}\mathbf{W}_m \left[\mathbf{m}_m - \mathbf{m}_b \right] \|_2^2. \tag{4}$$

- NEW: *Cross-updating* Approximation to the Simultaneous FWI:

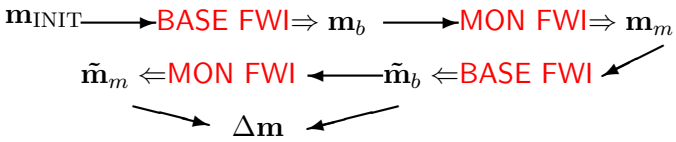

Total-variation difference regularization

- NEW: *Simultaneous FWI* of baseline and monitor with the *total-variation difference regularization*:

$$\text{Baseline Misfit} + \text{Monitor Misfit} + \tag{5}$$

$$\alpha |||\nabla \mathbf{W}_m \left[\mathbf{m}_m - \mathbf{m}_b\right] |||_1. \tag{6}$$

- The Total-variation (TV) seminorm (6) provides **edge-preserving** regularization that promotes model **"blockiness"** and helps to reduce spurious oscillations ("**ROF**" model of Rudin, Osher, and Fatemi, 1992).

7 dB = 2.2 SNR synthetic (reflections + refractions)

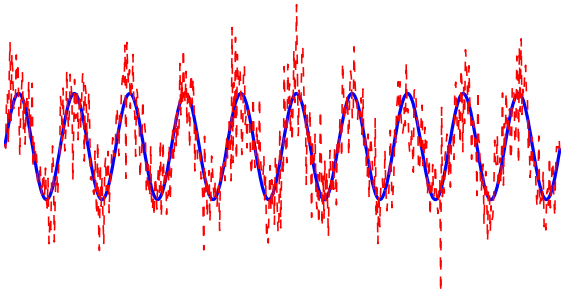

“Marmousi” model: true baseline

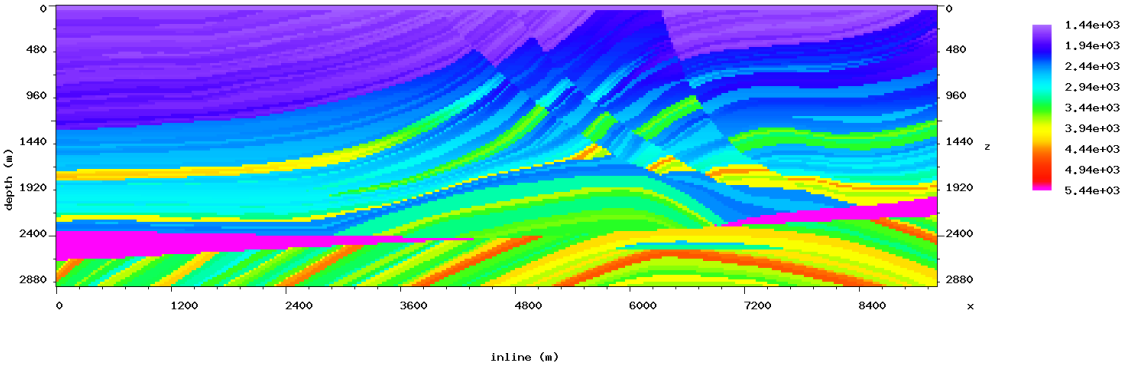

Modified "Marmousi": true monitor

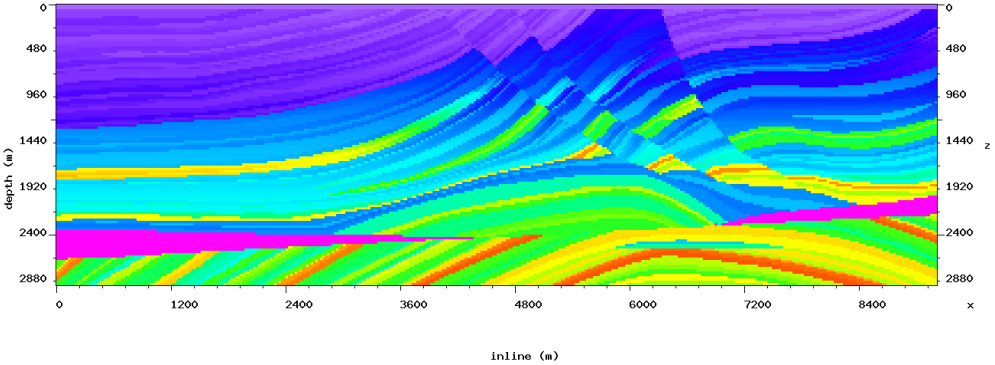

True difference

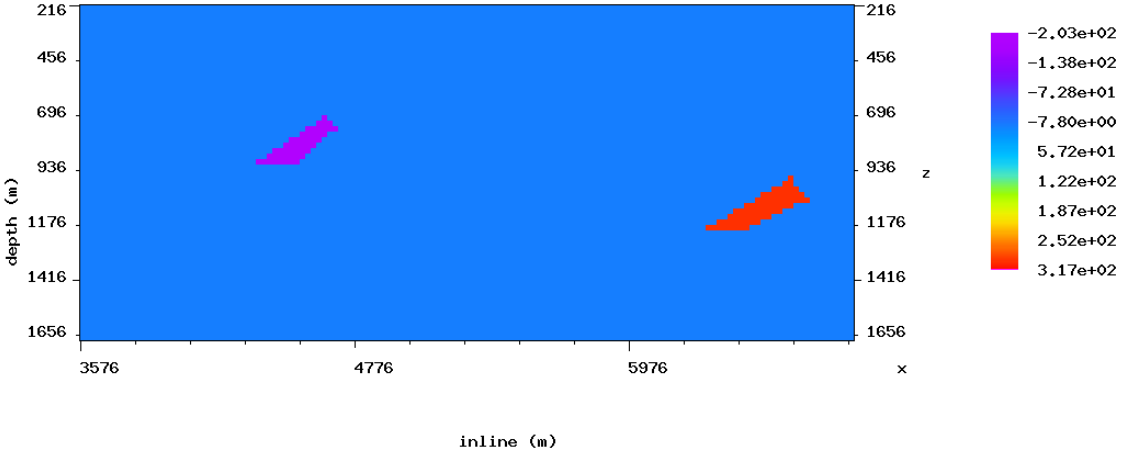

Parallel difference

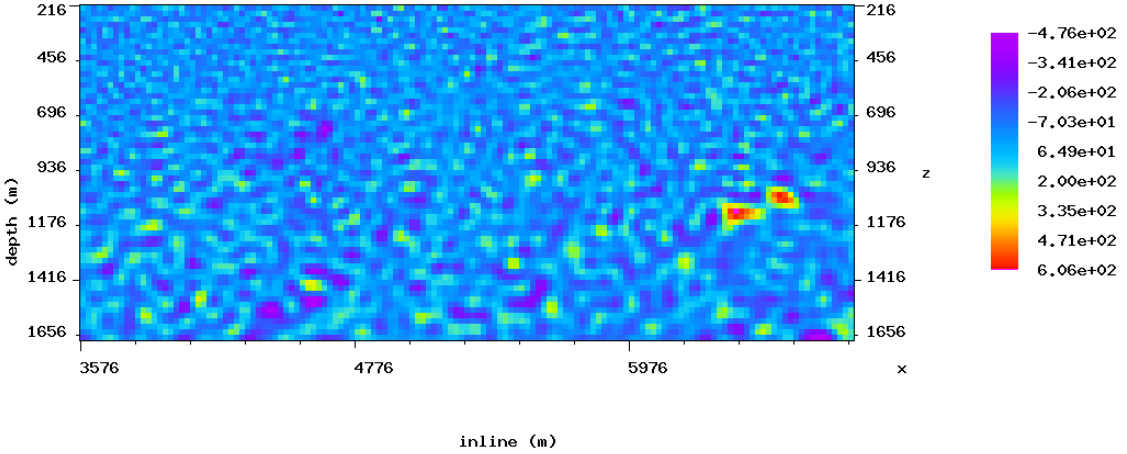

Sequential difference

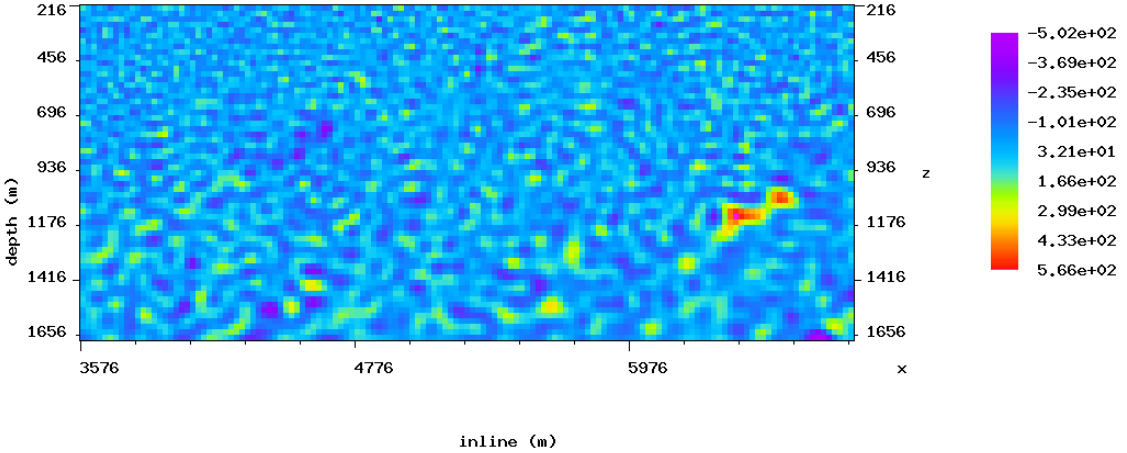

Cross-updating

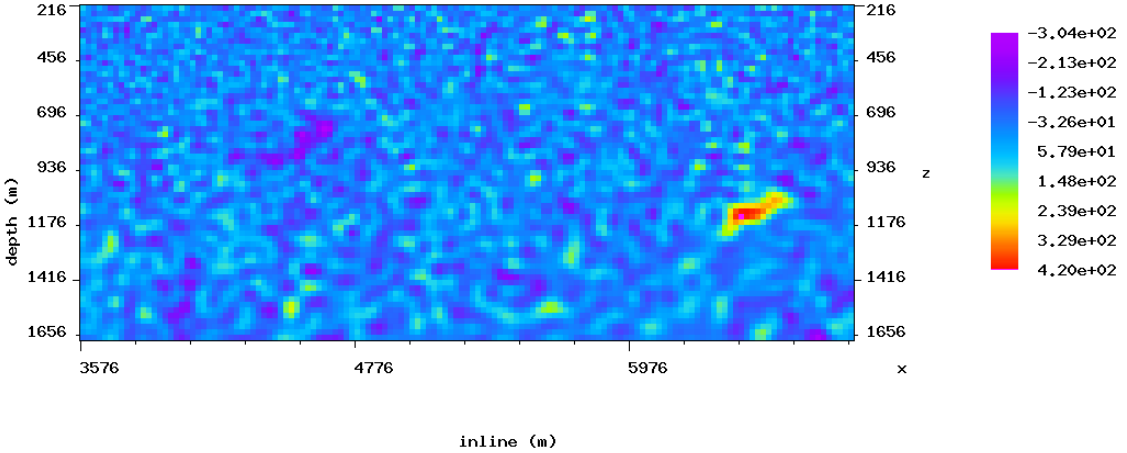

Total-variation difference regularization

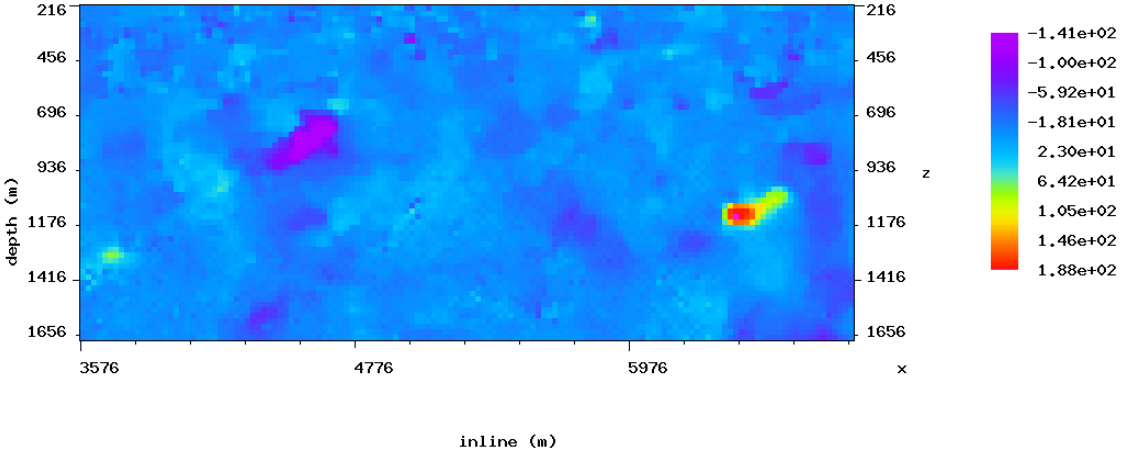

GoM Genesis field data: estimating production-induced overburden dilation

Genesis target (Magesan et al., 2008)

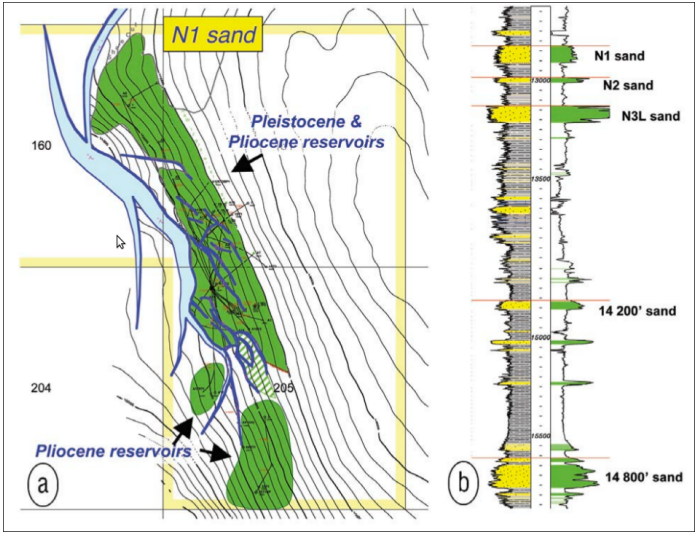

Genesis 2D FWI

- Frequency-domain inversion, 3-30Hz
- Shot gathers interpolated from the provided sparse CDP gathers
- Surveys: 1264 shots with up to 175 receivers each (a platform gap exists)
- Phase-only inversion to recover blocky velocity anomalies
- Maximum offset 5km, maximum target depth 4km
- **What is 4D FWI sensitivity to 1-2% overburden velocity change with such survey parameters?**

Genesis 2D FWI

- Frequency-domain inversion, 3-30Hz
- Shot gathers interpolated from the provided sparse CDP gathers
- Surveys: 1264 shots with up to 175 receivers each (a platform gap exists)
- Phase-only inversion to recover blocky velocity anomalies
- Maximum offset 5km, maximum target depth 4km
- **What is 4D FWI sensitivity to 1-2% overburden velocity change with such survey parameters?**

Sensitivity analysis for phase-only 4D FWI of reflection data

Test: 5km max offset, 4km target reservoir, true baseline model

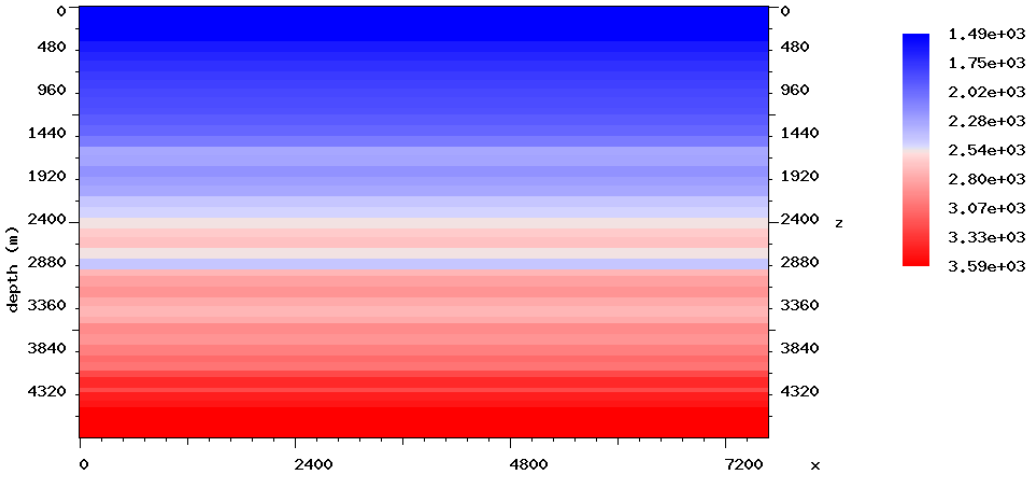

True monitor model

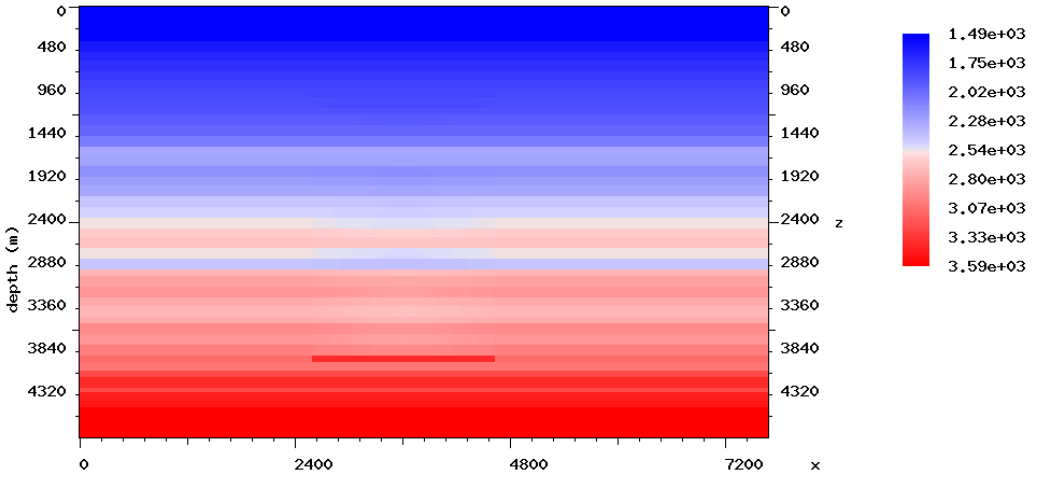

True 4D model difference

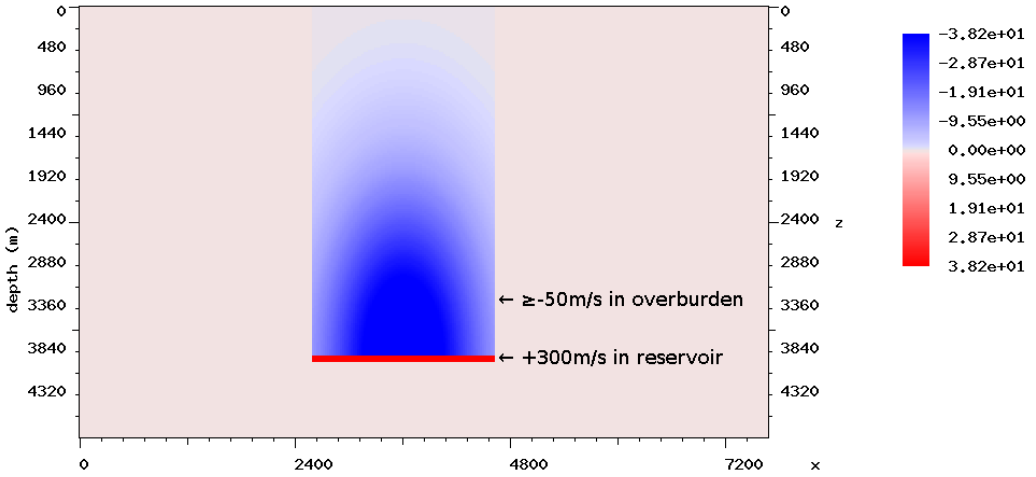

Observed travel-time dilation

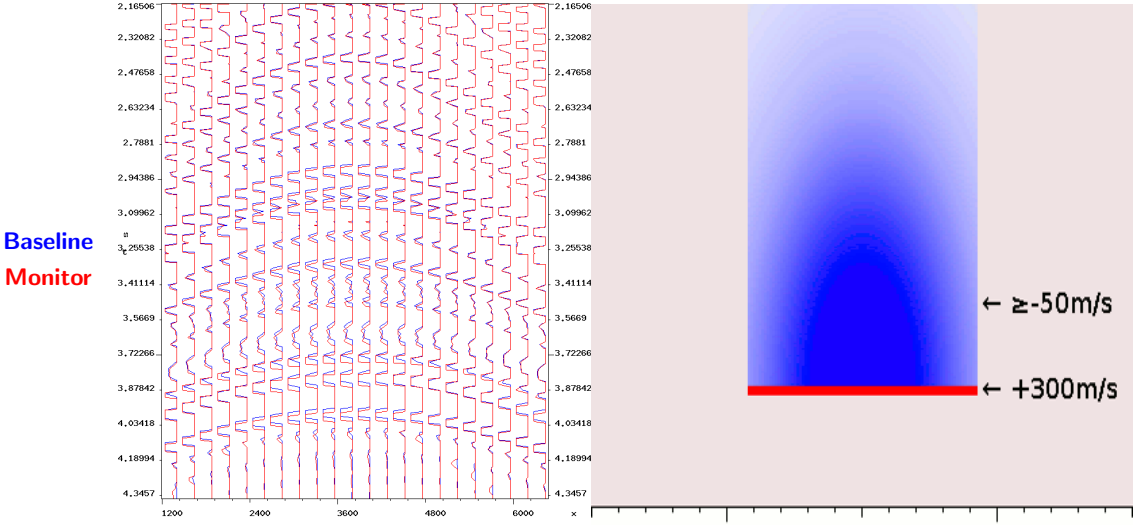

Parallel difference

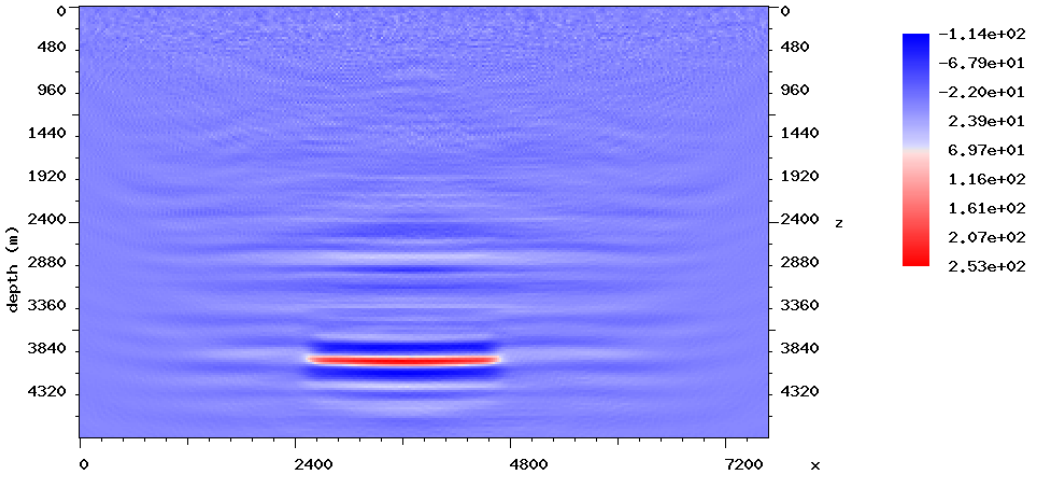

Cross-updated difference

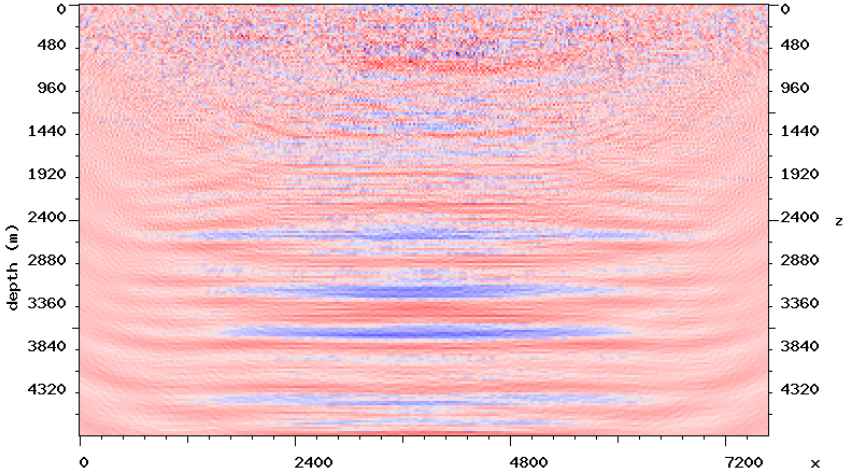

Simultaneous inversion with TV difference regularization

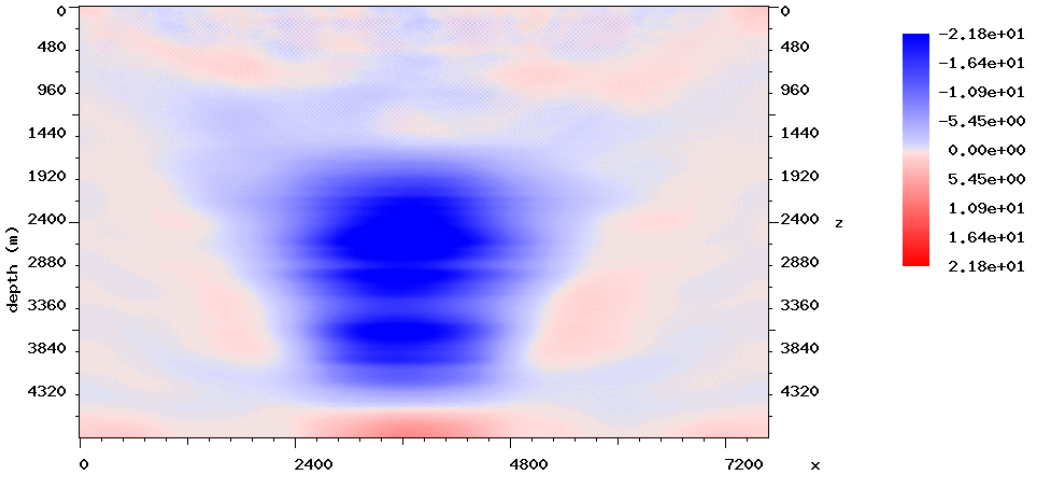

Multi-scale inversion: Maharramov and Biondi, 2015, SEP **160**

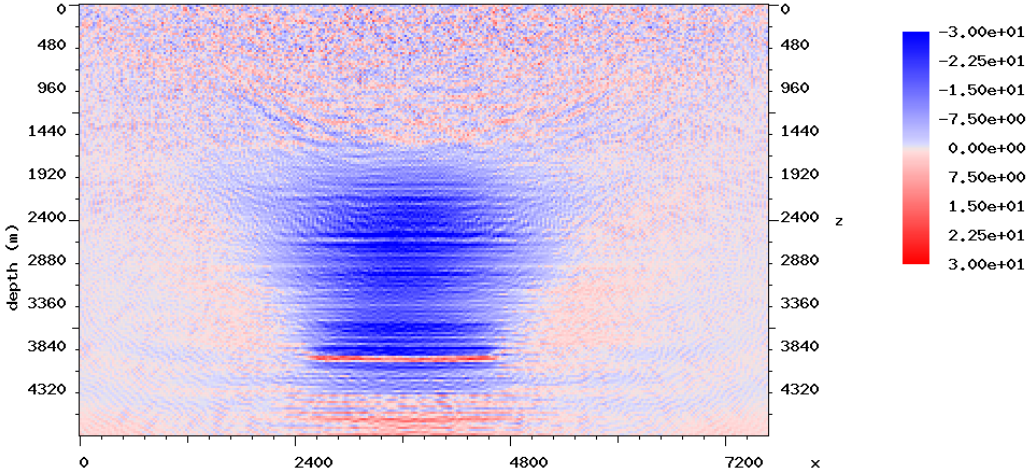

Migration with the updated velocity for image differencing

Baseline image, true baseline v

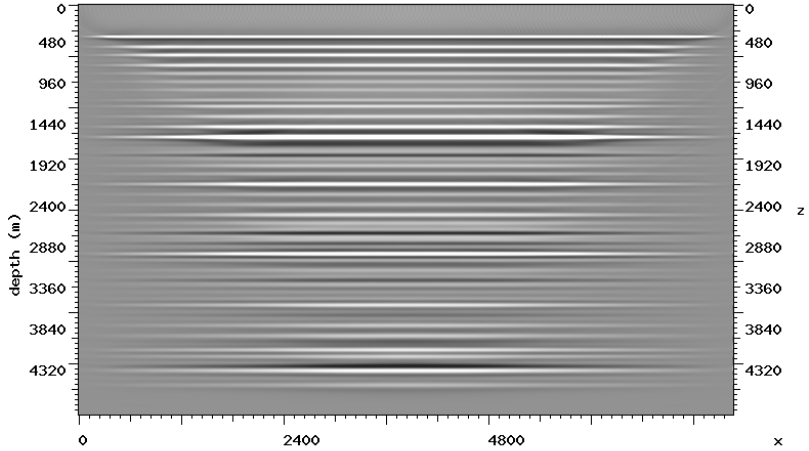

Monitor image, true monitor v – perfect alignment

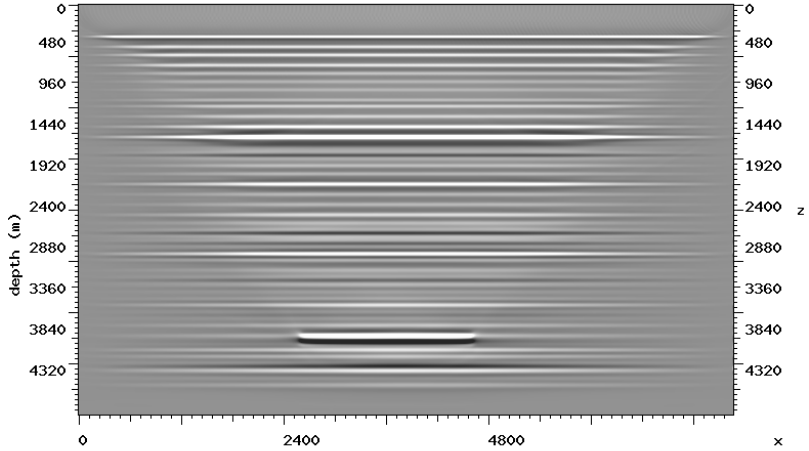

Baseline image, true baseline v

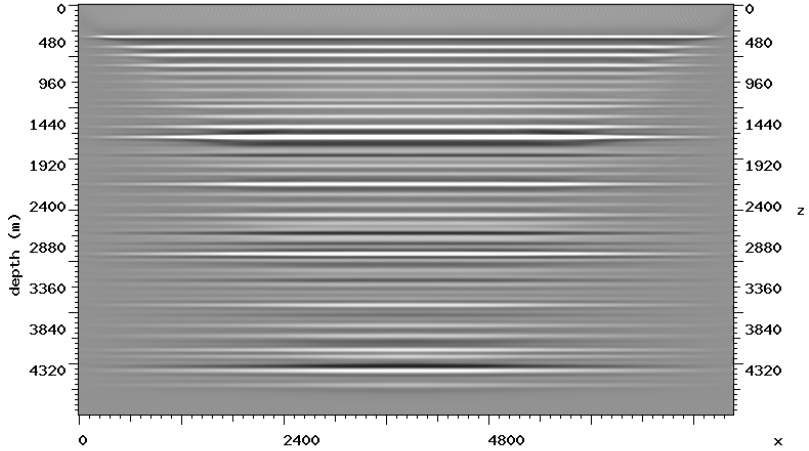

Monitor image, true **baseline** v – reflector shift

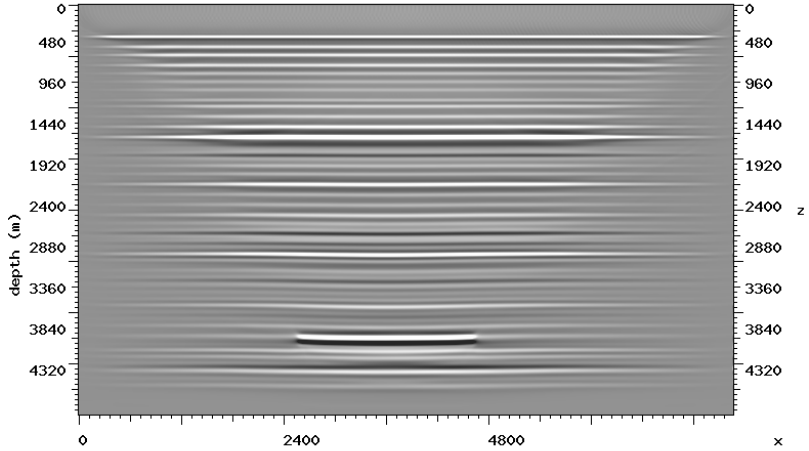

Baseline image, true baseline v

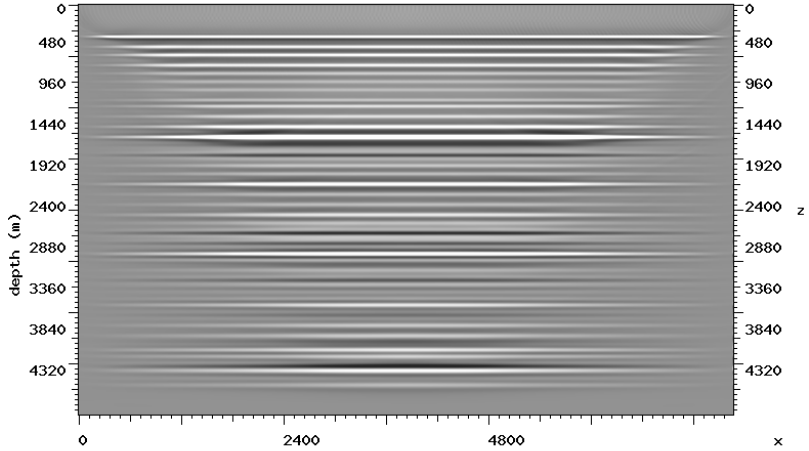

Monitor image, true updated $v + \Delta v$ – reduced shift

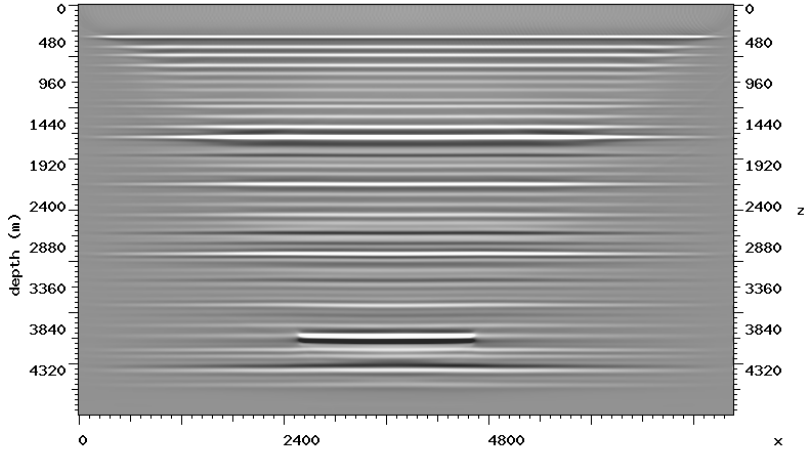

Sensitivity analysis of time-lapse overburden velocity inversion to wrong starting models

True velocity difference

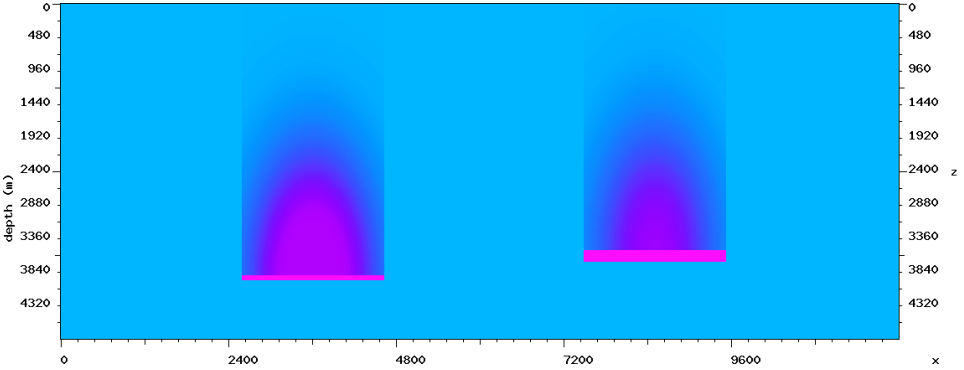

Inversion from good starting model

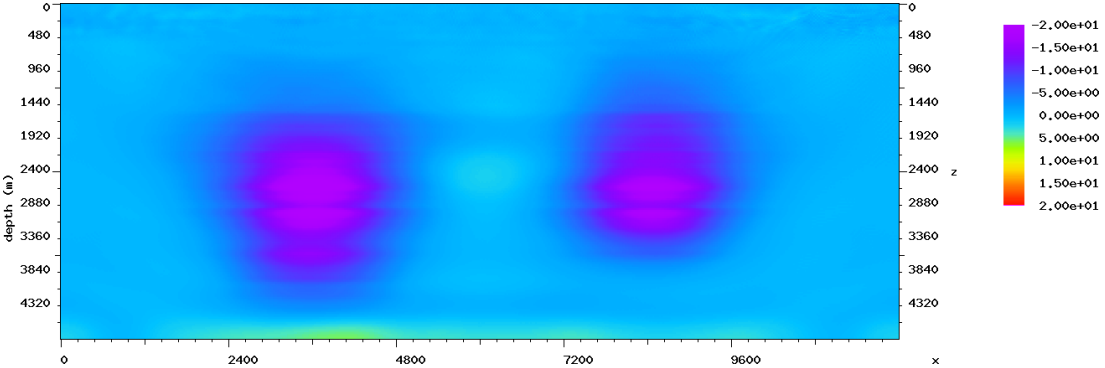

Inversion from bad starting model (cycle skipping)

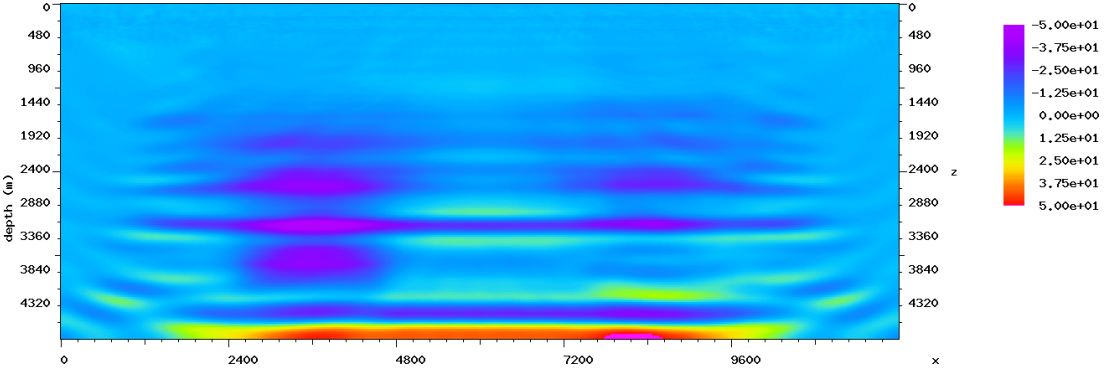

Inversion from bad starting model using strong regularization

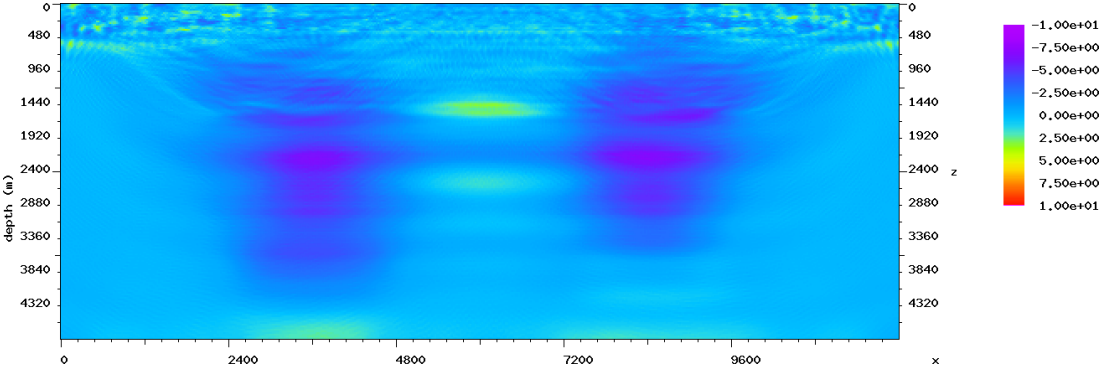

Overburden dilation: reflection field data

Baseline time migration image by Chevron

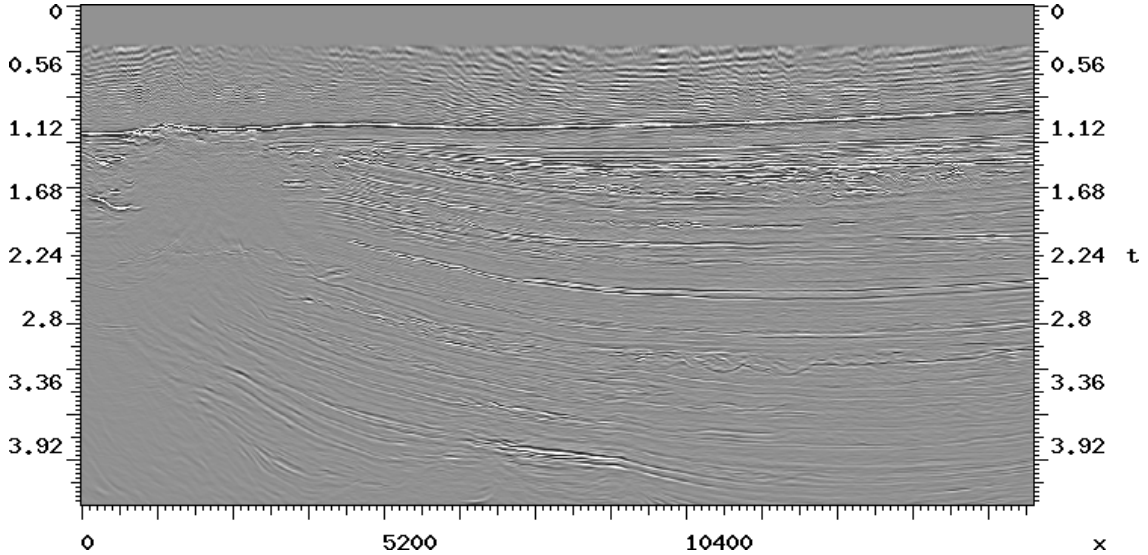

Monitor-Baseline image difference

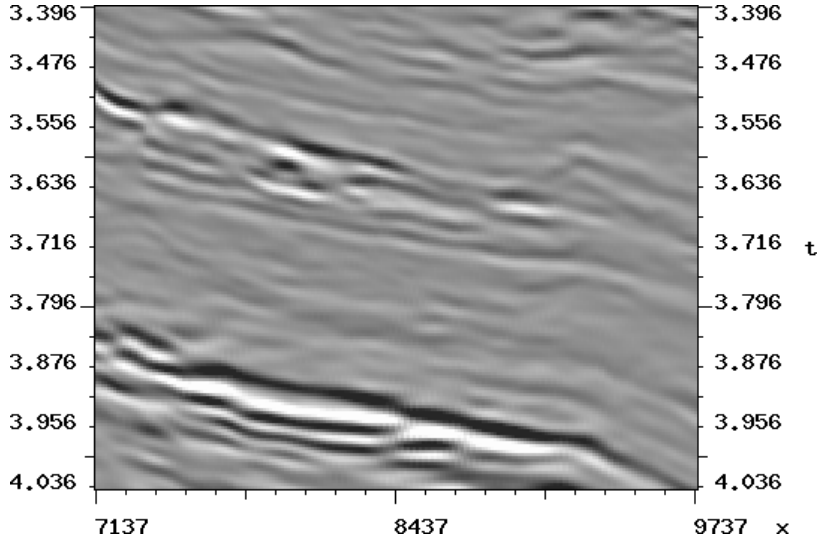

Kinematic differences (time shifts) in 1074m common-offset gathers

Baseline
Monitor

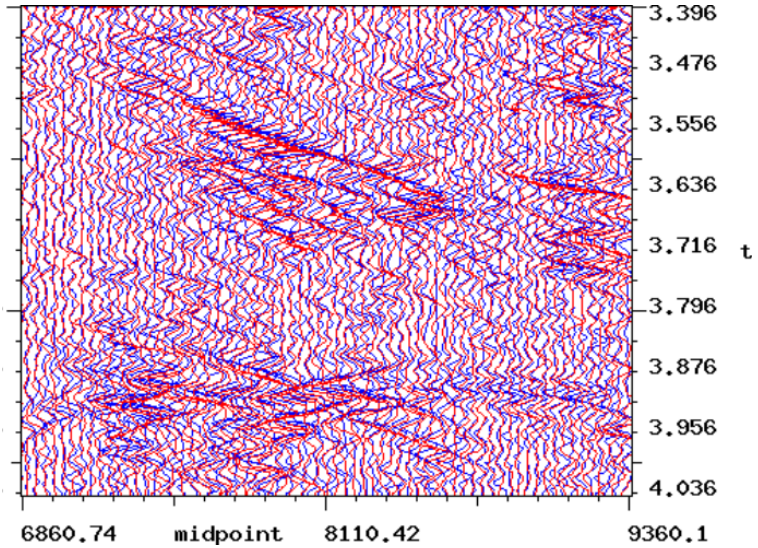

Baseline inversion, 3-30Hz

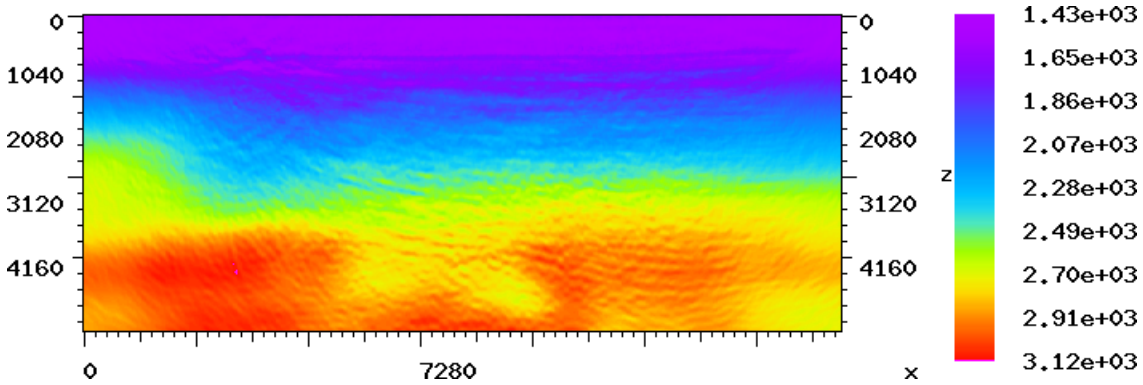

Baseline target

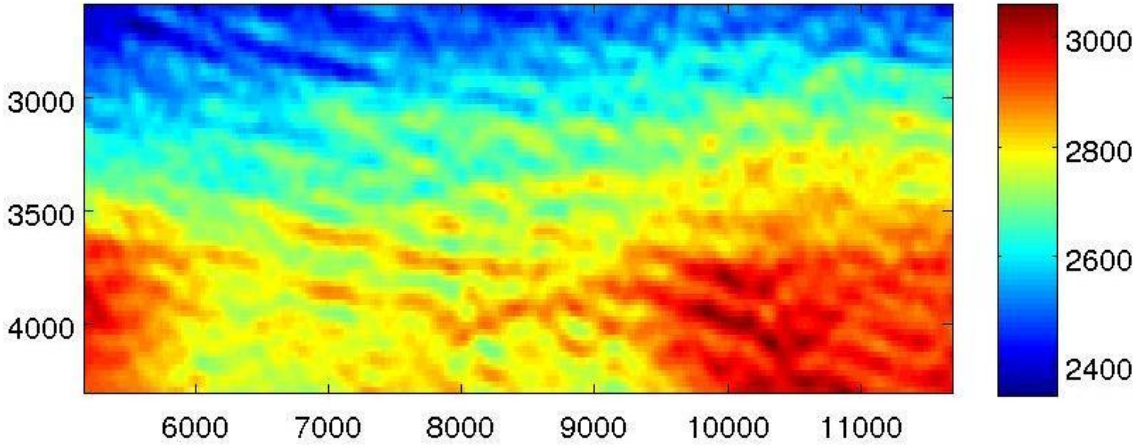

Parallel Difference

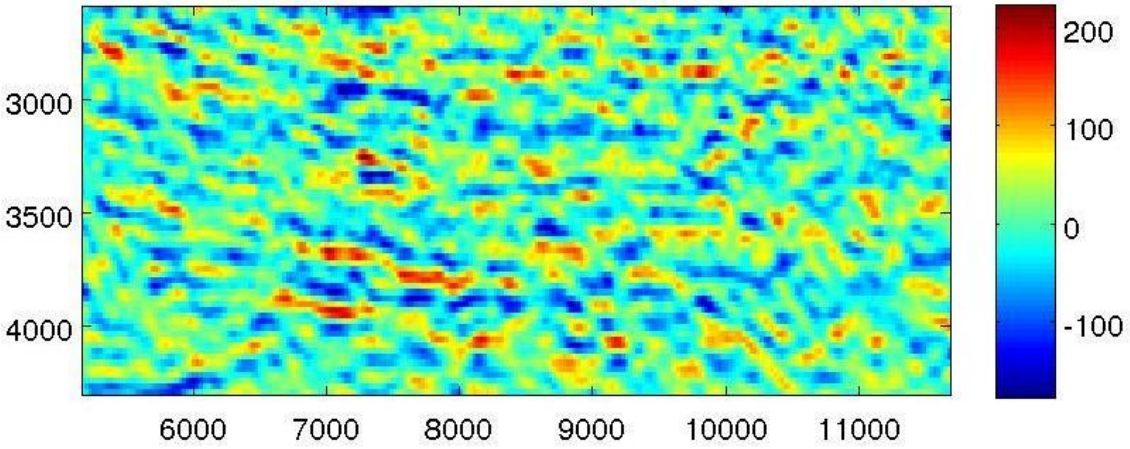

Baseline target

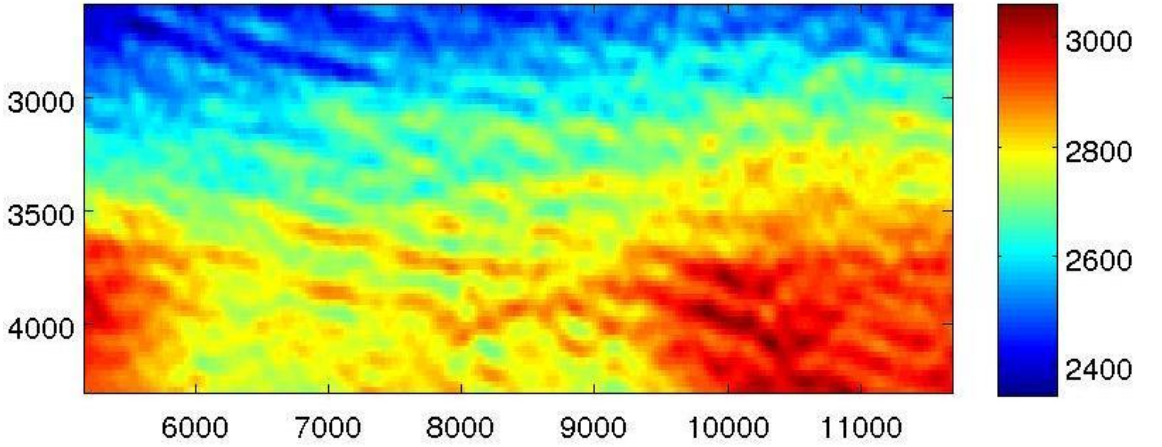

Model difference, strong TV regularization

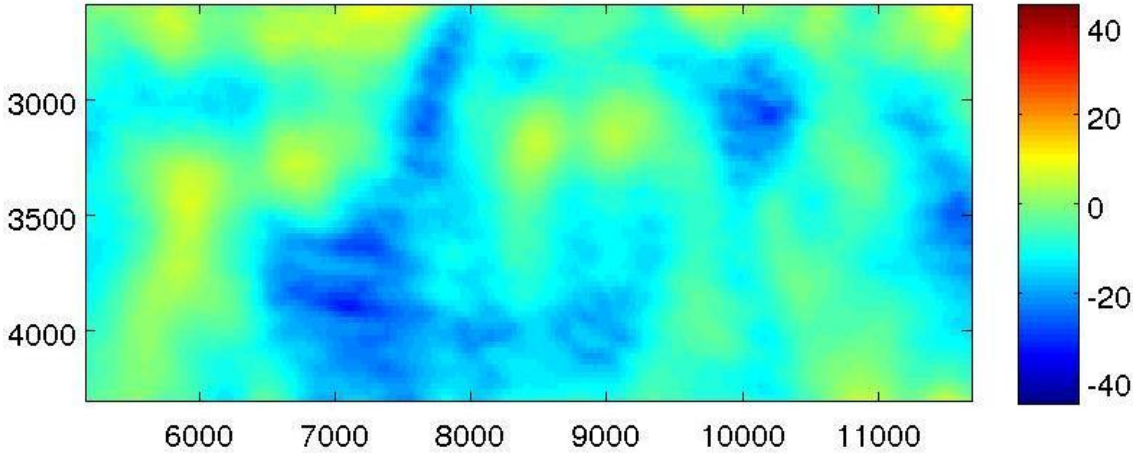

Zoomed-in baseline target

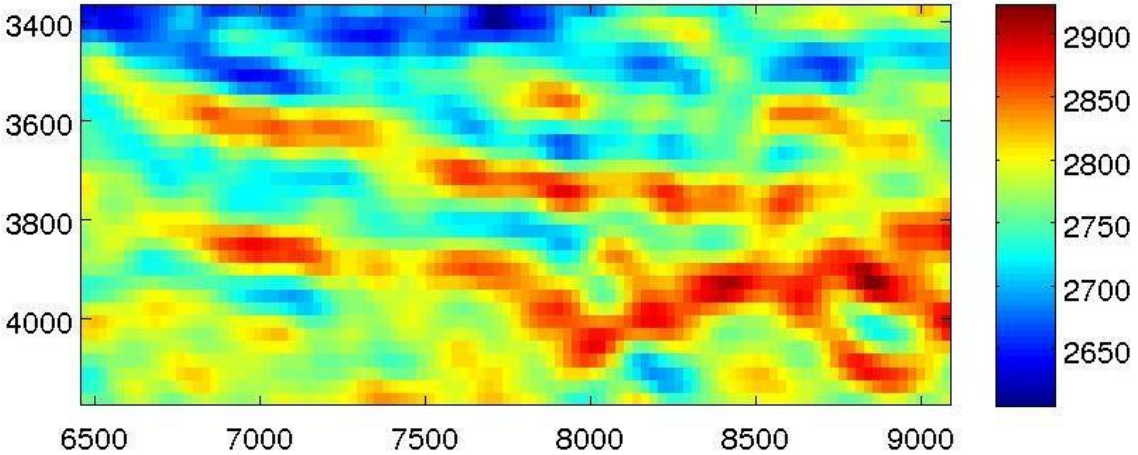

Zoomed-in model difference, strong TV regularization

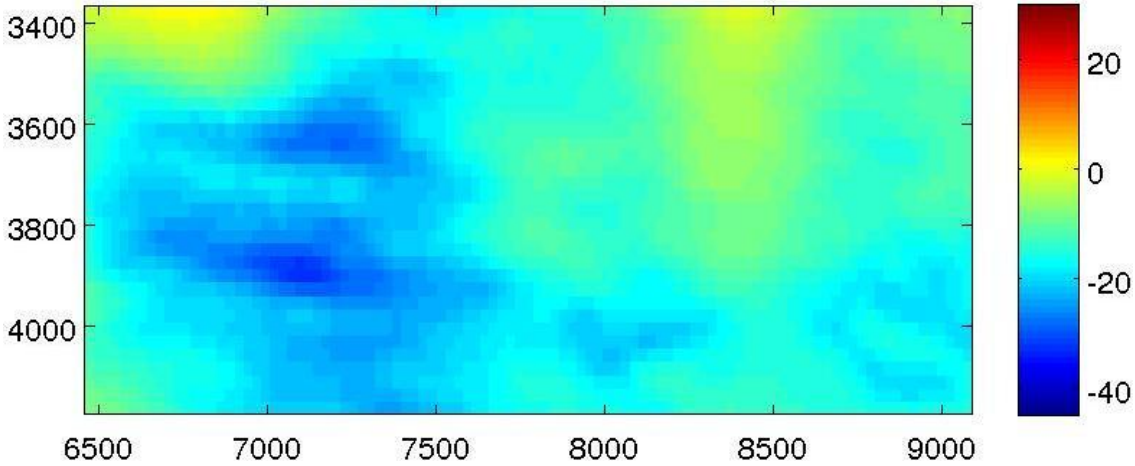

Migrated baseline image

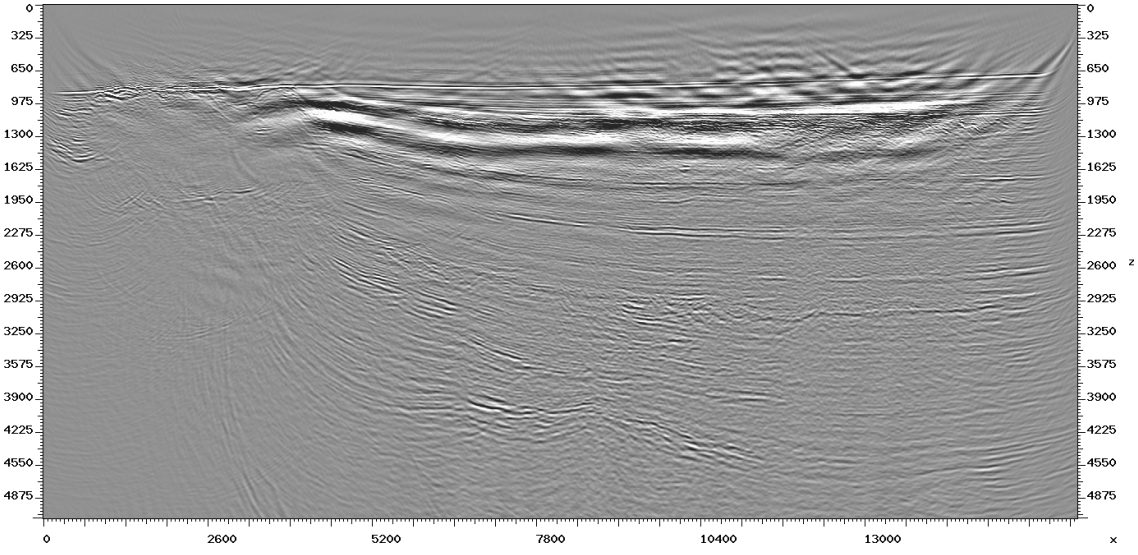

Migrated image difference (target area)

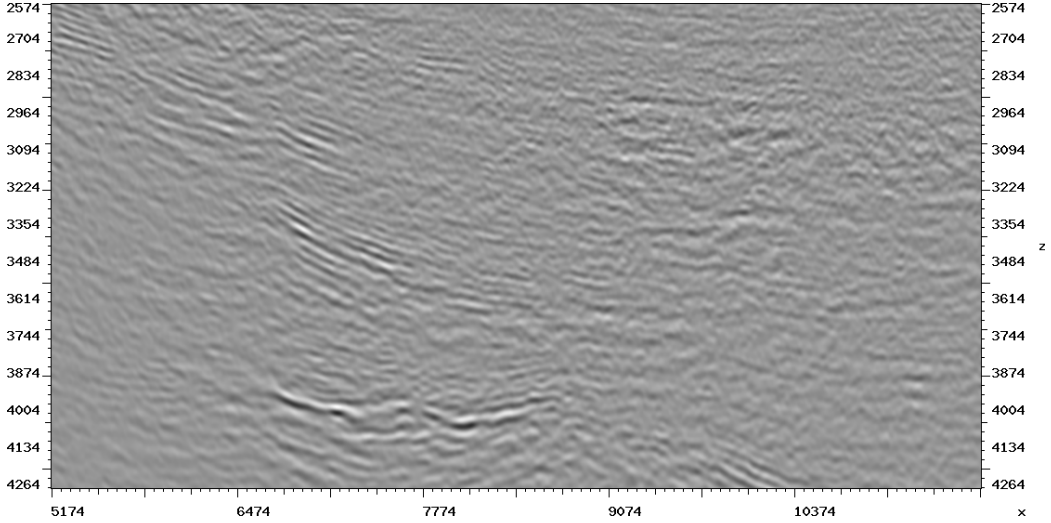

Velocity difference

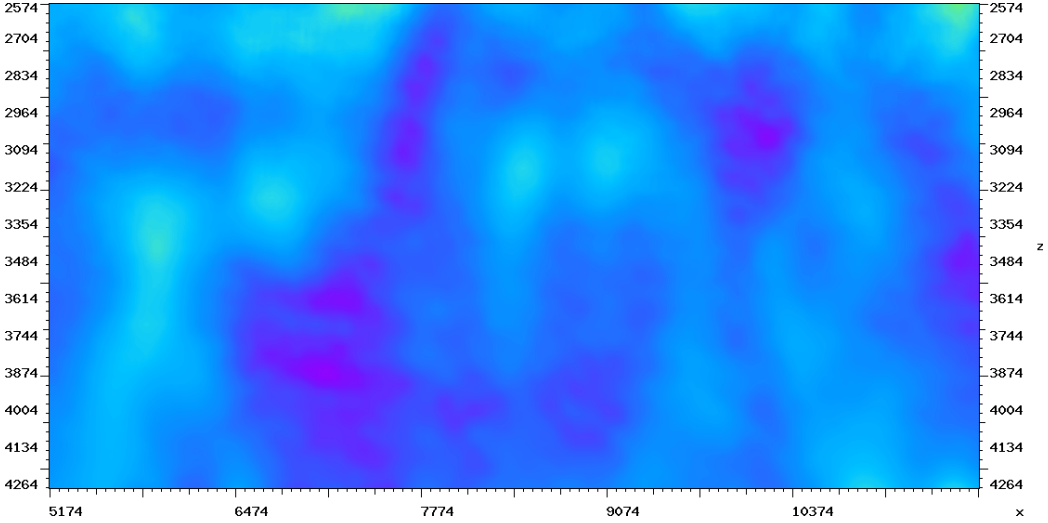

Image vs velocity difference

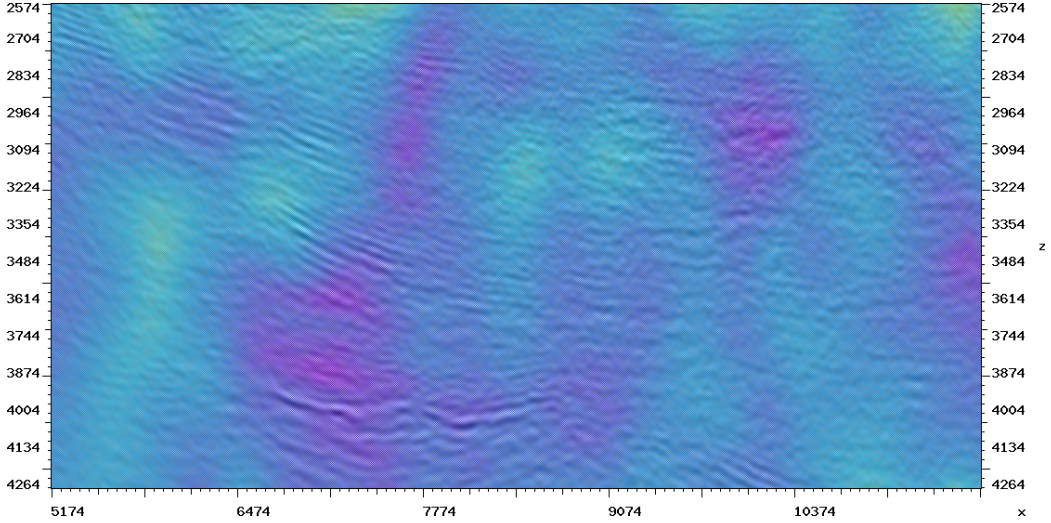

Overburden dilation appears even in non-masked inversion...

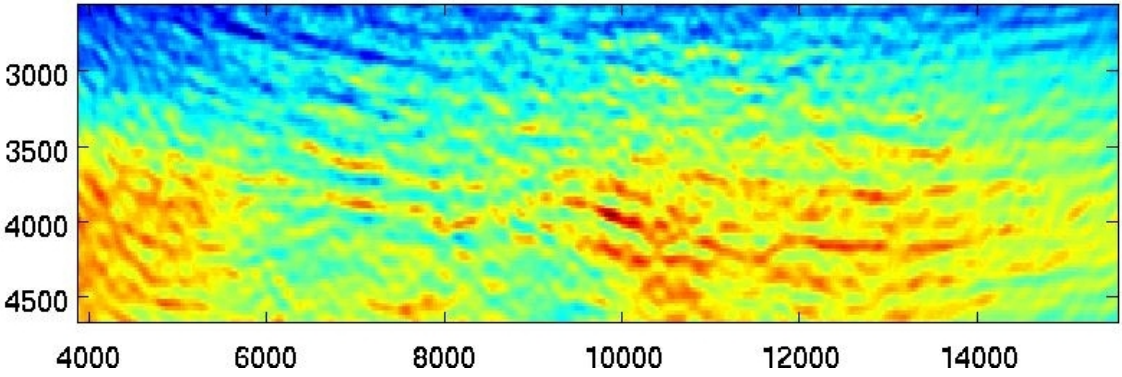

Overburden dilation appears even in non-masked inversion...

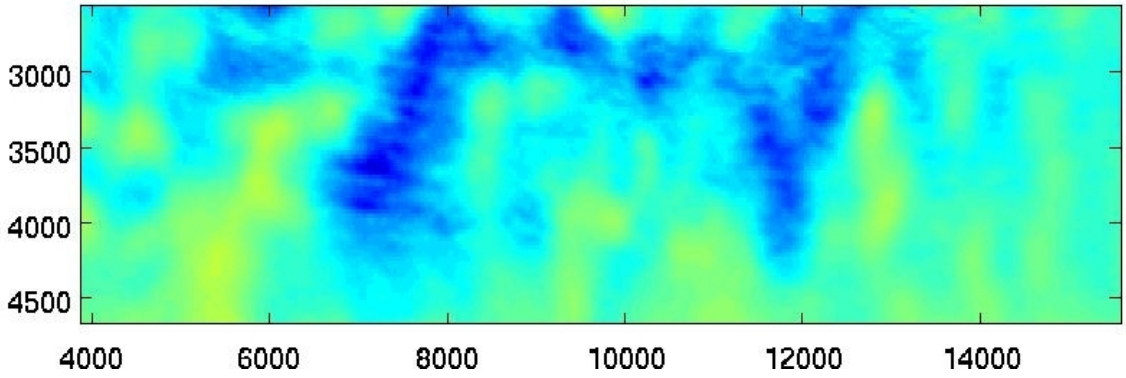

Genesis production wells (Rickett et al., 2007)

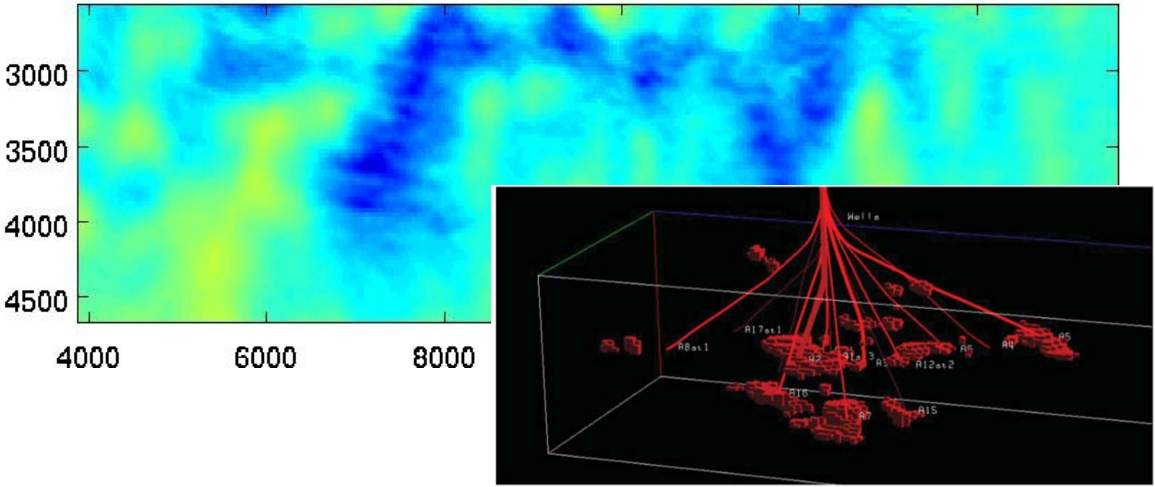

Genesis production wells

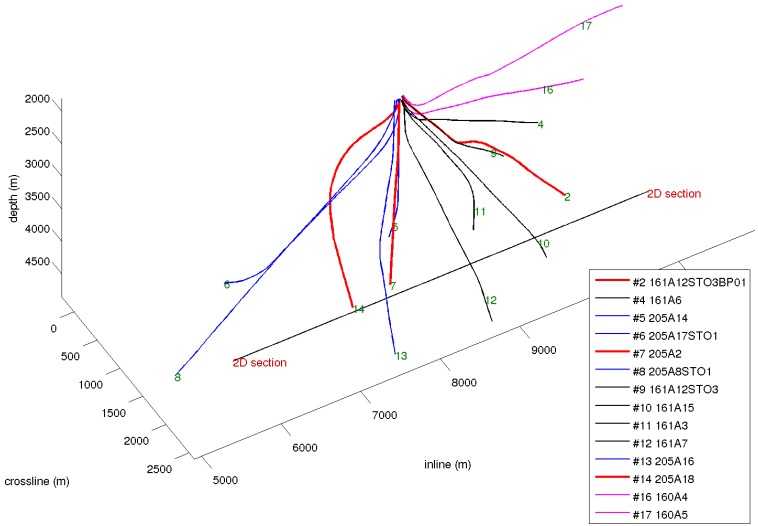

Global inversion with improved starting model vs Genesis wells

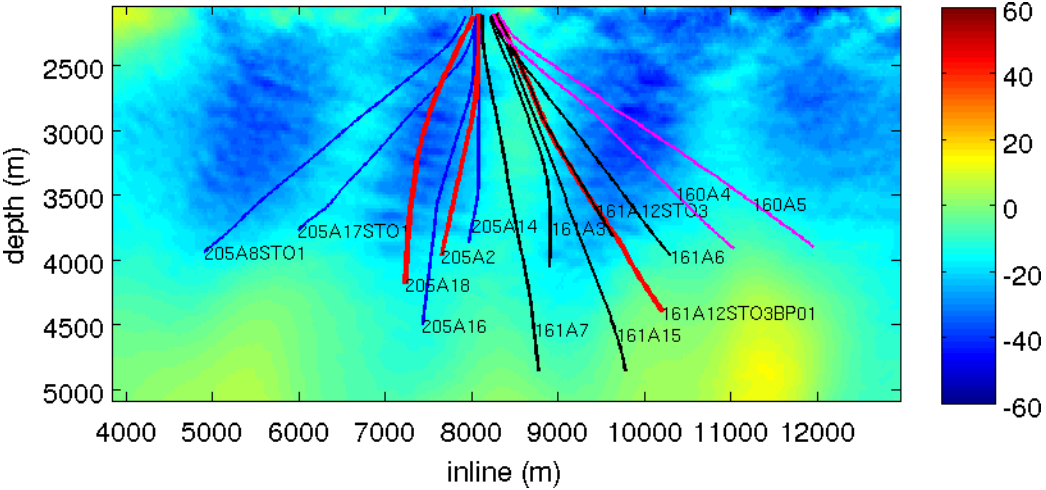

Genesis 3D FWI

- Frequency-domain inversion, 3-30Hz
- Shot gathers interpolated from the provided sparse CDP gathers
- Total of 60 shots with up to 175 receivers each
- 3D inversion for 5208m inline $\times$ 3600m crossline $\times$ 4500m depth
- Phase-only inversion to recover blocky velocity anomalies
- Maximum offset 5km, maximum target depth 4km

Genesis production wells

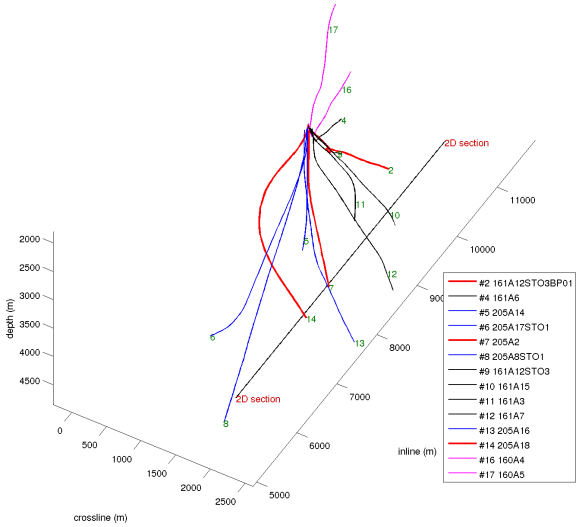

Genesis production wells

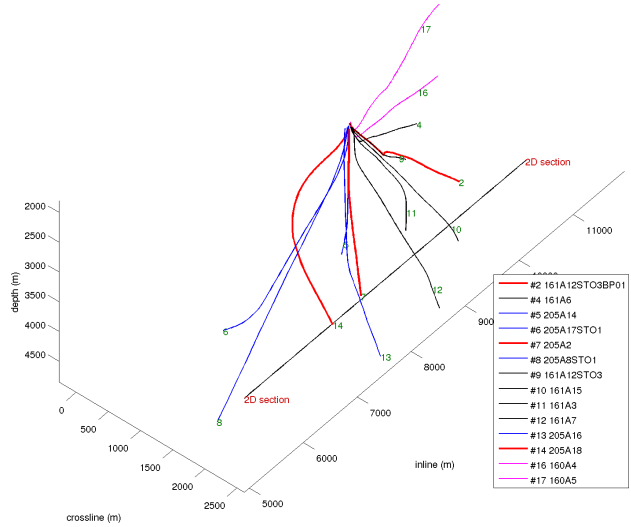

Genesis production wells

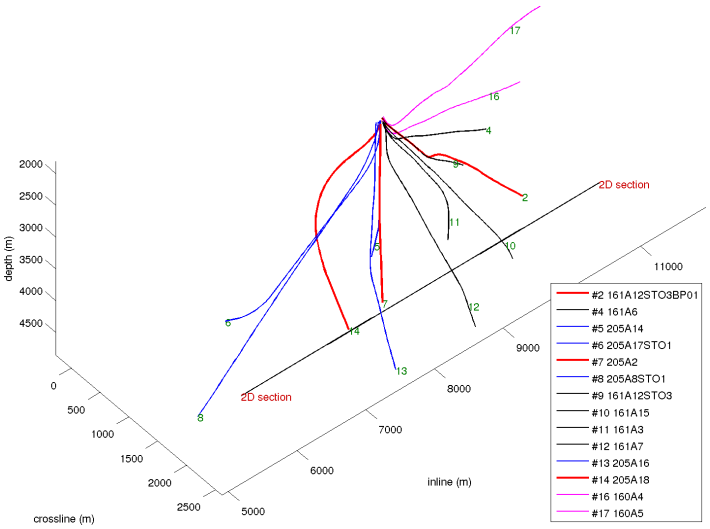

Genesis production wells

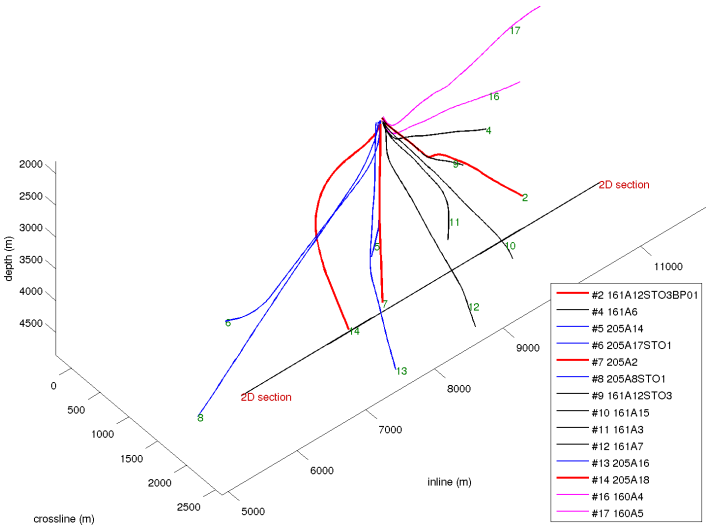

Genesis production wells

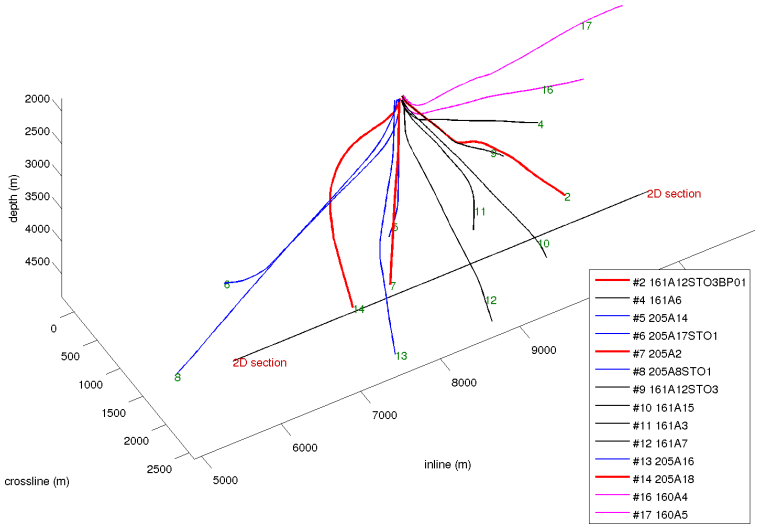

Genesis production wells

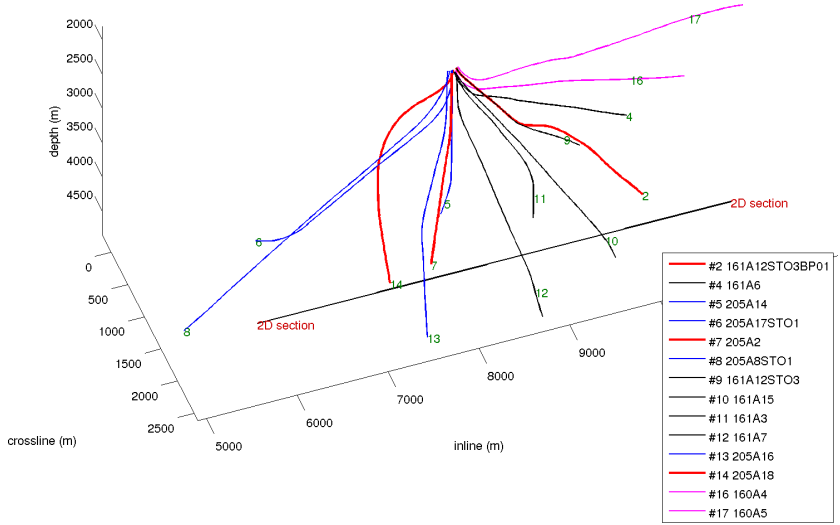

Genesis production wells

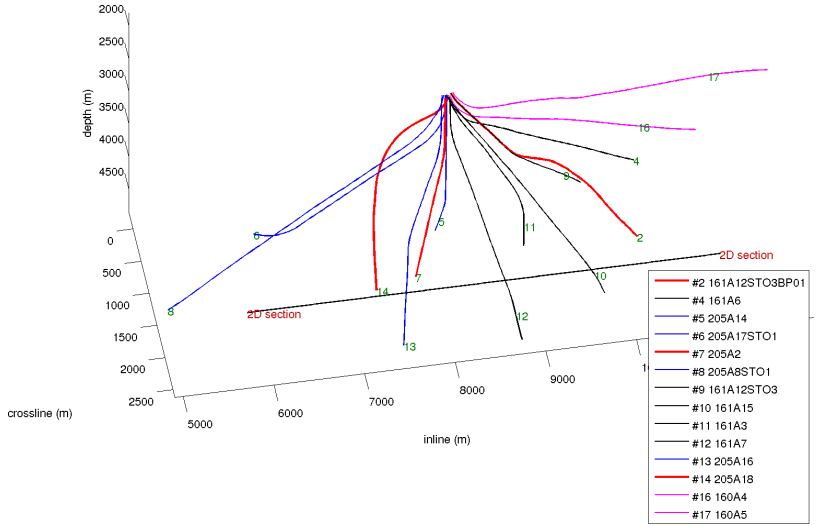

Genesis production wells

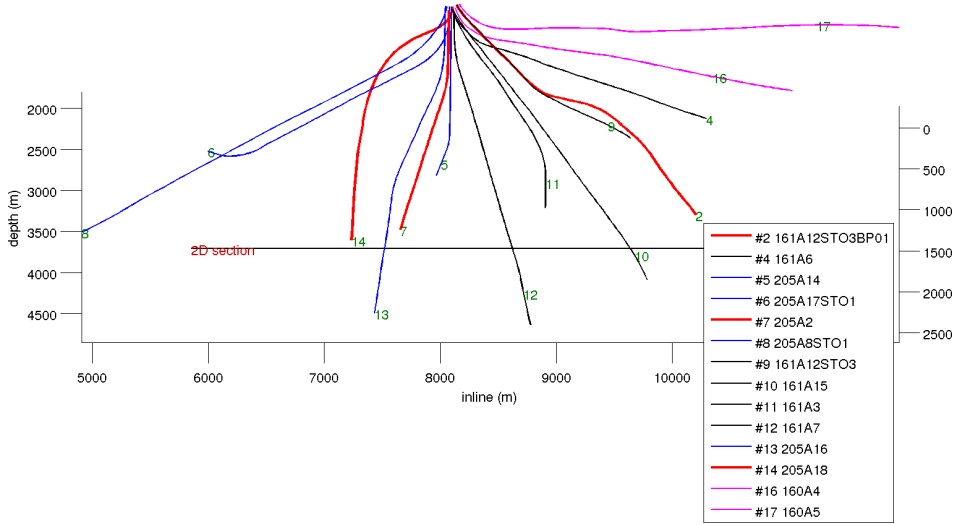

Genesis production wells

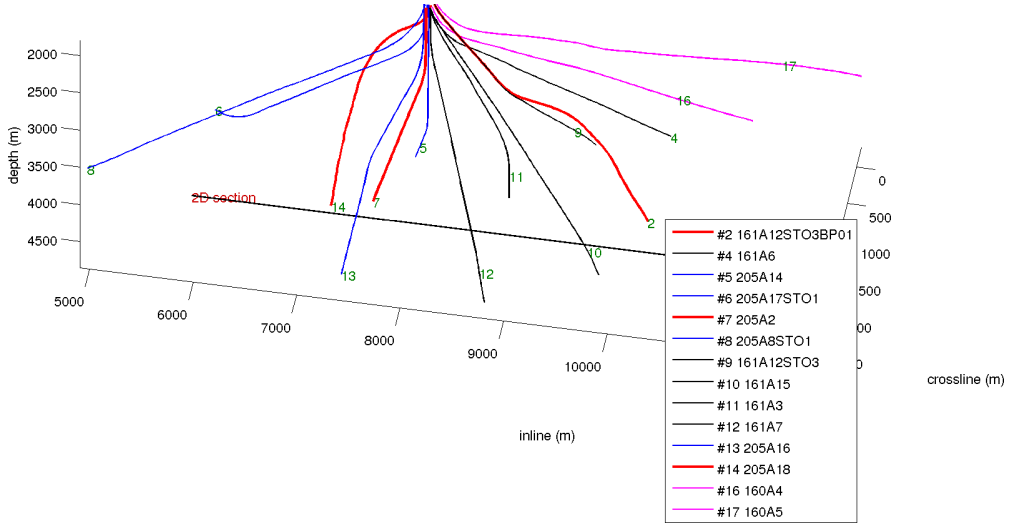

Genesis production wells

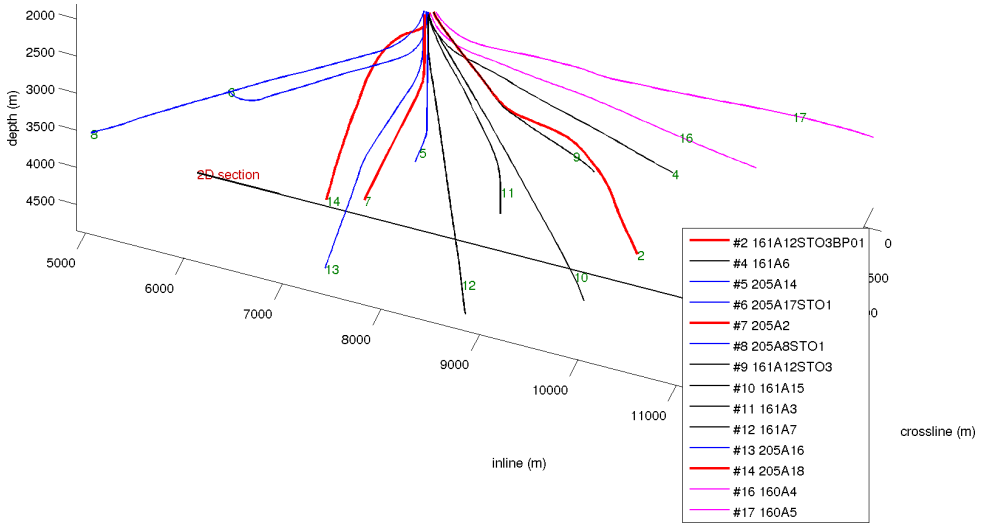

Genesis production wells

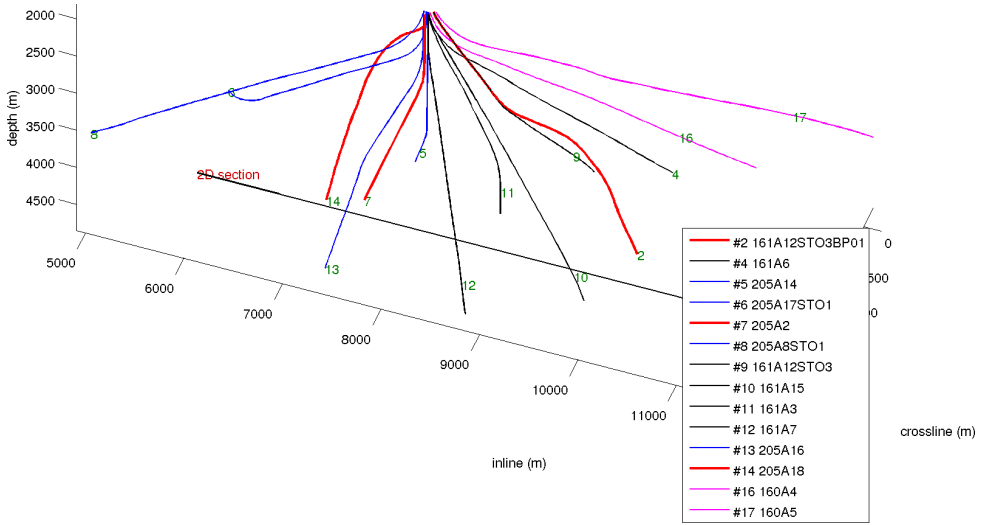

Genesis production wells

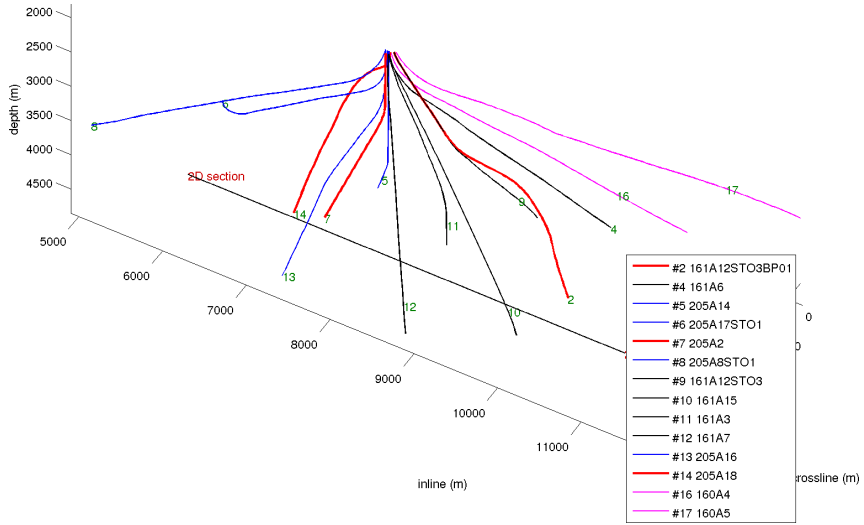

Genesis production wells

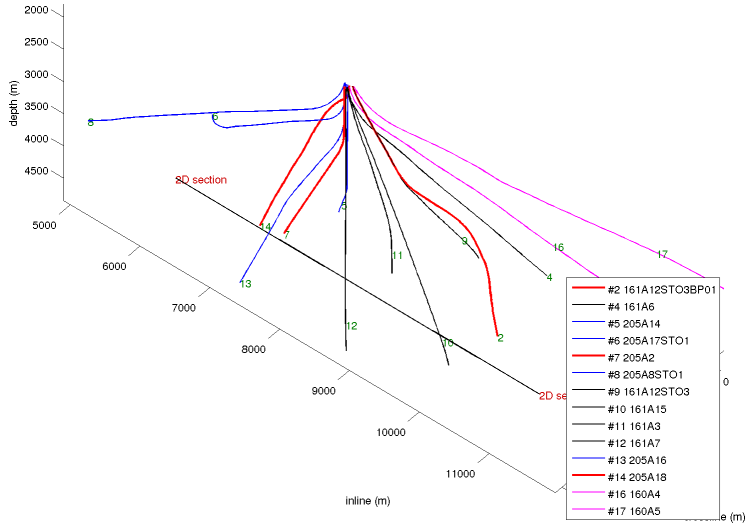

Genesis production wells

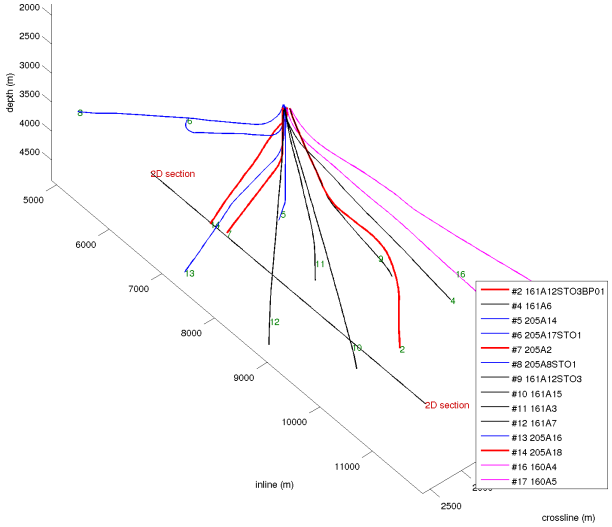

Genesis production wells

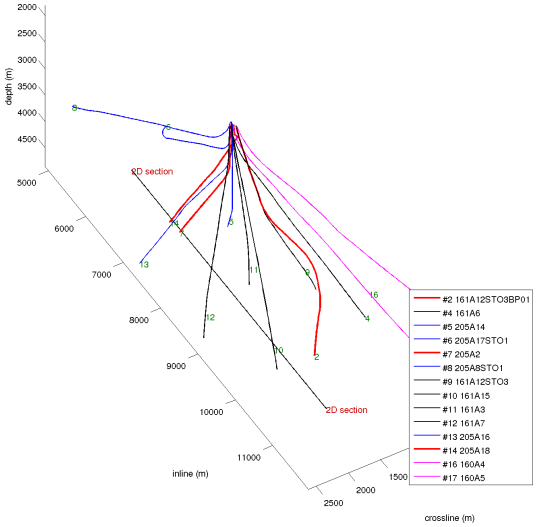

Anomalies with $\Delta v <= -50$m/s (60 shots)

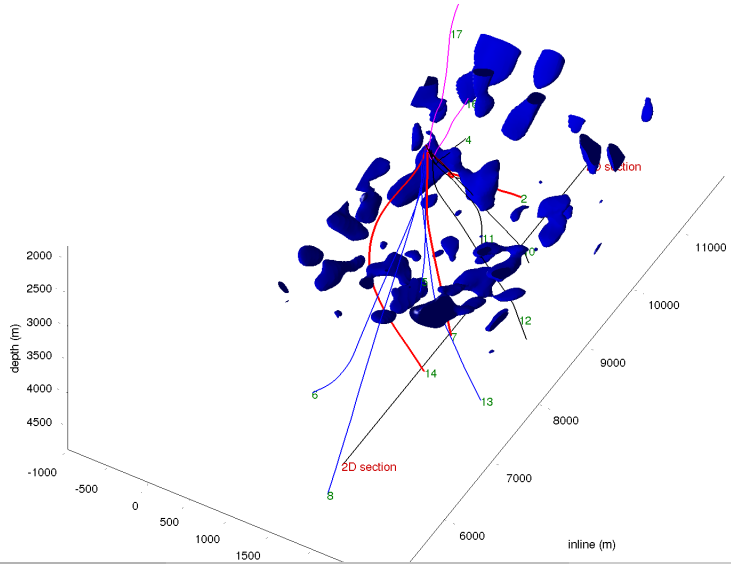

Anomalies with $\Delta v <= -50$m/s (60 shots)

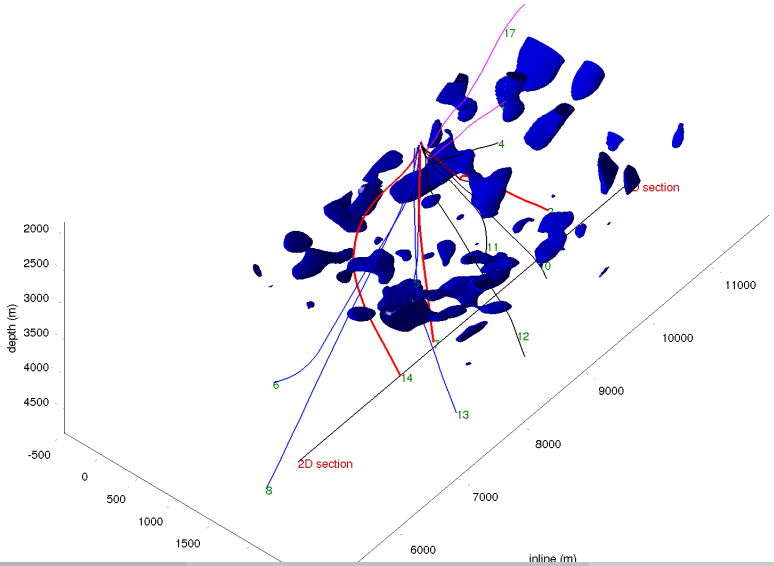

Anomalies with $\Delta v <= -50$m/s (60 shots)

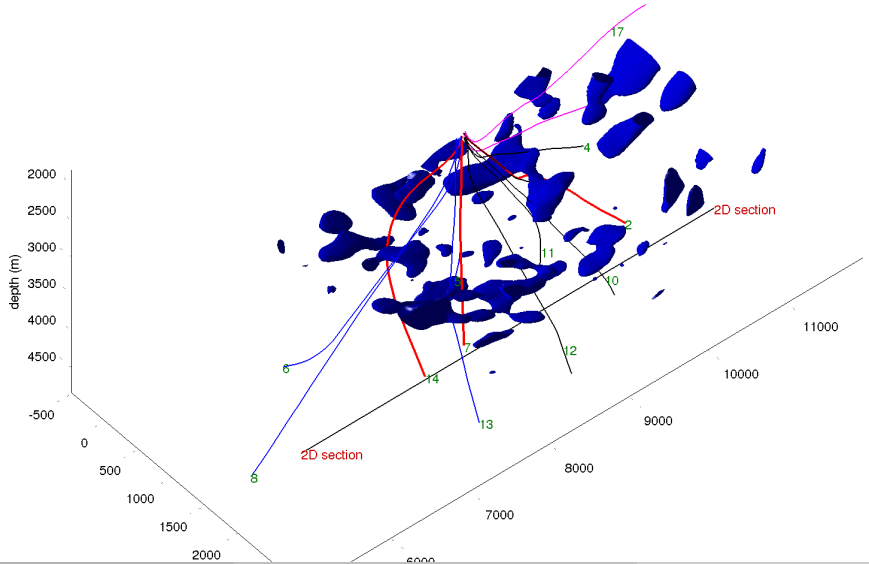

Anomalies with $\Delta v <= -50$m/s (60 shots)

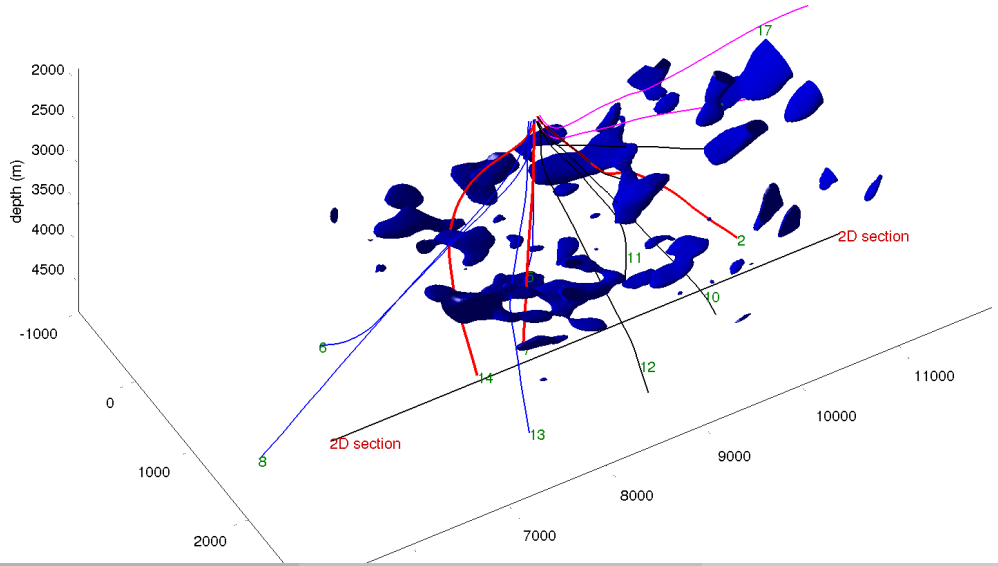

Anomalies with $\Delta v <= -50$m/s (60 shots)

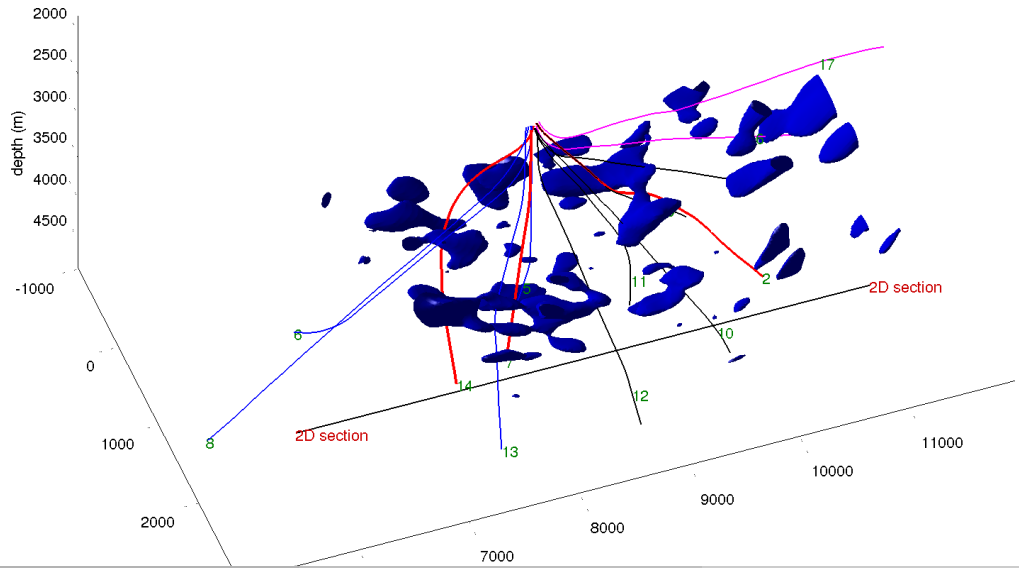

Anomalies with $\Delta v <= -50$m/s (60 shots)

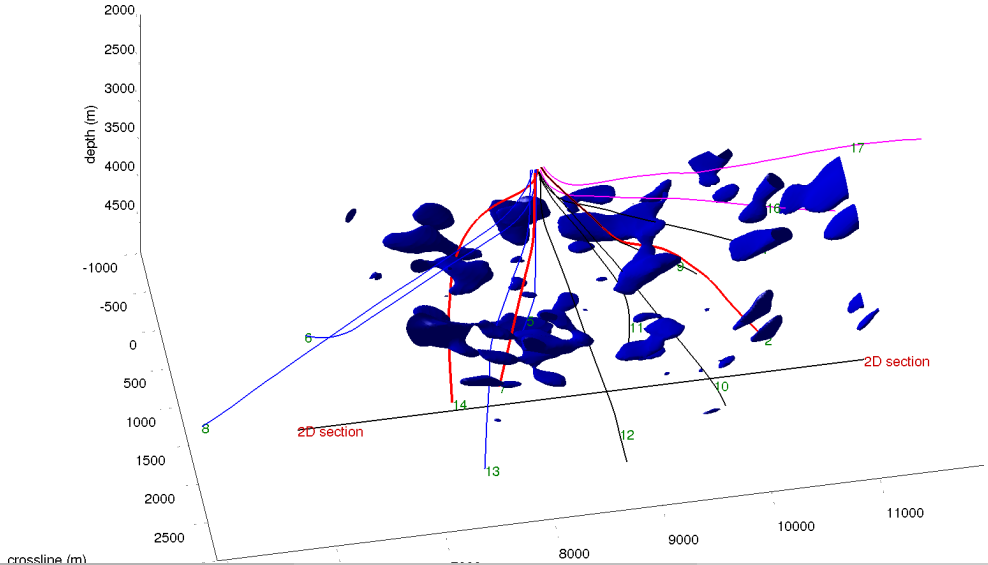

Anomalies with $\Delta v <= -50$m/s (60 shots)

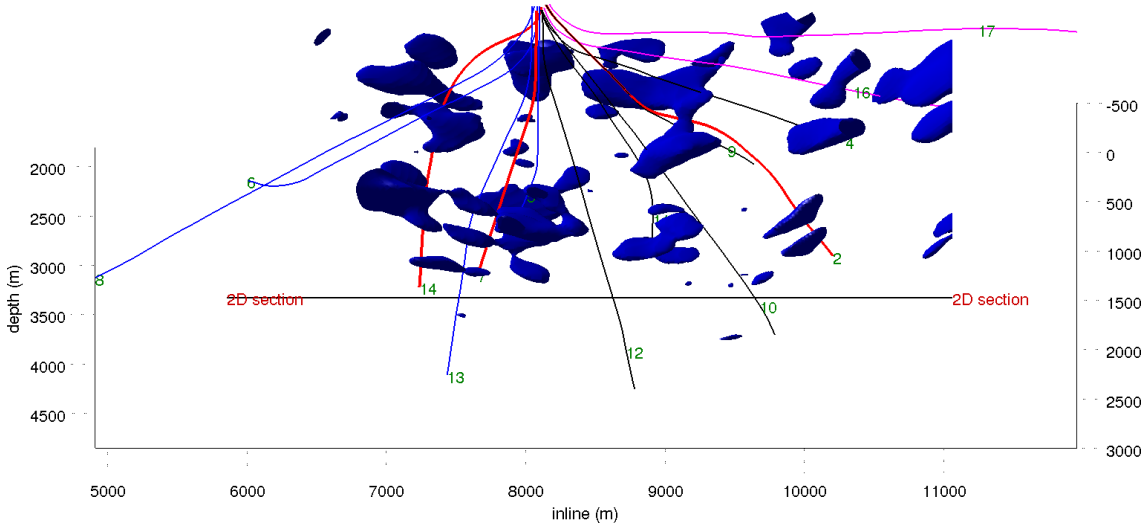

Anomalies with $\Delta v <= -50$m/s (60 shots)

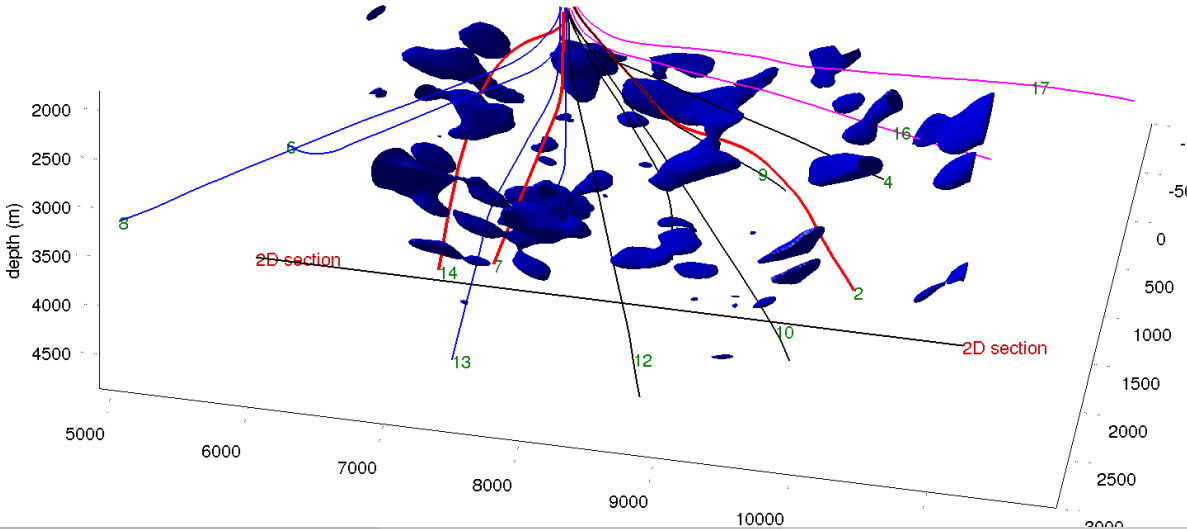

Anomalies with $\Delta v <= -50$m/s (60 shots)

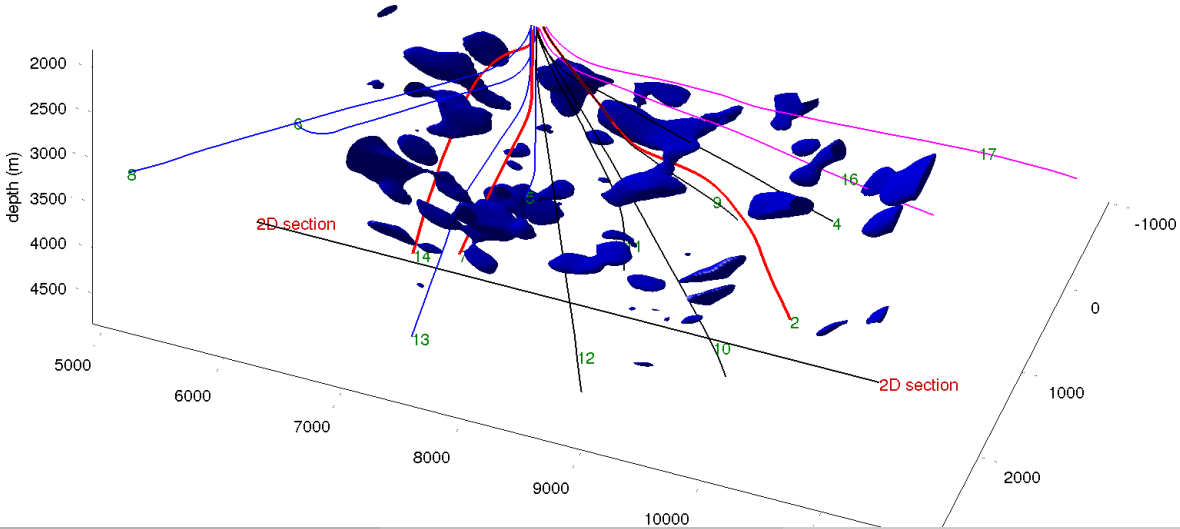

Anomalies with $\Delta v <= -50$m/s (60 shots)

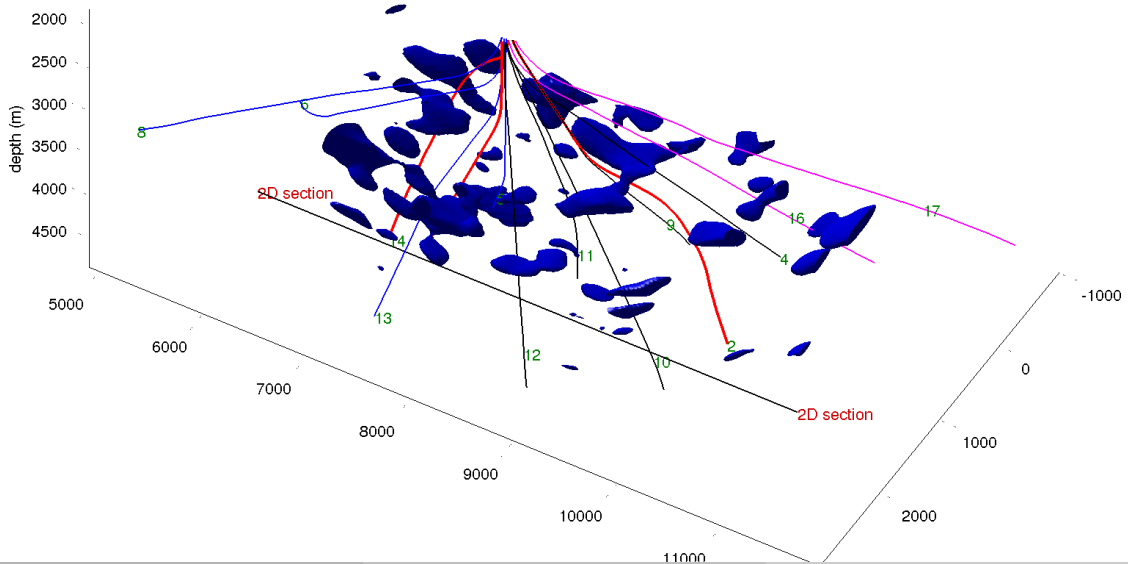

Anomalies with $\Delta v <= -50$m/s (60 shots)

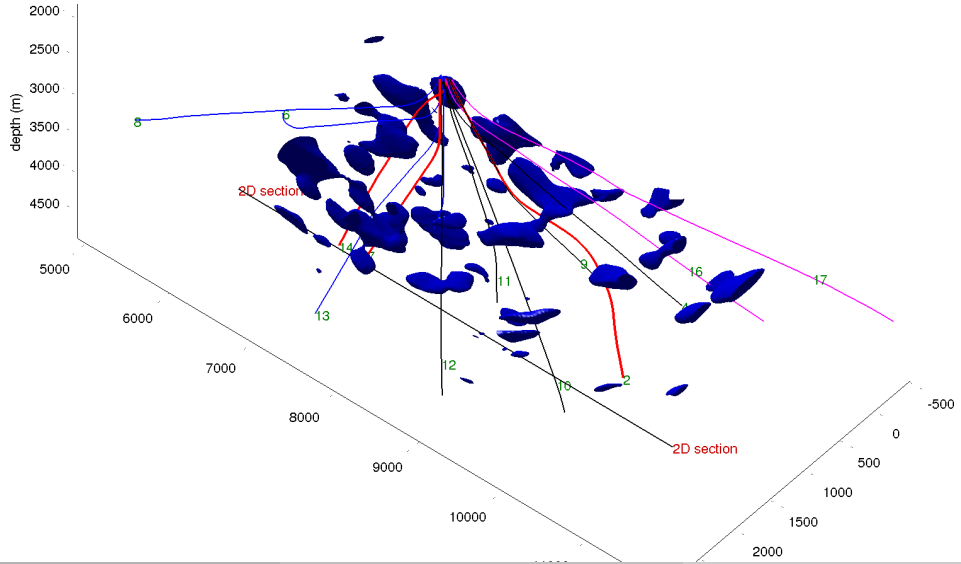

Anomalies with $\Delta v <= -50$m/s (60 shots)

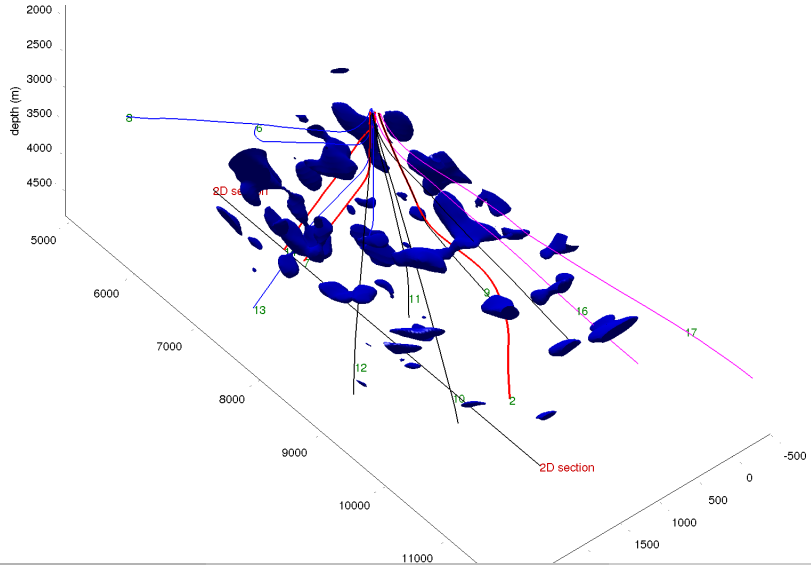

Anomalies with $\Delta v <= -50$m/s (60 shots)

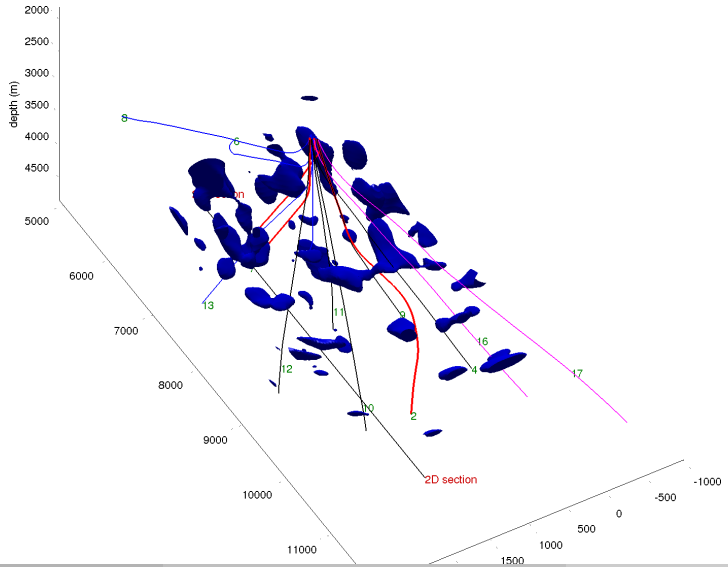

Conclusions and perspectives

- TV-regularized simultaneous time-lapse FWI can resolve velocity changes induced by overburden dilation
- Resolving fine features of compacting reservoirs requires multi-scale or hierarchical inversion
- Computationally intensive, requires multiple inversion experiments
- Reflection 4D FWI capability $\Rightarrow$ 4D land seismic perspectives

Time-lapse geomechanical analysis

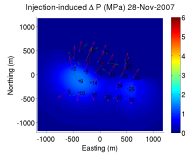

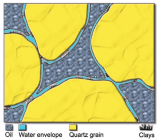

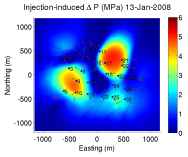

CSS: http://birchwoodresources.ca/node/23

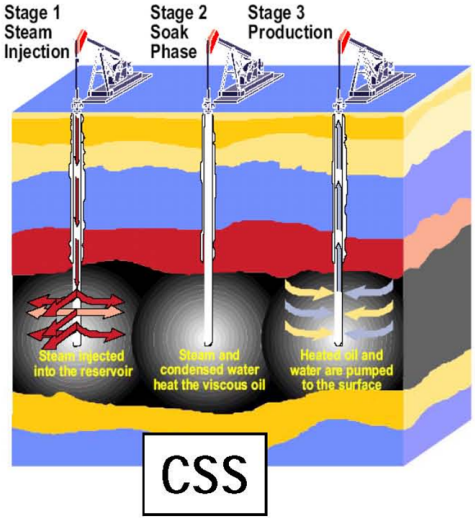

Motivation: improved reservoir monitoring

- Extraction of heavy oil from deep formations relies on Cyclic Steam Stimulation (CSS) or Steam-Assisted Gravity Drainage (SAGD).
- Effective steam injection requires understanding pressure front propagation and reservoir heterogeneity.
- Goal: design a robust computational framework for estimating pressure fronts from measurable surface deformation.

A heavy oil reservoir undergoing a 60-day steam injection

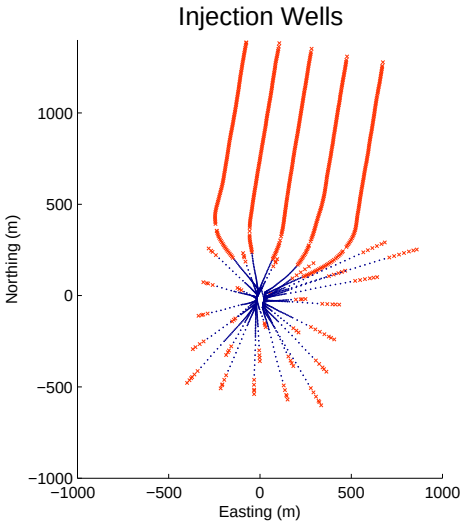

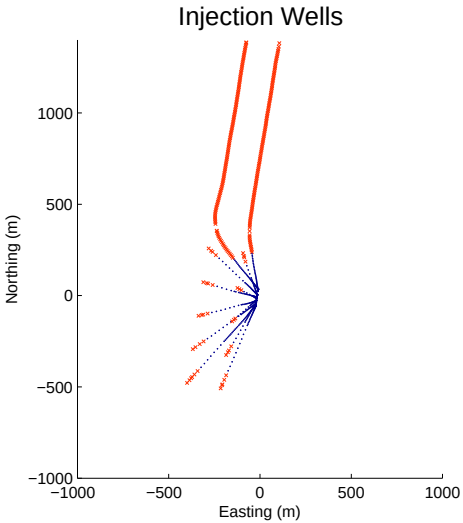
Injection Wells
Northing (m)
Easting (m)
1000
500
0
−500
−1000
−1000
−500
0
500
1000

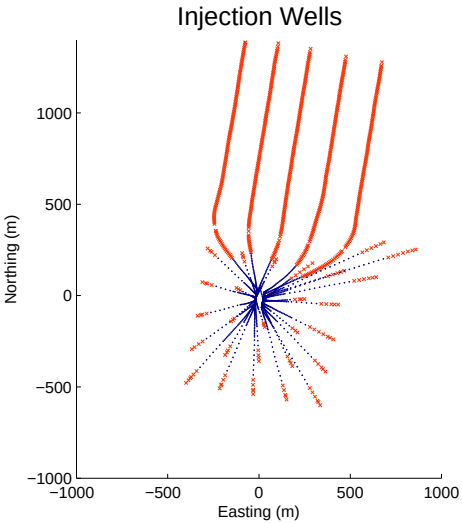
Injection Wells
Northing (m)
Easting (m)
1000
500
0
−500
−1000
−1000
−500
0
500
1000

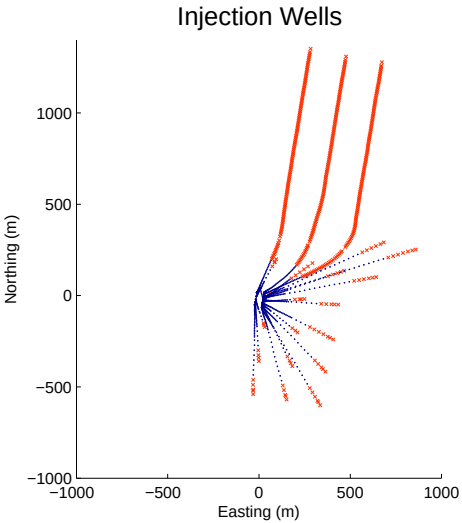
Injection Wells
Northing (m)
Easting (m)
1000
500
0
−500
−1000
−1000
−500
0
500
1000

Relate deformation and pore pressure change using Biot's theory (Rice and Cleary, 1976; Segall, 1985; Segall, 2010):

$$\mu\nabla^2 u_i + \frac{\mu}{1-2\nu}\frac{\partial^2 u_j}{\partial x_i \partial x_j} = \boxed{\alpha\frac{\partial p}{\partial x_i}} - f_i = 0,\ i = 1,2,3, \qquad \text{(ELAST)}$$

and

$$S_\alpha \frac{\partial p}{\partial t} - \frac{\kappa}{\eta}\nabla^2 p = -\alpha\frac{\partial}{\partial t}\left(\nabla\cdot\mathbf{u}\right), \qquad \text{(FLOW)}$$

where $\mathbf{u}$ is displacement, p is the pore pressure change, f_i is a differential body-force distribution, μ,ν,α,κ, and η are the shear modulus, Poisson's ratio, Biot coefficient, permeability, and fluid viscosity;

$$S_\alpha = \frac{3\alpha(1-2\nu)(1-\alpha B)}{2\mu B(1+\nu)}, \qquad \text{(STORAGE)}$$

where B is Skempton's coefficient.

Relate deformation and pore pressure change using Biot's theory (Rice and Cleary, 1976; Segall, 1985; Segall, 2010):

$$\mu\nabla^2 u_i + \frac{\mu}{1-2\nu}\frac{\partial^2 u_j}{\partial x_i \partial x_j} = \boxed{\alpha\frac{\partial p}{\partial x_i}} - f_i = 0,\ i = 1,2,3, \qquad \text{(ELAST)}$$

and

$$S_\alpha \frac{\partial p}{\partial t} - \frac{\kappa}{\eta}\nabla^2 p = -\alpha\frac{\partial}{\partial t}\left(\nabla\cdot\mathbf{u}\right), \qquad \text{(FLOW)}$$

where $\mathbf{u}$ is displacement, p is the pore pressure change, f_i is a differential body-force distribution, μ,ν,α,κ, and η are the shear modulus, Poisson's ratio, Biot coefficient, permeability, and fluid viscosity;

$$S_\alpha = \frac{3\alpha(1-2\nu)(1-\alpha B)}{2\mu B(1+\nu)}, \qquad \text{(STORAGE)}$$

where B is Skempton's coefficient.

- Regard (ELAST) as a deformation modeling operator $\mathbf{A}p = \mathbf{u}$ and **decouple** it from the flow equation (FLOW) (Vasco et al., 2000; Du and Olson, 2001; Hodgson, 2007).

- Solve the regularized constrained optimization problem

$$\|\mathbf{A}p - \mathbf{u}\|_{L_2}^2 + \epsilon\|\Delta p\|_{L_2}^2 \rightarrow \min, \quad 0 \leq p \leq p_{\max}. \quad \text{(BOUNDREG)}$$

Inverted pore pressure change, $\epsilon = 10^{-3}$

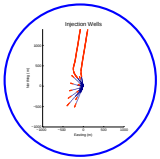

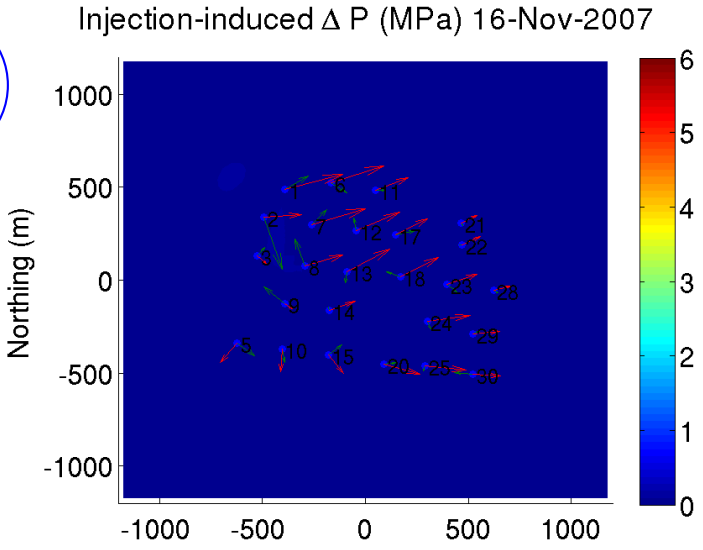

Inverted pore pressure change, $\epsilon = 10^{-3}$

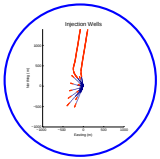

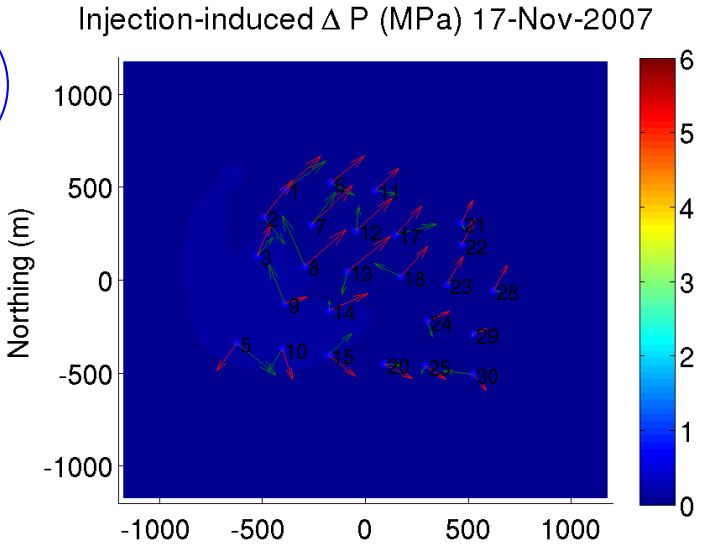

Inverted pore pressure change, $\epsilon = 10^{-3}$

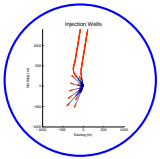

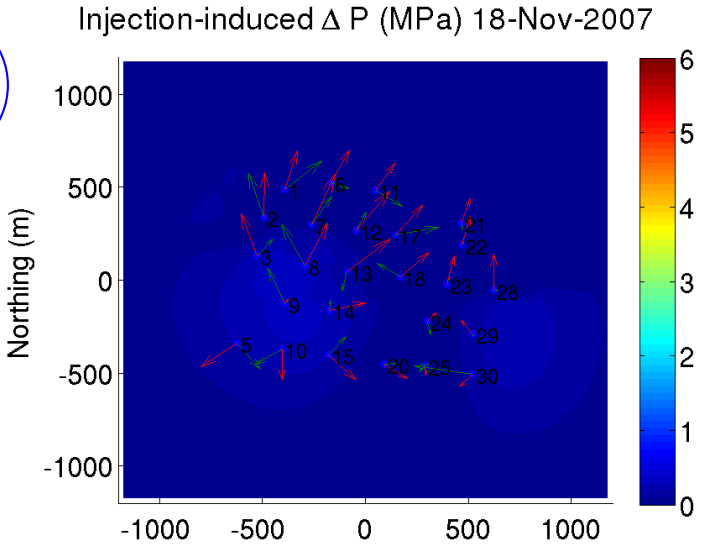

Inverted pore pressure change, $\epsilon = 10^{-3}$

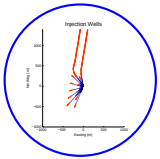

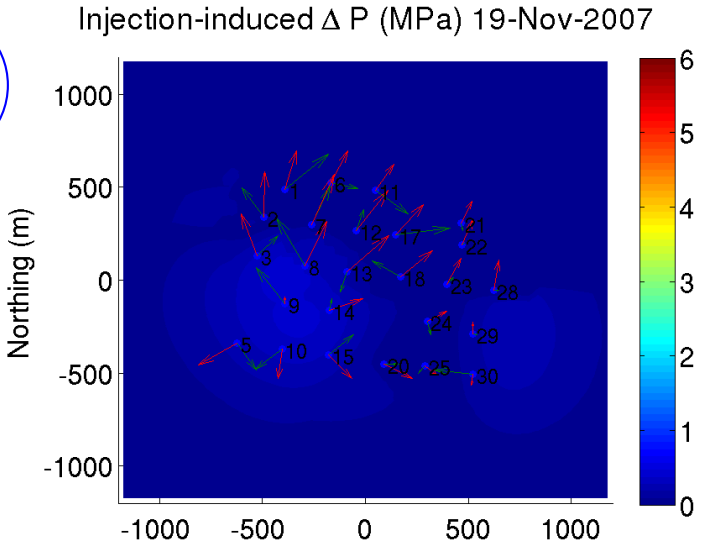

Inverted pore pressure change, $\epsilon = 10^{-3}$

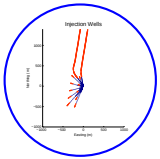

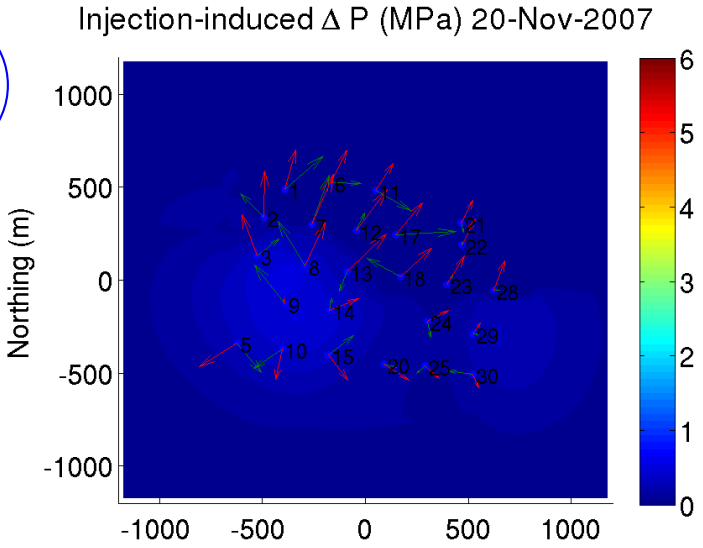

Inverted pore pressure change, $\epsilon = 10^{-3}$

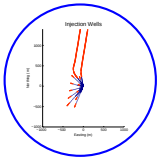

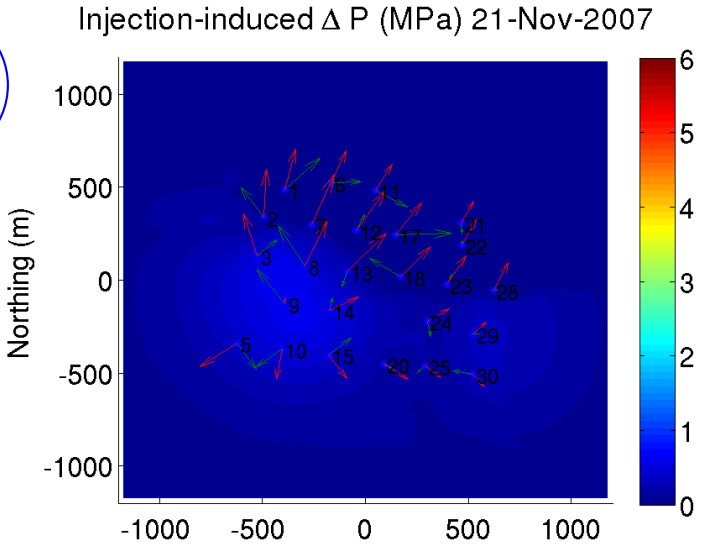

Inverted pore pressure change, $\epsilon = 10^{-3}$

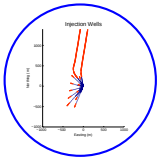

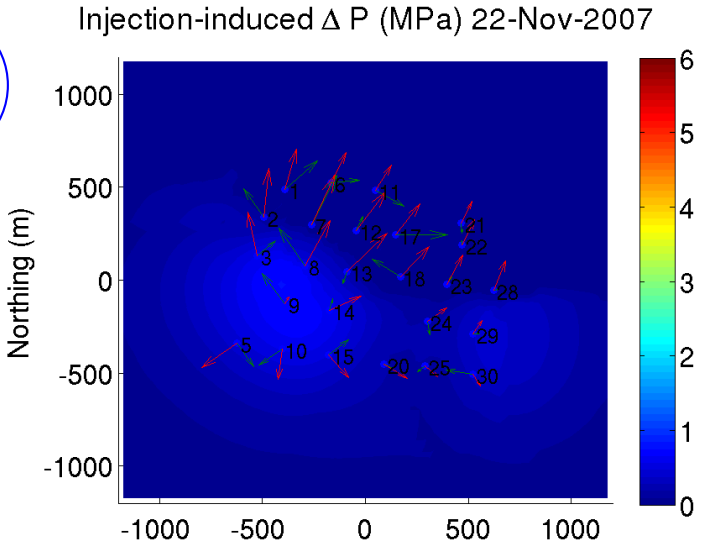

Inverted pore pressure change, $\epsilon = 10^{-3}$

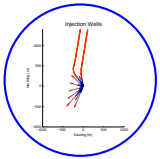

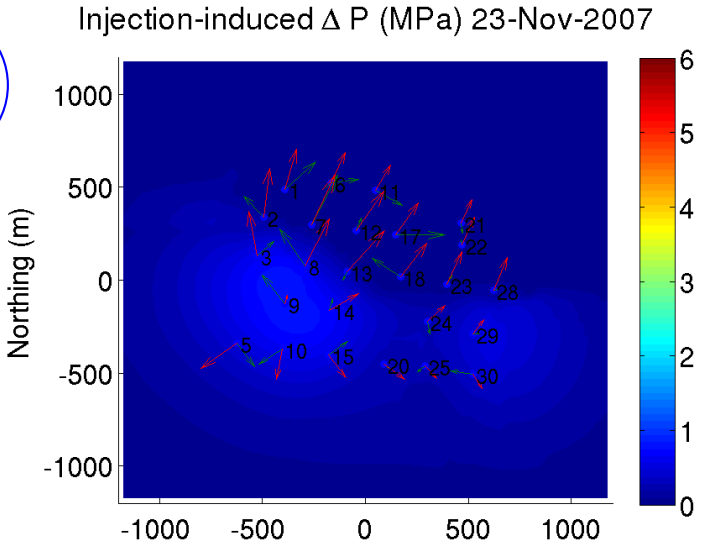

Inverted pore pressure change, $\epsilon = 10^{-3}$

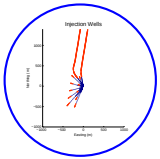

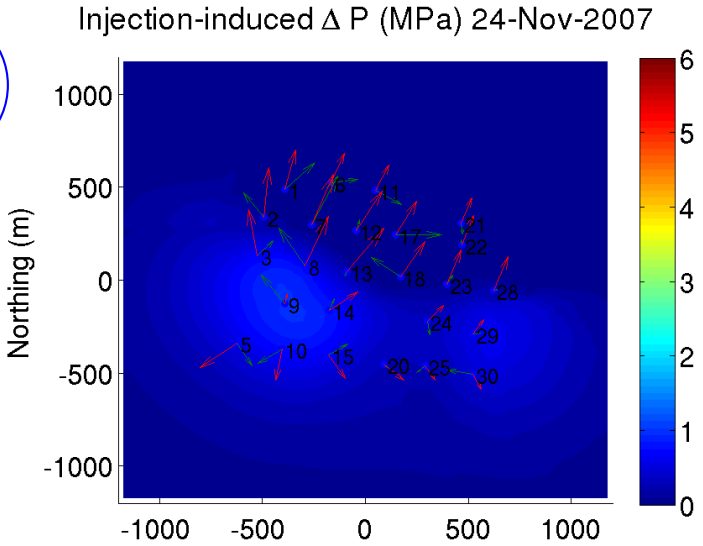

Inverted pore pressure change, $\epsilon = 10^{-3}$

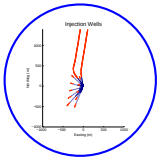

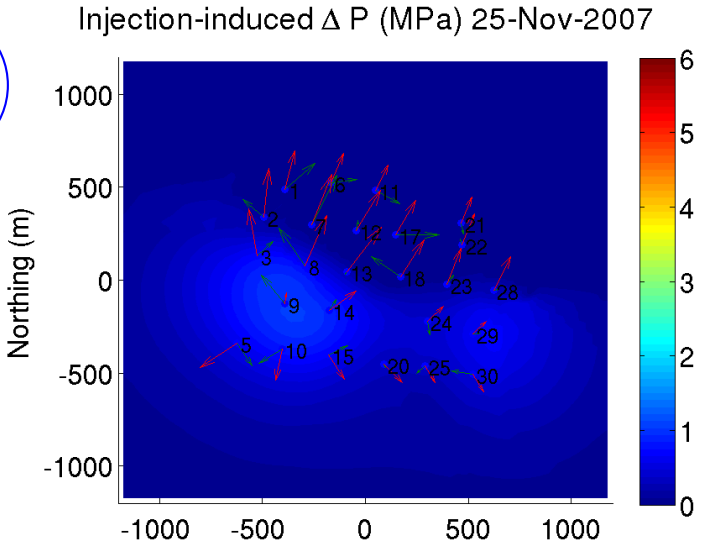

Inverted pore pressure change, $\epsilon = 10^{-3}$

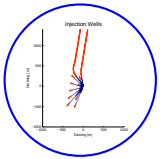

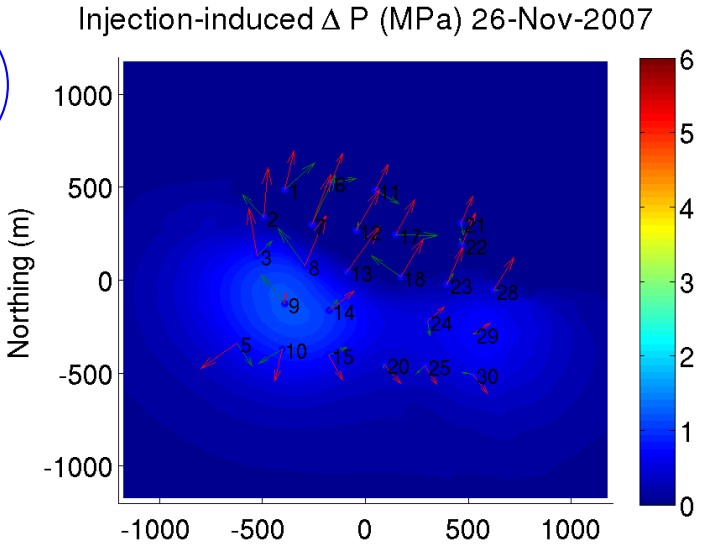

Inverted pore pressure change, $\epsilon = 10^{-3}$

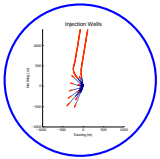

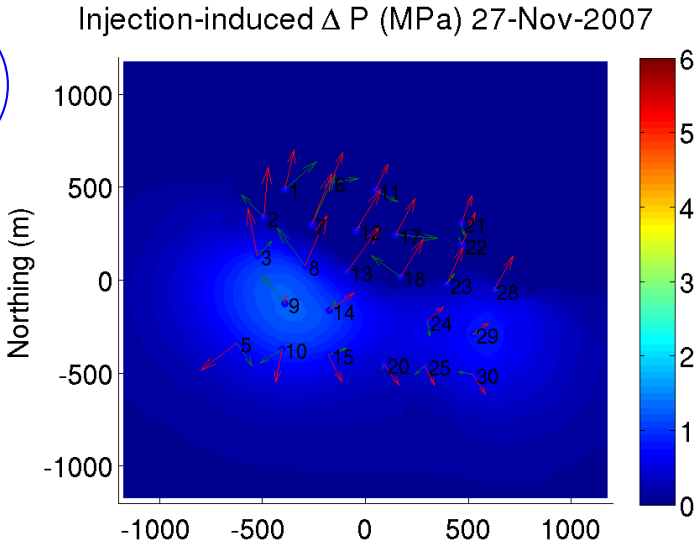

Inverted pore pressure change, $\epsilon = 10^{-3}$

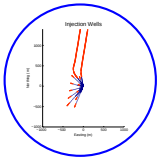

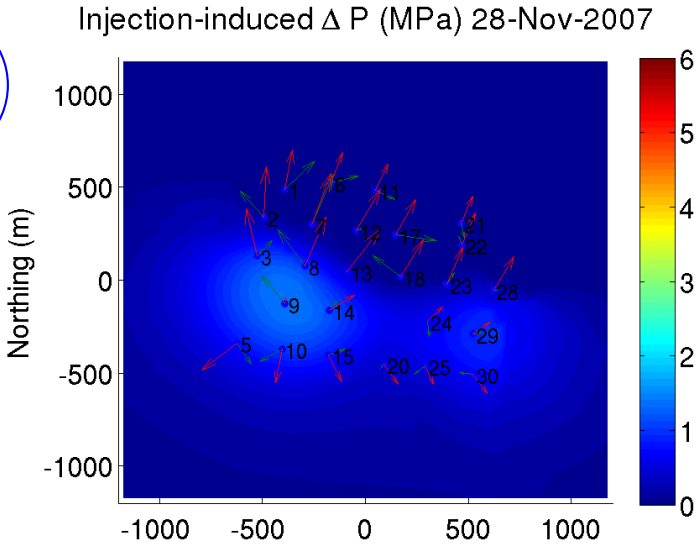

Inverted pore pressure change, $\epsilon = 10^{-3}$

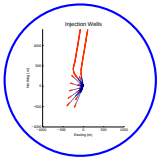

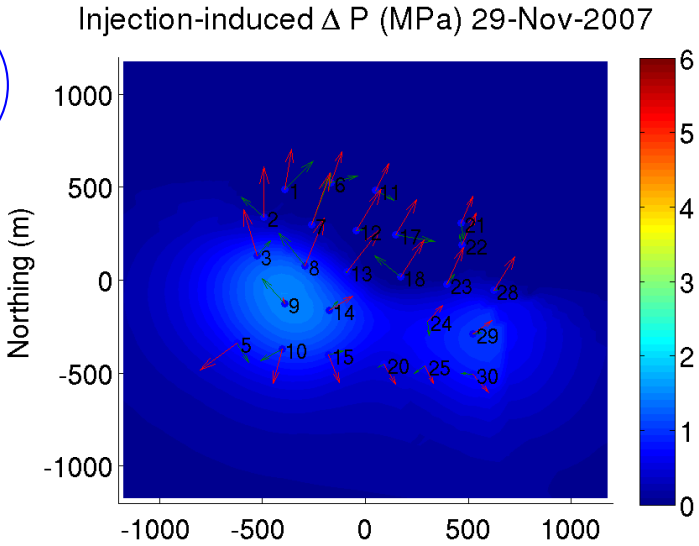

Inverted pore pressure change, $\epsilon = 10^{-3}$

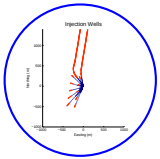

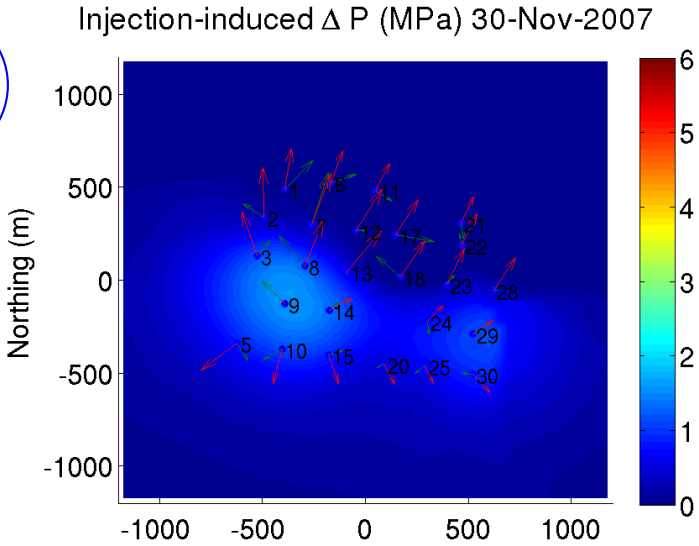

Inverted pore pressure change, $\epsilon = 10^{-3}$

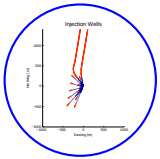

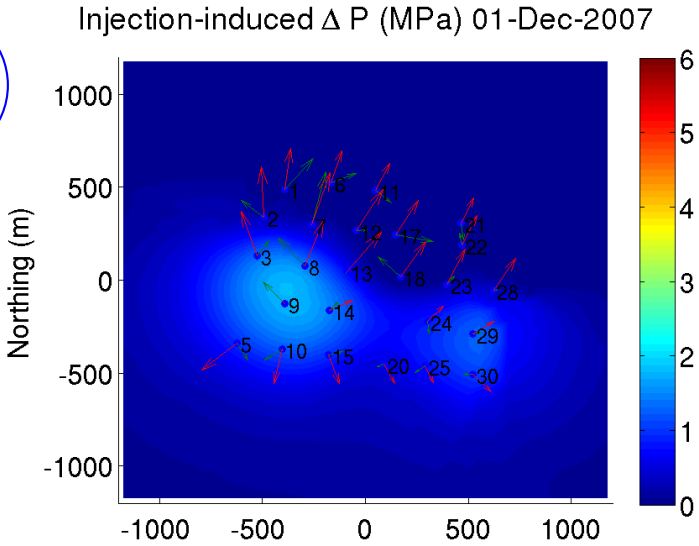

Inverted pore pressure change, $\epsilon = 10^{-3}$

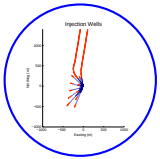

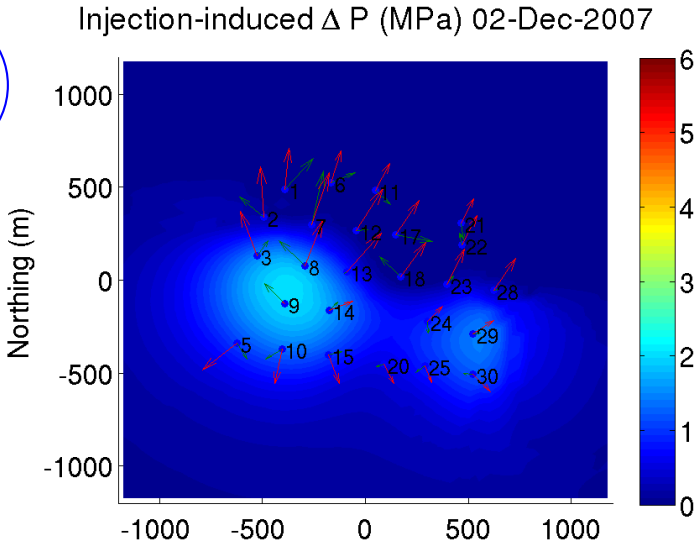

Inverted pore pressure change, $\epsilon = 10^{-3}$

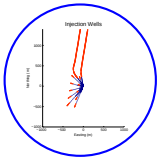

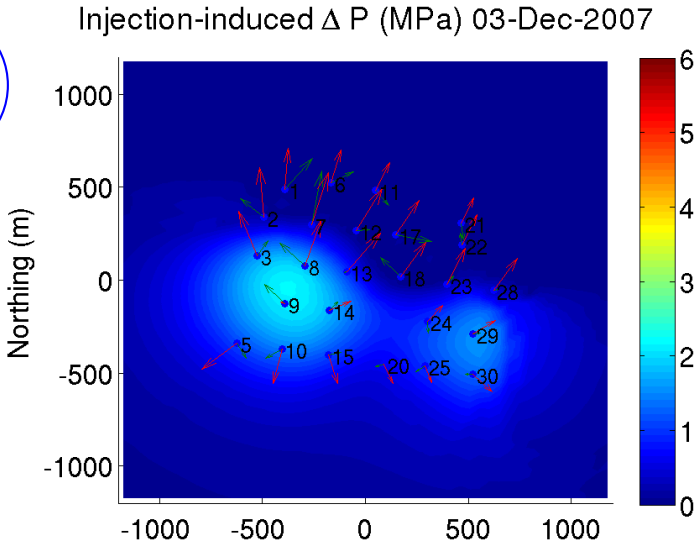

Inverted pore pressure change, $\epsilon = 10^{-3}$

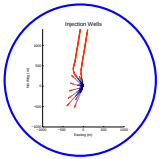

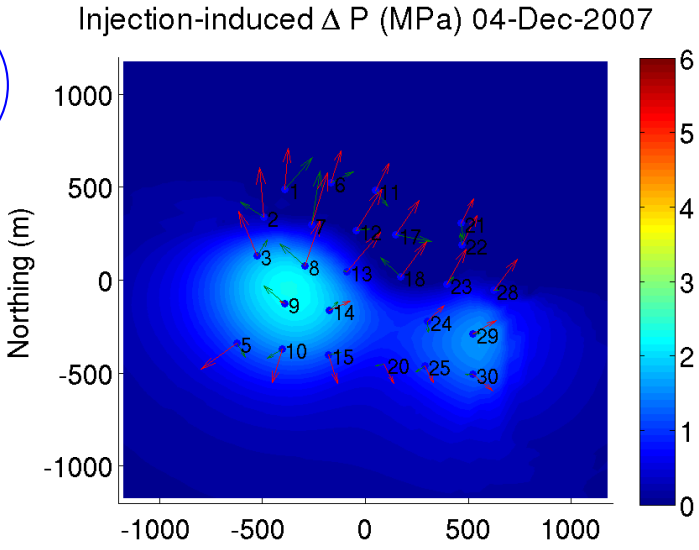

Inverted pore pressure change, $\epsilon = 10^{-3}$

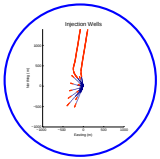

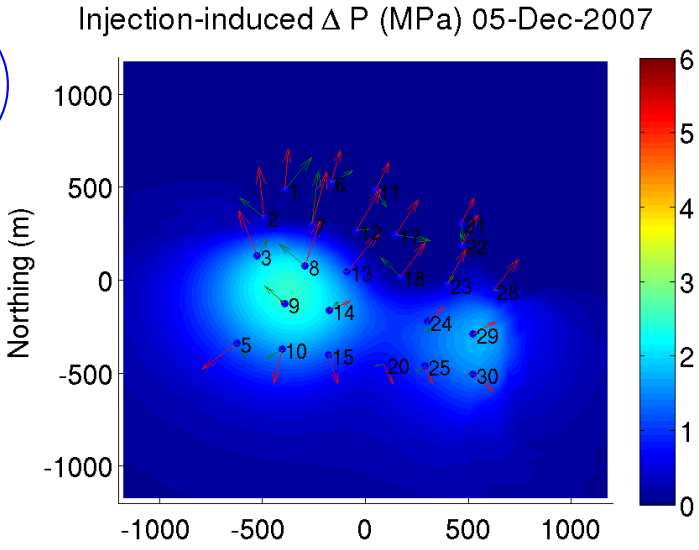

Inverted pore pressure change, $\epsilon = 10^{-3}$

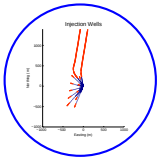

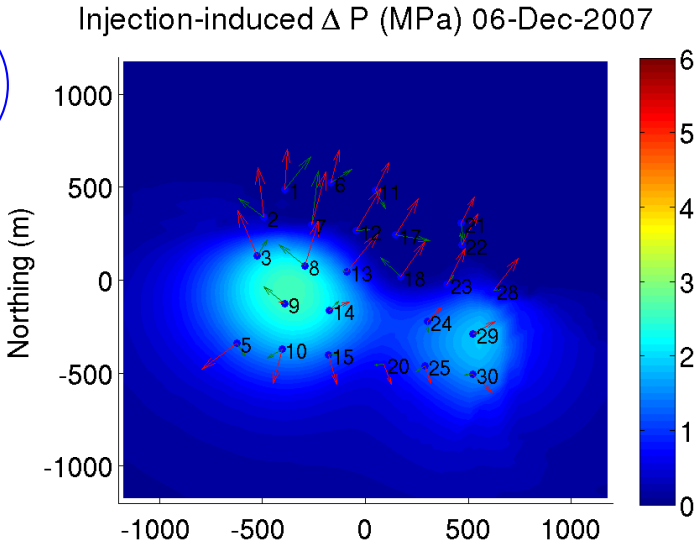

Inverted pore pressure change, $\epsilon = 10^{-3}$

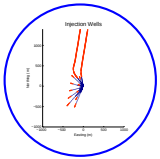

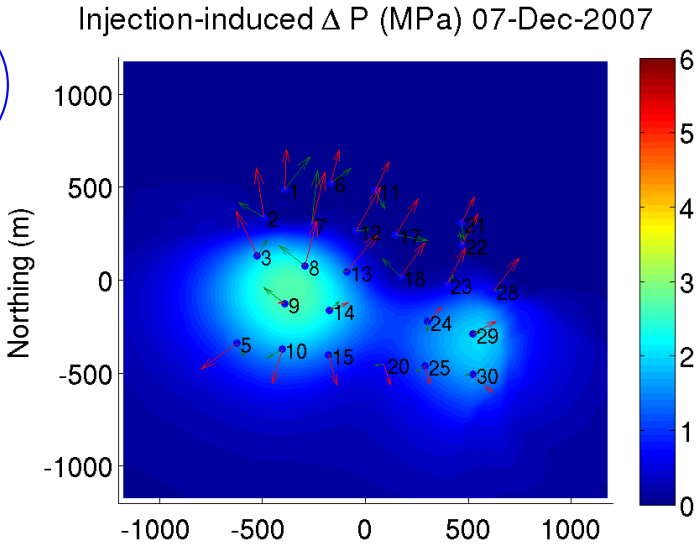

Inverted pore pressure change, $\epsilon = 10^{-3}$

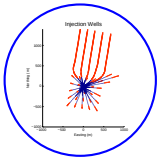

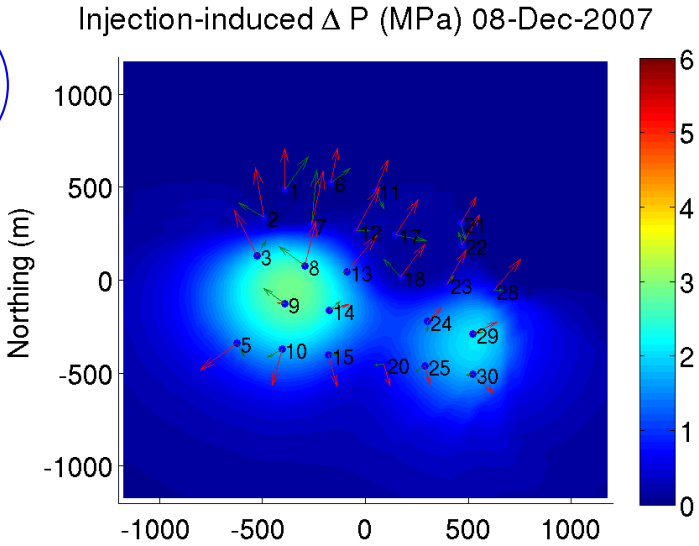

Inverted pore pressure change, $\epsilon = 10^{-3}$

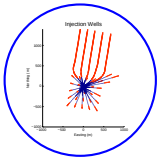

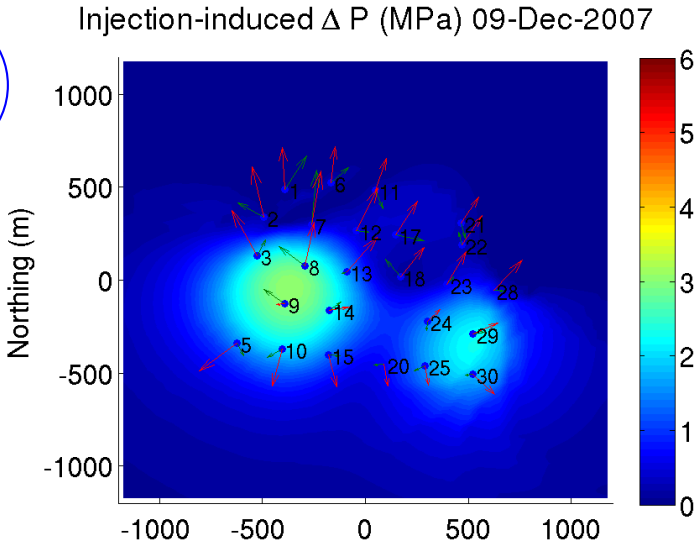

Inverted pore pressure change, $\epsilon = 10^{-3}$

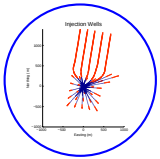

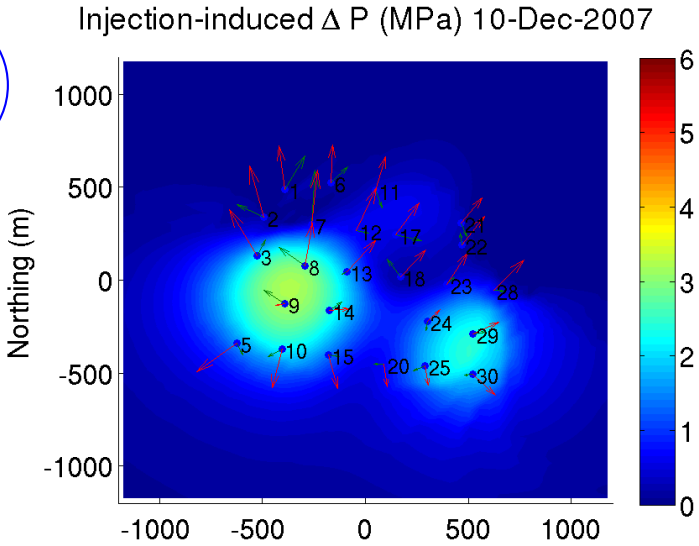

Inverted pore pressure change, $\epsilon = 10^{-3}$

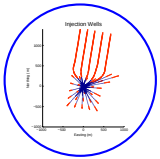

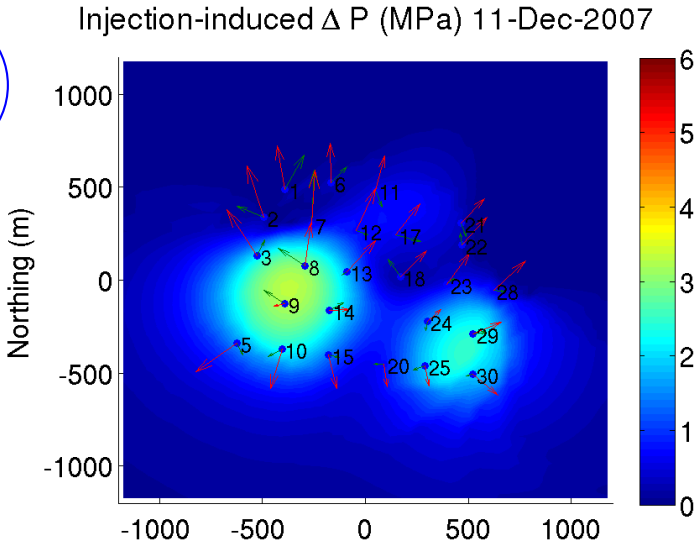

Inverted pore pressure change, $\epsilon = 10^{-3}$

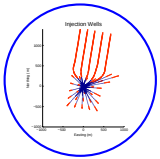

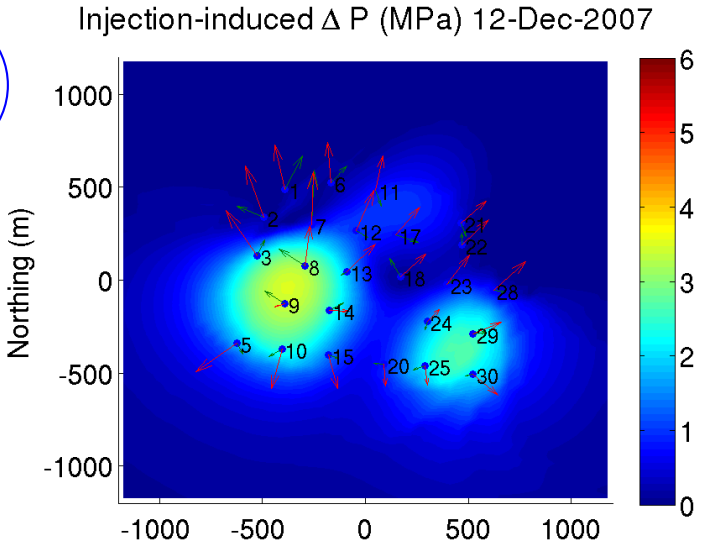

Inverted pore pressure change, $\epsilon = 10^{-3}$

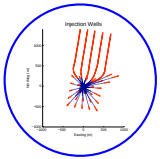

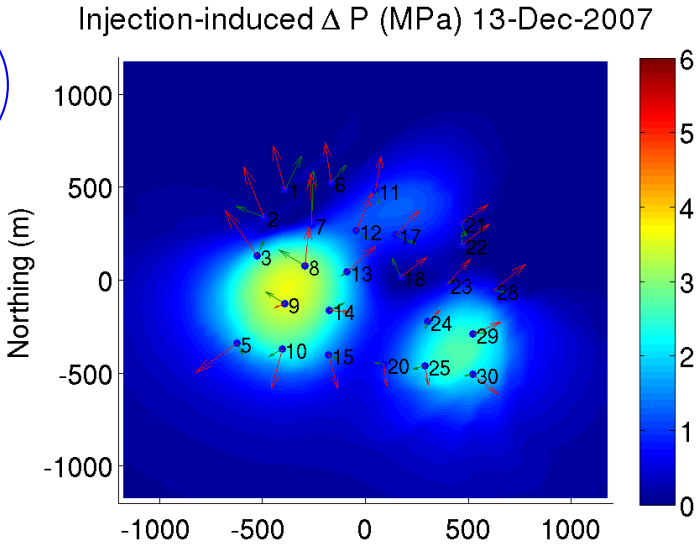

Inverted pore pressure change, $\epsilon = 10^{-3}$

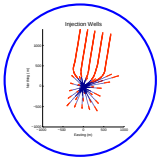

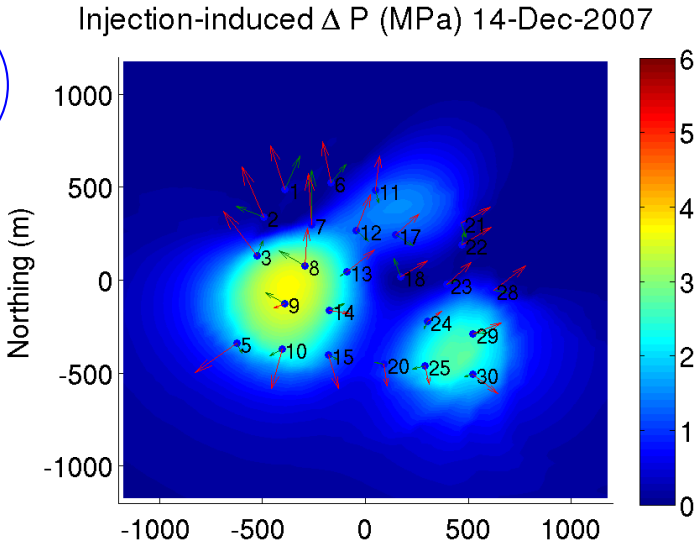

Inverted pore pressure change, $\epsilon = 10^{-3}$

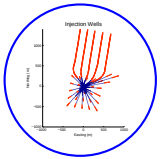

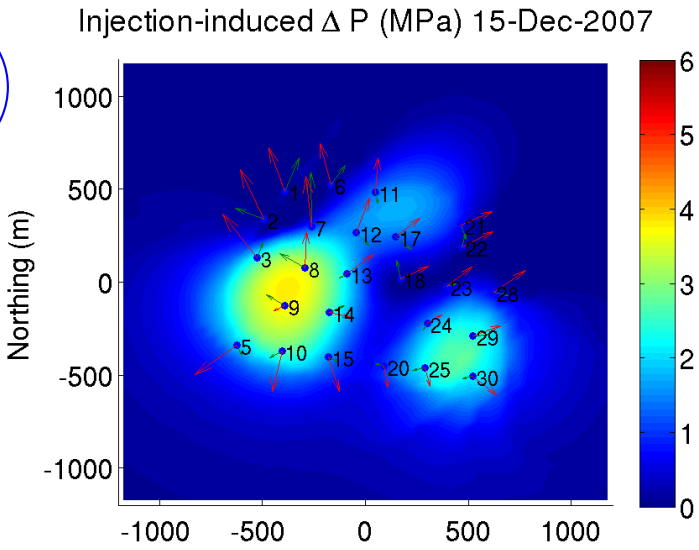

Inverted pore pressure change, $\epsilon = 10^{-3}$

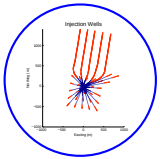

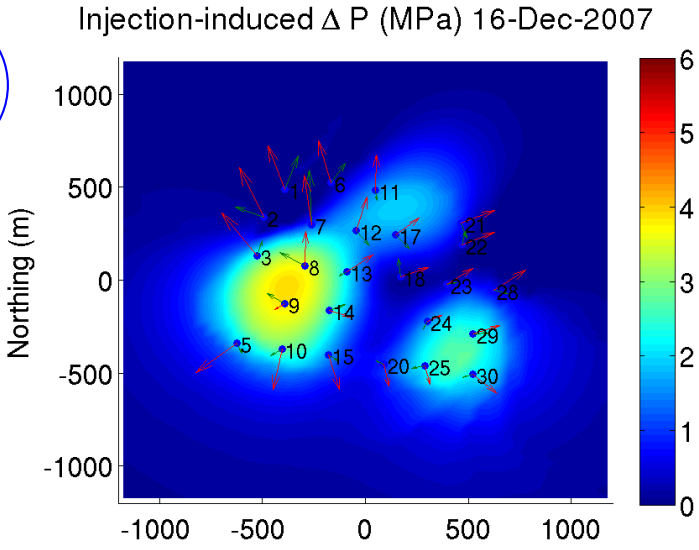

Inverted pore pressure change, $\epsilon = 10^{-3}$

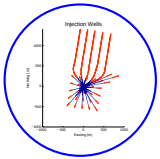

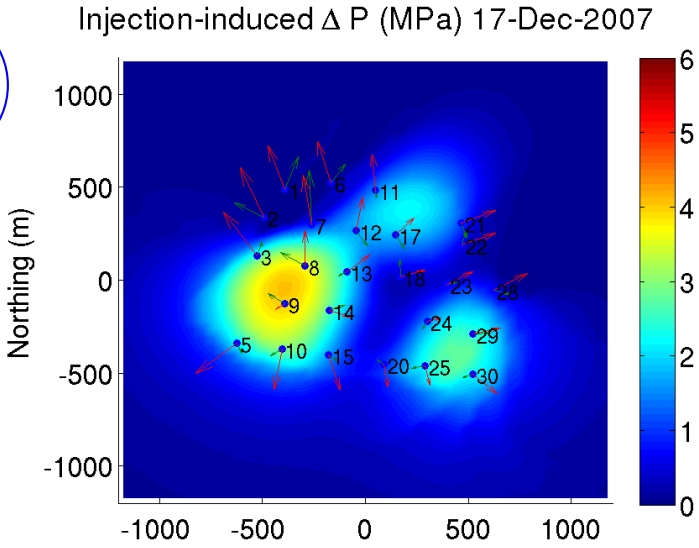

Inverted pore pressure change, $\epsilon = 10^{-3}$

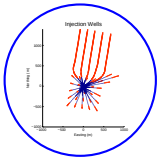

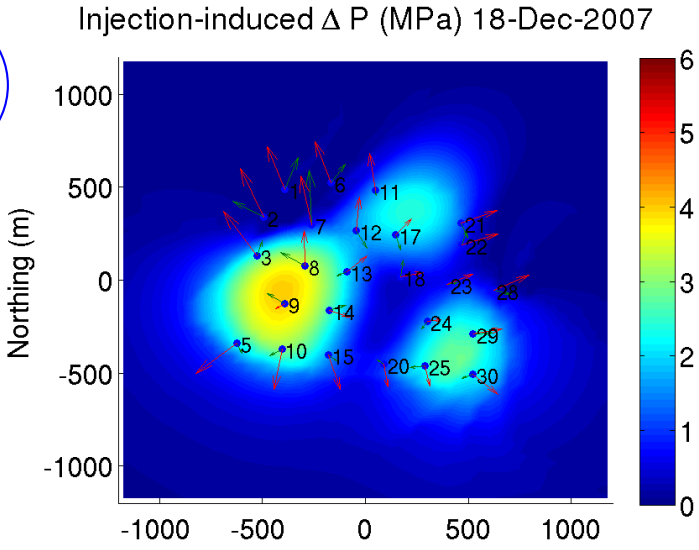

Inverted pore pressure change, $\epsilon = 10^{-3}$

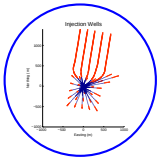

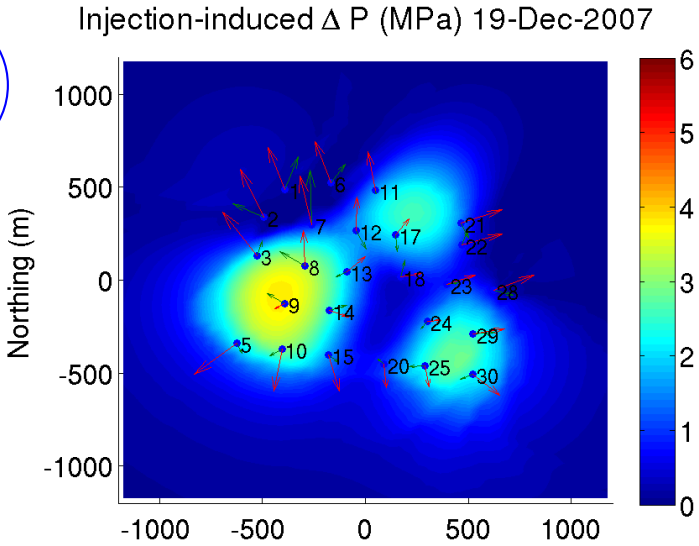

Inverted pore pressure change, $\epsilon = 10^{-3}$

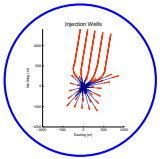

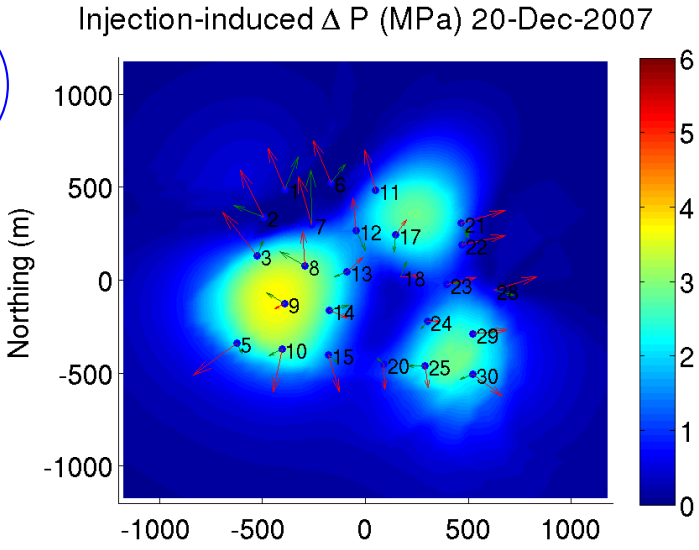

Inverted pore pressure change, $\epsilon = 10^{-3}$

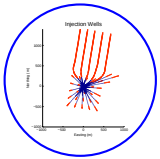

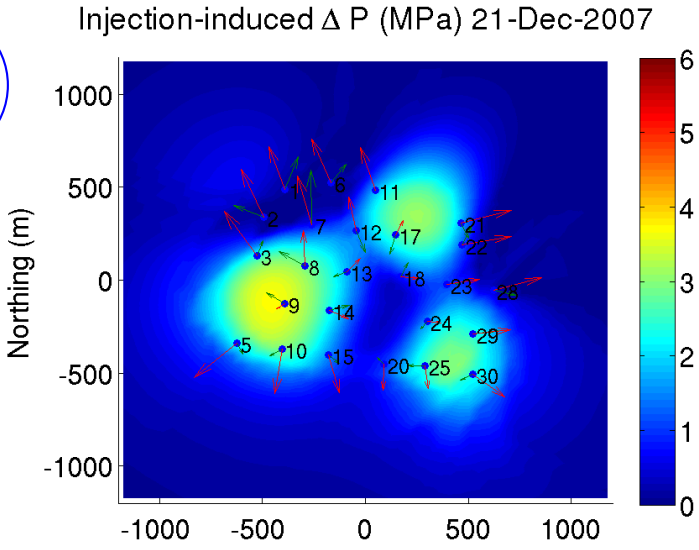

Inverted pore pressure change, $\epsilon = 10^{-3}$

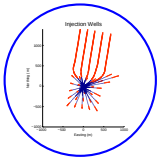

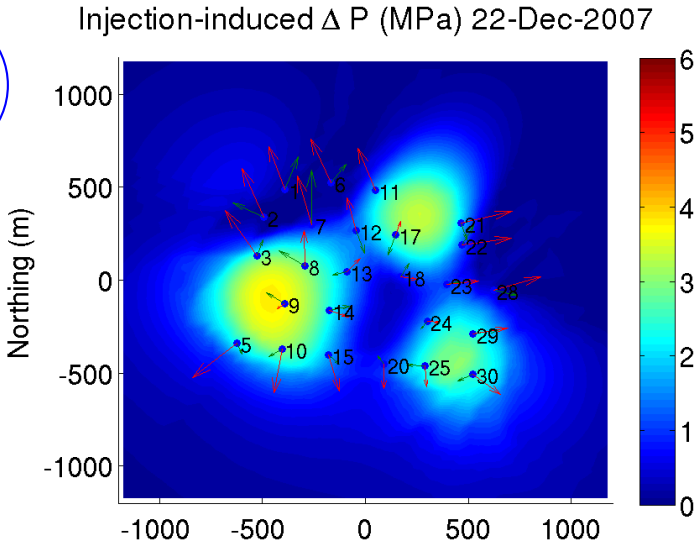

Inverted pore pressure change, $\epsilon = 10^{-3}$

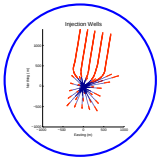

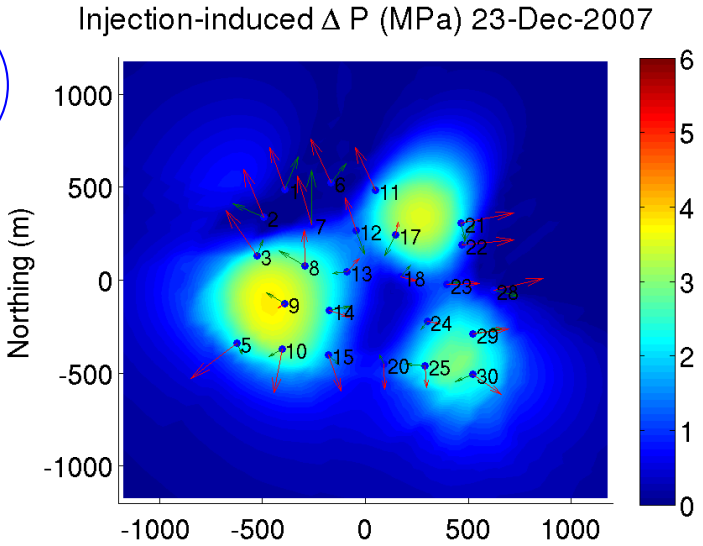

Inverted pore pressure change, $\epsilon = 10^{-3}$

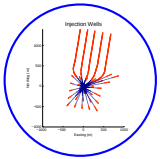

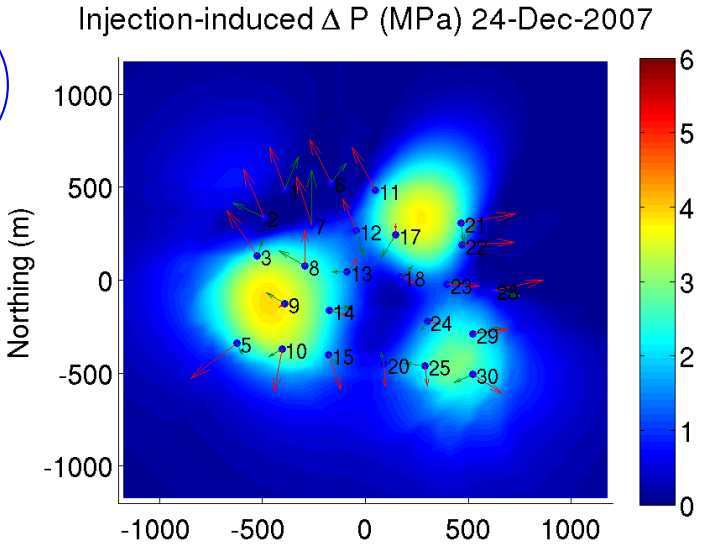

Inverted pore pressure change, $\epsilon = 10^{-3}$

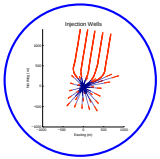

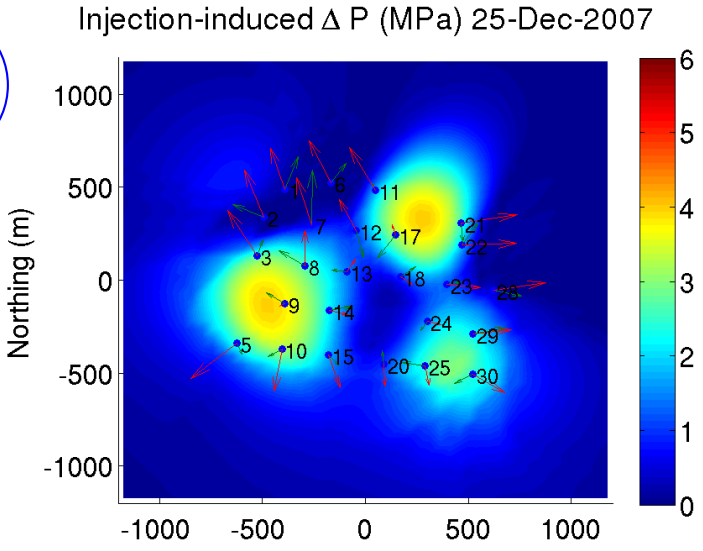

Inverted pore pressure change, $\epsilon = 10^{-3}$

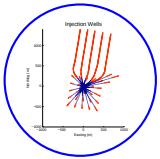

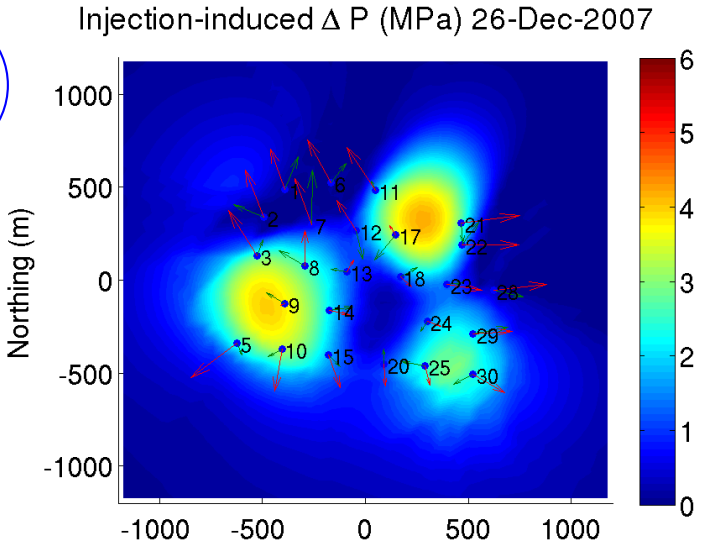

Inverted pore pressure change, $\epsilon = 10^{-3}$

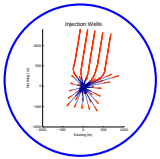

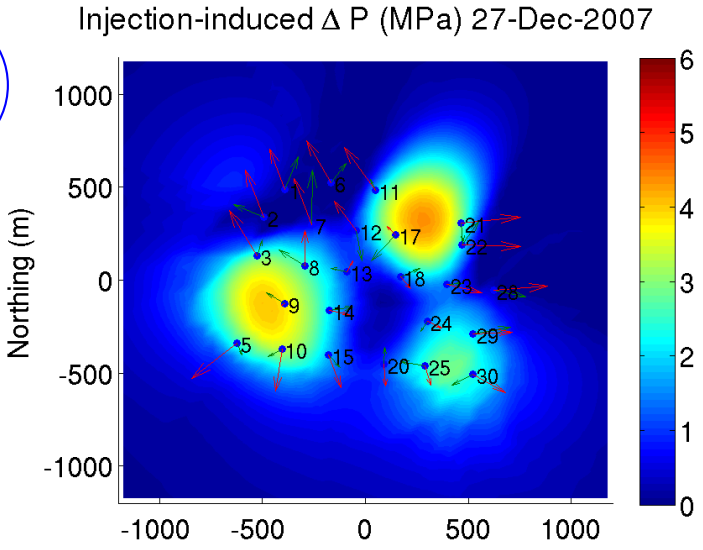

Inverted pore pressure change, $\epsilon = 10^{-3}$

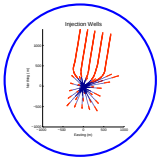

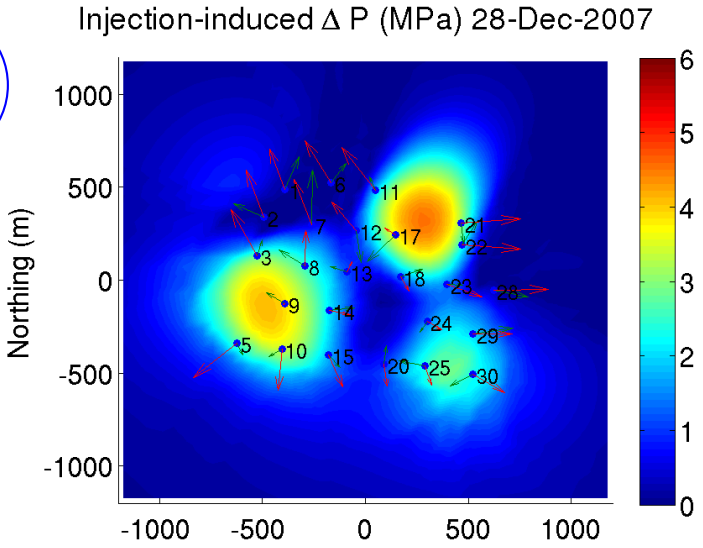

Inverted pore pressure change, $\epsilon = 10^{-3}$

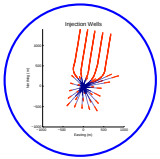

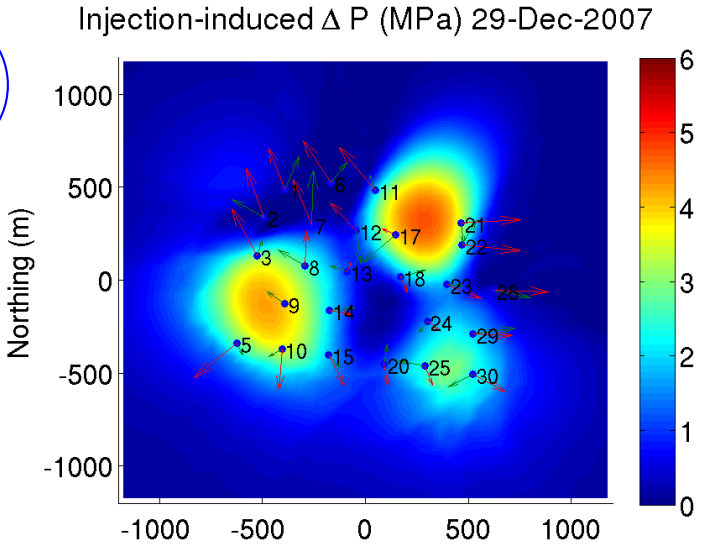

Inverted pore pressure change, $\epsilon = 10^{-3}$

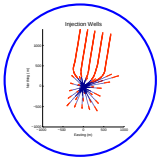

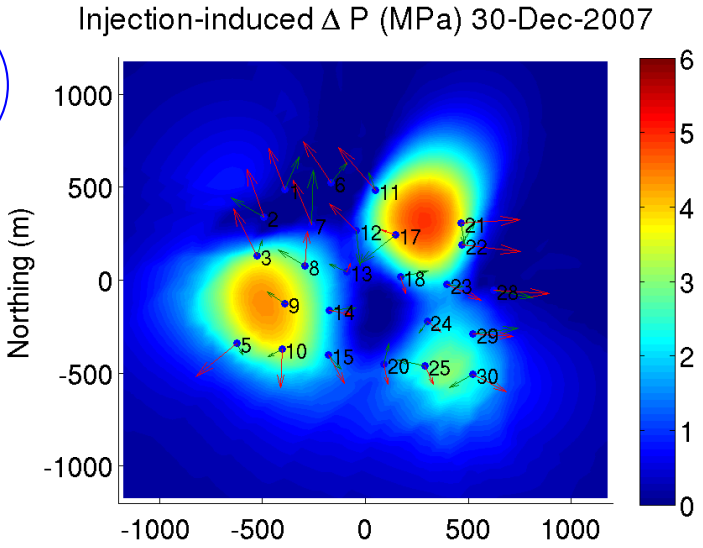

Inverted pore pressure change, $\epsilon = 10^{-3}$

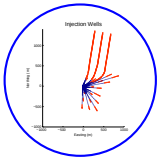

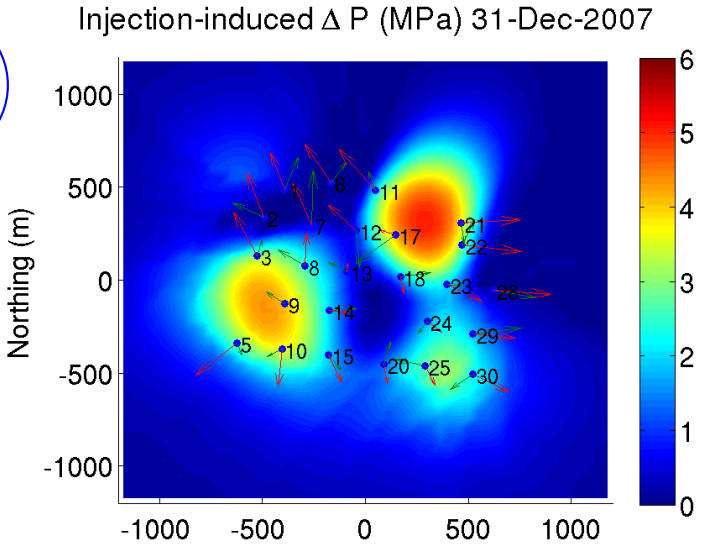

Inverted pore pressure change, $\epsilon = 10^{-3}$

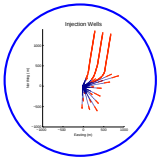

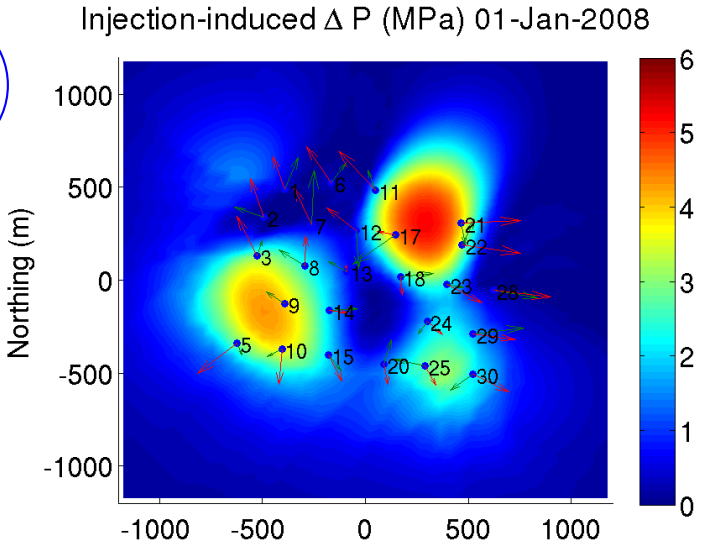

Inverted pore pressure change, $\epsilon = 10^{-3}$

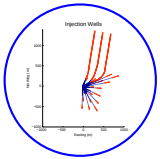

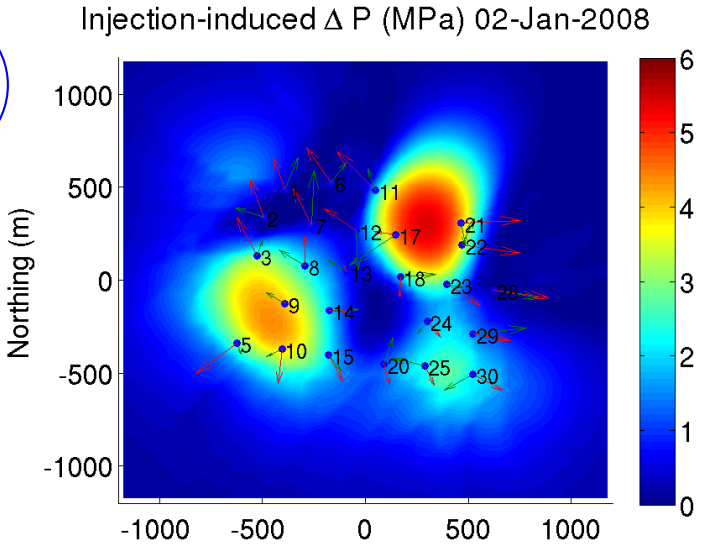

Inverted pore pressure change, $\epsilon = 10^{-3}$

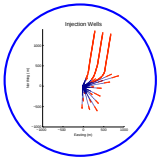

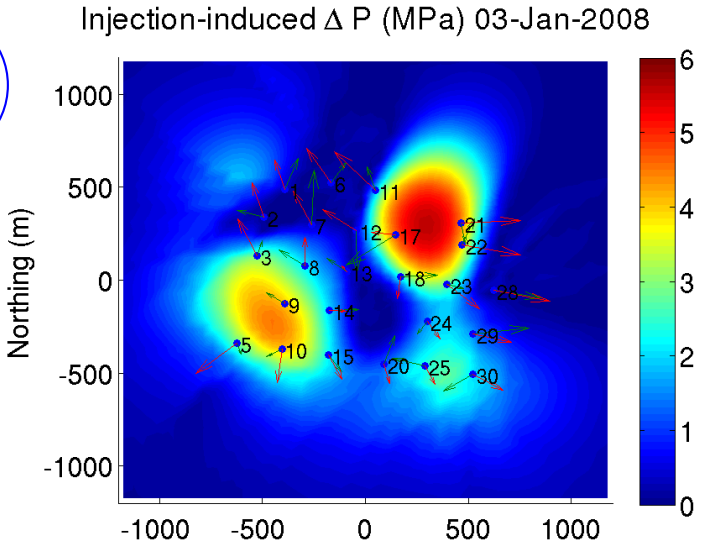

Inverted pore pressure change, $\epsilon = 10^{-3}$

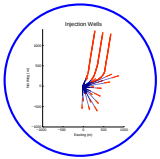

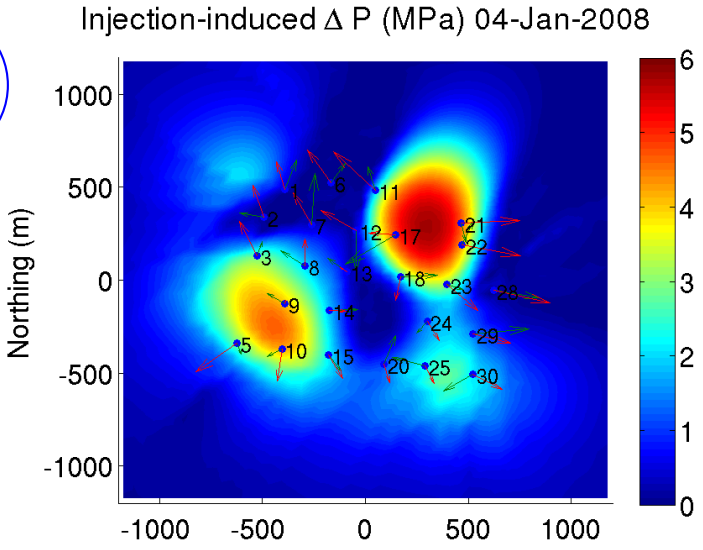

Inverted pore pressure change, $\epsilon = 10^{-3}$

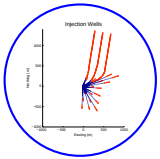

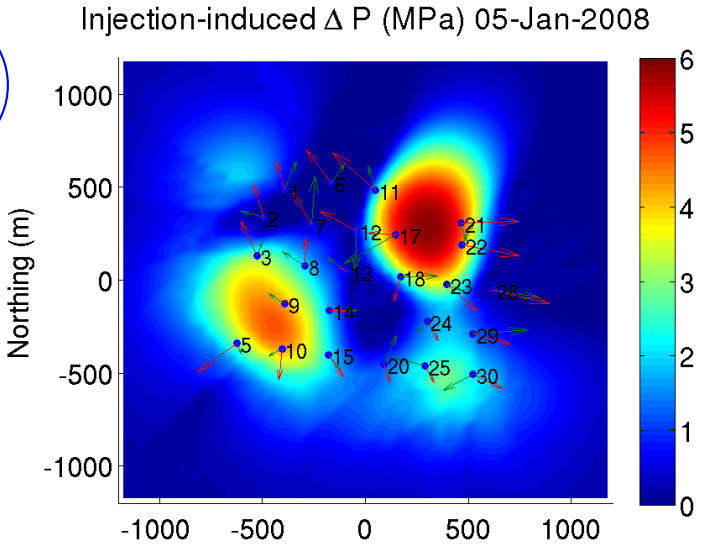

Inverted pore pressure change, $\epsilon = 10^{-3}$

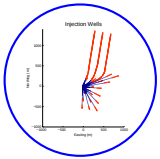

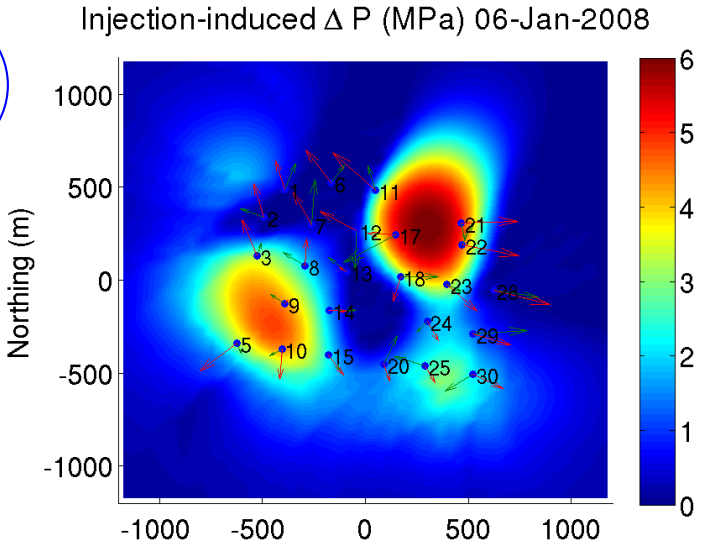

Inverted pore pressure change, $\epsilon = 10^{-3}$

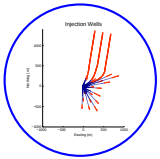

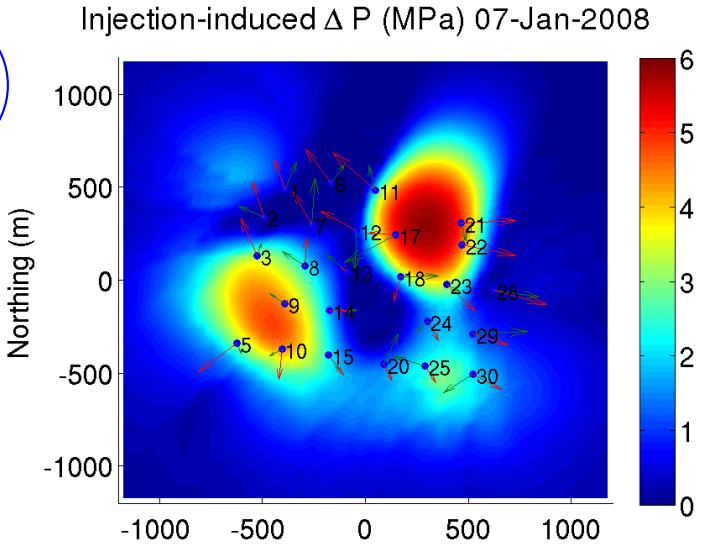

Inverted pore pressure change, $\epsilon = 10^{-3}$

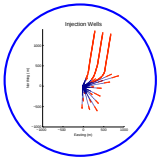

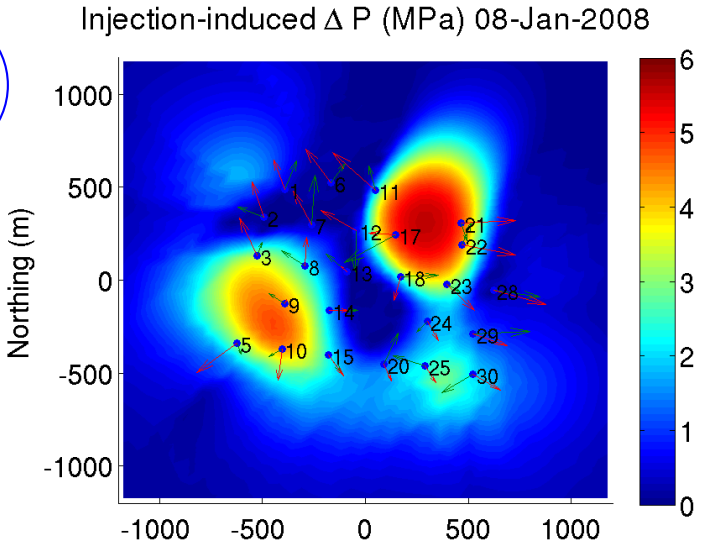

Inverted pore pressure change, $\epsilon = 10^{-3}$

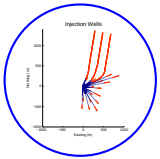

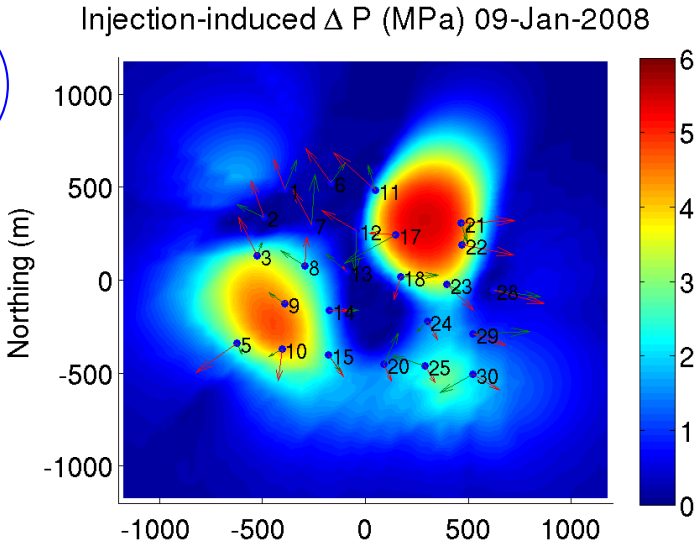

Inverted pore pressure change, $\epsilon = 10^{-3}$

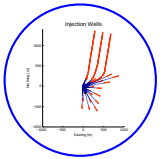

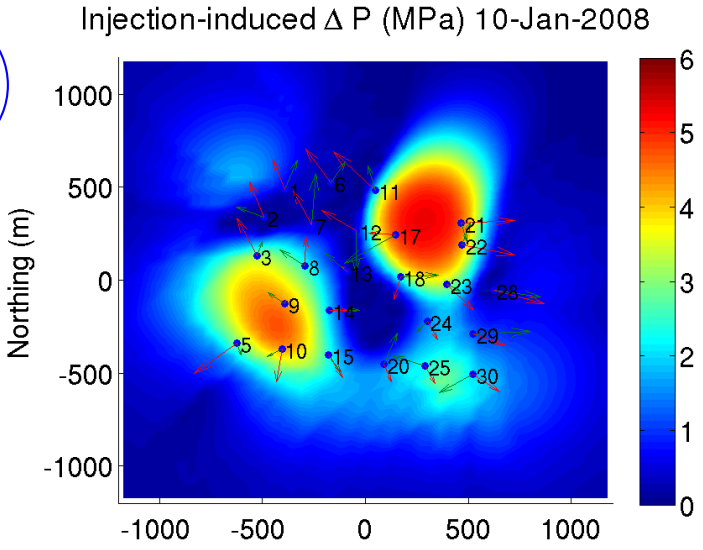

Inverted pore pressure change, $\epsilon = 10^{-3}$

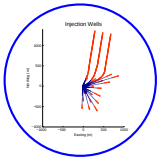

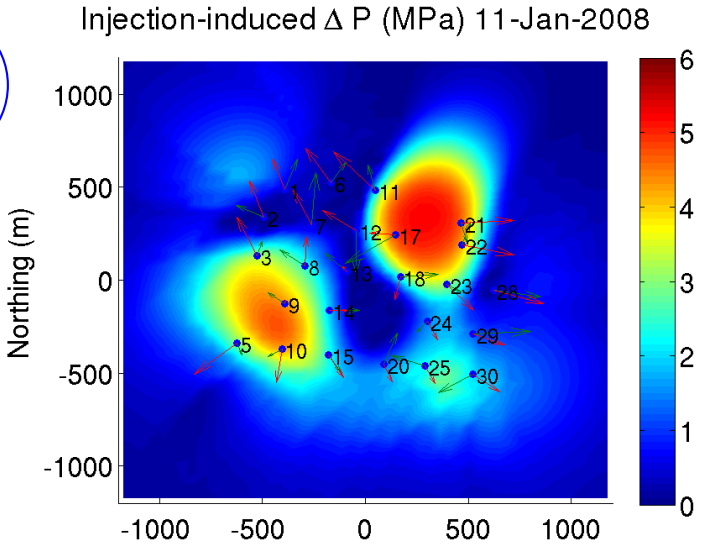

Inverted pore pressure change, $\epsilon = 10^{-3}$

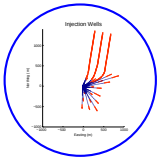

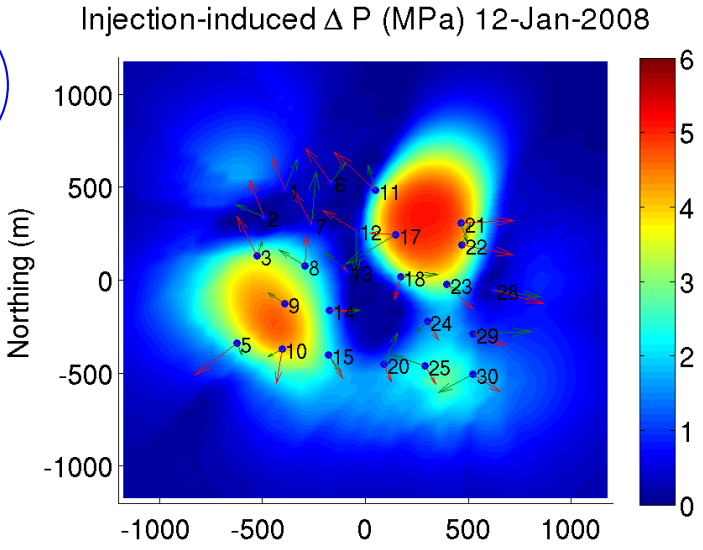

Inverted pore pressure change, $\epsilon = 10^{-3}$

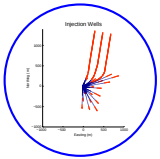

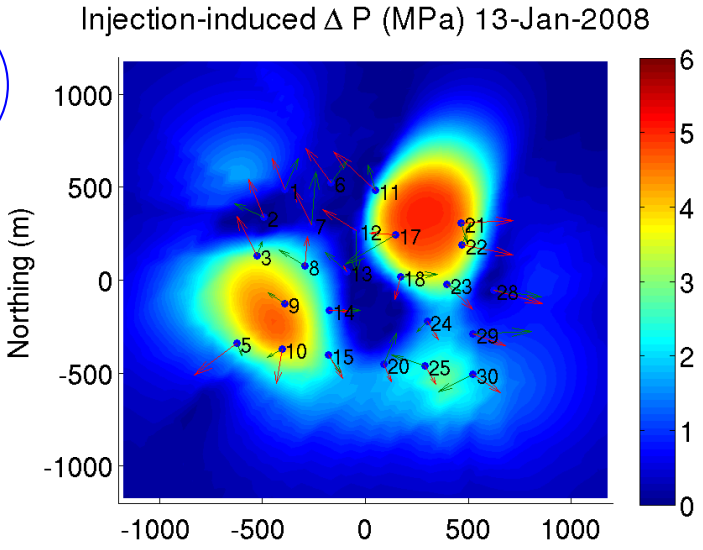

Stability with respect to regularization, $\epsilon = 10^{-3}$

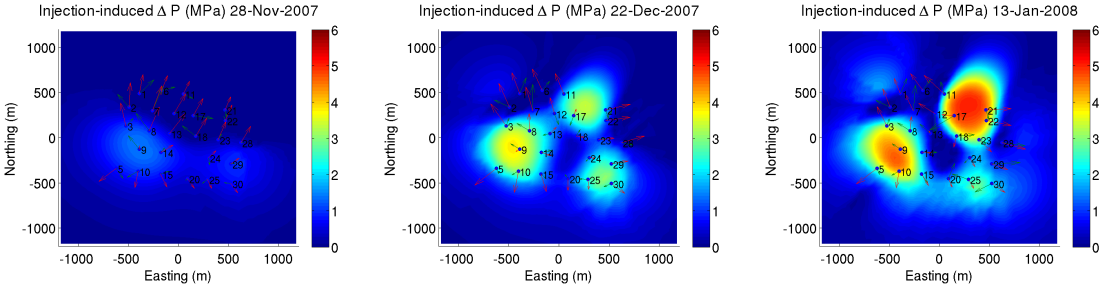

Stability with respect to regularization, $\epsilon = 5 \times 10^{-3}$

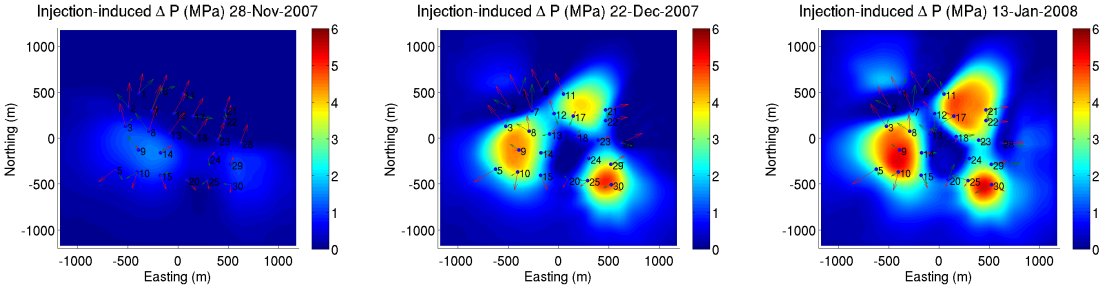

Stability with respect to regularization, $\epsilon = 10^{-2}$

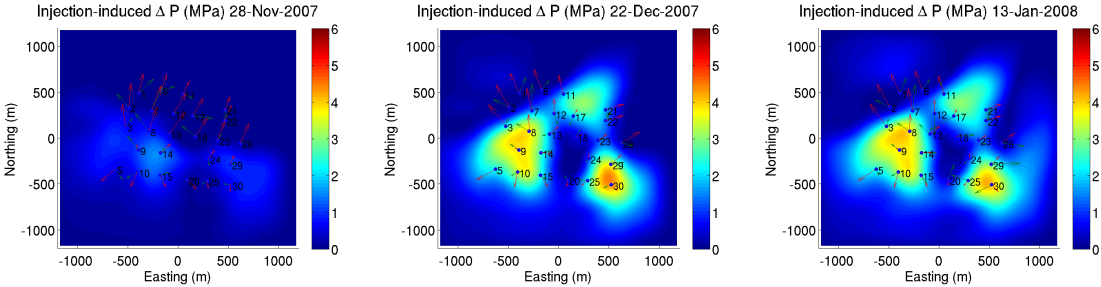

Resolving sharp pressure contrasts

(methodology and a synthetic example)

Achieve better resolution of subsurface heterogeneities (e.g, **permeability barriers**) by using edge-preserving total-variation regularization:

$$\|\mathbf{A}p - \mathbf{u}\|_{L_2}^2 + \boxed{\epsilon \||\nabla \mathbf{p}|\|_{L_1}} \rightarrow \min, \qquad p_1 \leq p \leq p_2. \tag{BOUNDTVREG}$$

Achieve better resolution of subsurface heterogeneities (e.g, **permeability barriers**) by using edge-preserving total-variation regularization:

$$\|\mathbf{A}p - \mathbf{u}\|_{L_2}^2 + \epsilon \||\nabla \mathbf{p}|\|_{L_1} \rightarrow \min, \quad p_1 \leq p \leq p_2. \qquad \text{(BOUNDTVREG)}$$

Resolving sharp pressure contrasts

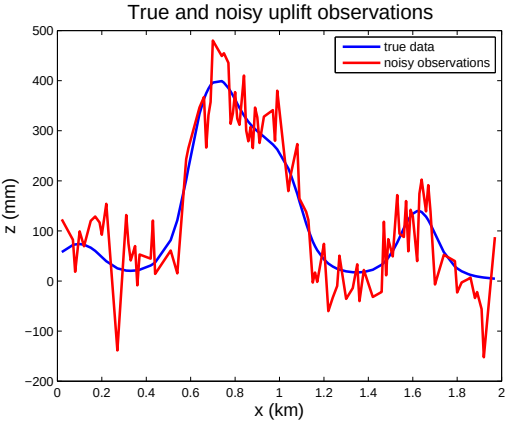

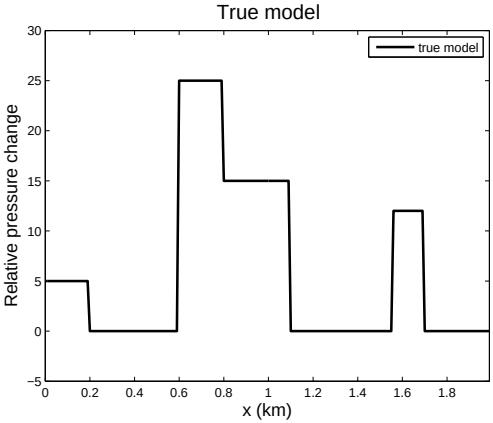

Naive constrained inversion—false contrasts

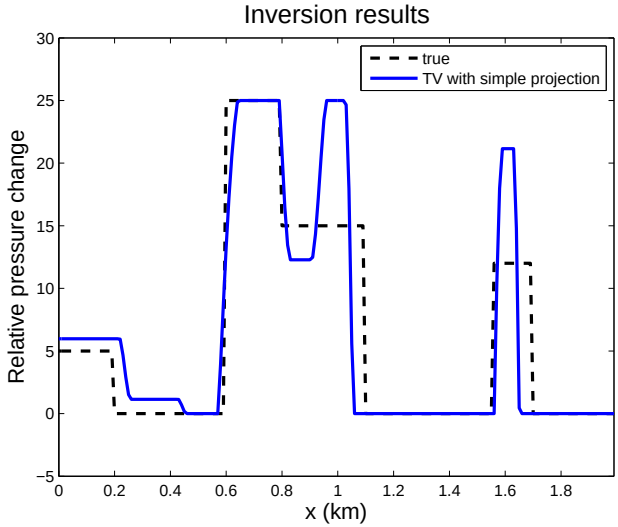

Unconstrained inversion—false contrasts and violated bounds

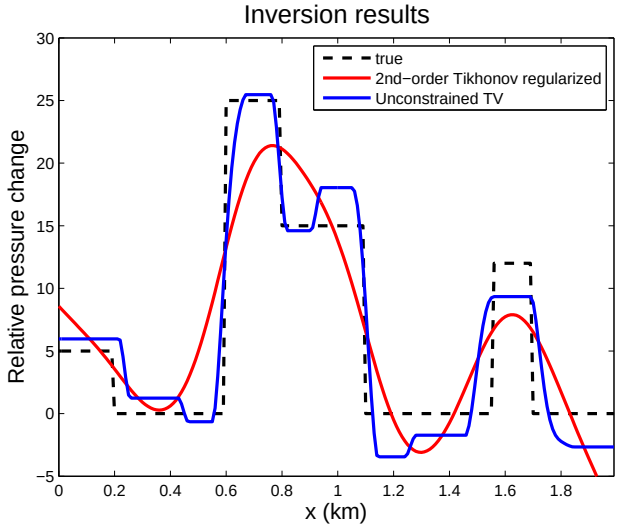

New constrained inversion

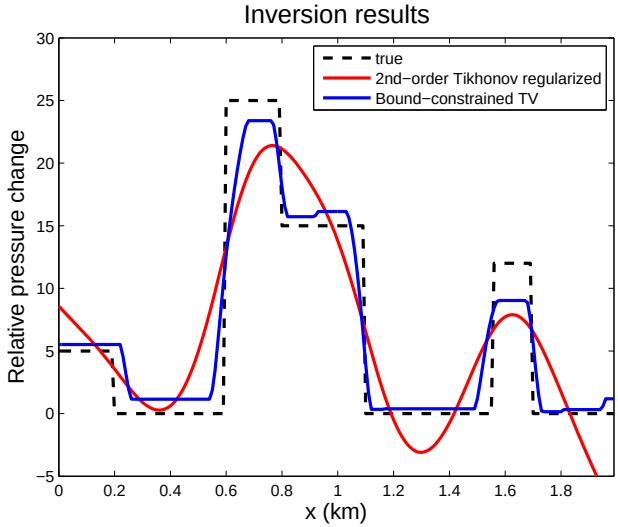

Motivation: characterization of reservoir heterogeneity

- Fluid injection is a key tool in EOR, waste water disposal, carbon sequestration, and hydraulic fracturing.
- Effective injection strategies requires understanding pressure front propagation and reservoir heterogeneity.
- Goal: design a robust computational framework for estimating **permeability and flow contrasts** from measurable surface deformation.

Water injection into a formation with a low permeability barrier

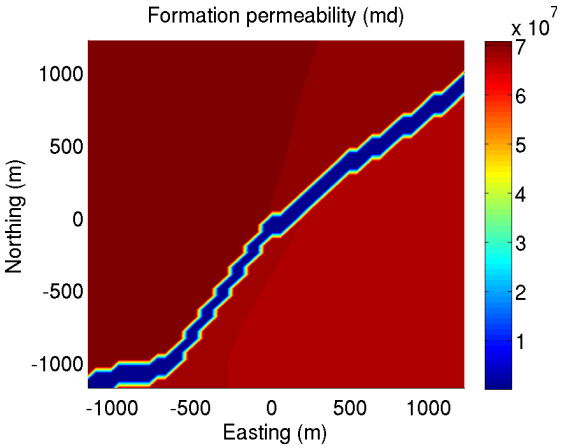

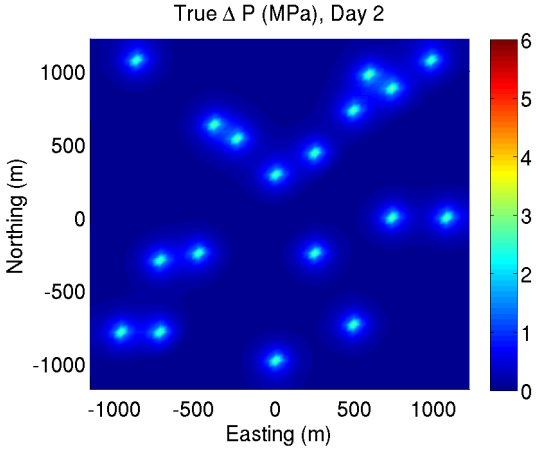

Relate deformation and pore pressure change using Biot's theory (Rice and Cleary, 1976; Segall, 1985; Segall, 2010):

$$\mu\nabla^2 u_i + \frac{\mu}{1-2\nu}\frac{\partial^2 u_j}{\partial x_i \partial x_j} = \boxed{\alpha\frac{\partial p}{\partial x_i}} - f_i = 0,\ i = 1,2,3, \qquad \text{(ELAST)}$$

and

$$S_\alpha \frac{\partial p}{\partial t} - \frac{\kappa}{\eta}\nabla^2 p = -\alpha\frac{\partial}{\partial t}\left(\nabla\cdot\mathbf{u}\right), \qquad \text{(FLOW)}$$

where $\mathbf{u}$ is displacement, p is the pore pressure change, f_i is a differential body-force distribution, μ,ν,α,κ, and η are the shear modulus, Poisson's ratio, Biot coefficient, permeability, and fluid viscosity;

$$S_\alpha = \frac{3\alpha(1-2\nu)(1-\alpha B)}{2\mu B(1+\nu)}, \qquad \text{(STORAGE)}$$

where B is Skempton's coefficient.

Relate deformation and pore pressure change using Biot's theory (Rice and Cleary, 1976; Segall, 1985; Segall, 2010):

$$\mu\nabla^2 u_i + \frac{\mu}{1-2\nu}\frac{\partial^2 u_j}{\partial x_i \partial x_j} = \boxed{\alpha\frac{\partial p}{\partial x_i}} - f_i = 0,\ i = 1,2,3, \qquad \text{(ELAST)}$$

and

$$S_\alpha \frac{\partial p}{\partial t} - \frac{\kappa}{\eta}\nabla^2 p = -\alpha\frac{\partial}{\partial t}\left(\nabla\cdot\mathbf{u}\right), \qquad \text{(FLOW)}$$

where $\mathbf{u}$ is displacement, p is the pore pressure change, f_i is a differential body-force distribution, μ,ν,α,κ, and η are the shear modulus, Poisson's ratio, Biot coefficient, permeability, and fluid viscosity;

$$S_\alpha = \frac{3\alpha(1-2\nu)(1-\alpha B)}{2\mu B(1+\nu)}, \qquad \text{(STORAGE)}$$

where B is Skempton's coefficient.

- Regard (ELAST) as a deformation modeling operator $\mathbf{A}p = \mathbf{u}$ and **decouple** it from the flow equation (FLOW) (Vasco et al., 2000; Du and Olson, 2001; Hodgson, 2007).

- Solve the regularized constrained optimization problem

$$\begin{aligned} &\|\mathbf{A}p - \mathbf{u}\|^2_{L_2} \; + \; \epsilon\|\Delta p\|^2_{L_2} \; \rightarrow \; \min, \\ &0 \; \leq \; p \; \leq \; p_{\max}. \end{aligned} \tag{LS}$$

Achieve better resolution of subsurface heterogeneities (e.g, **permeability barriers**) by using edge-preserving total-variation regularization:

$$\|\mathbf{A}p - \mathbf{u}\|_{L_2}^2 \; + \; \boxed{\epsilon \||\nabla \mathbf{p}|\|_{L_1}} \; \rightarrow \; \min, \qquad 0 \; \leq \; p \; \leq \; p_{\max}. \tag{TV}$$

Achieve better resolution of subsurface heterogeneities (e.g, **permeability barriers**) by using edge-preserving total-variation regularization:

$$\begin{aligned} &\|\mathbf{A}p-\mathbf{u}\|_{L_2}^2 \;+\; \boxed{\epsilon\||\nabla \mathbf{p}|\|_{L_1}} \;\rightarrow\; \min, \\ &0 \;\leq\; p \;\leq\; p_{\max}. \end{aligned} \tag{TV}$$

True pressure, noisy surface uplift measurements

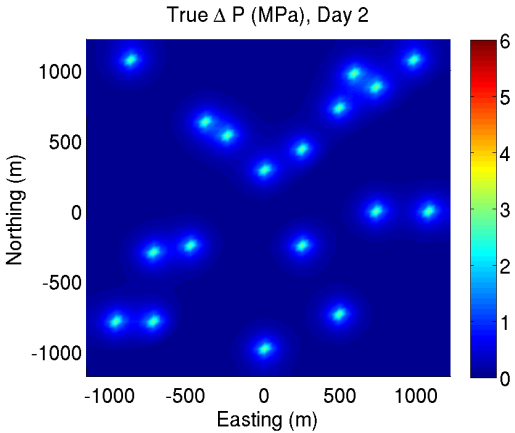

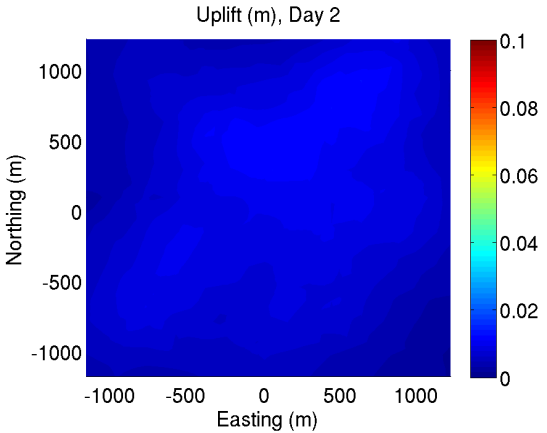

True pressure, noisy surface uplift measurements

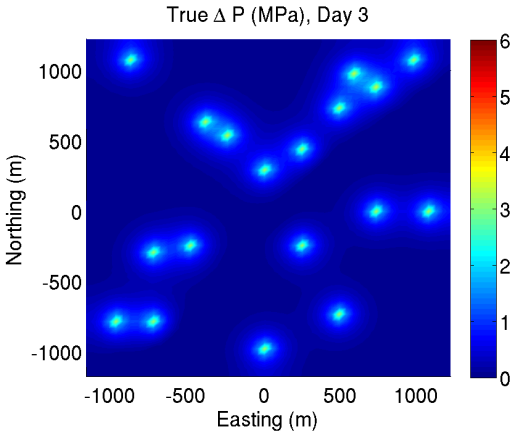

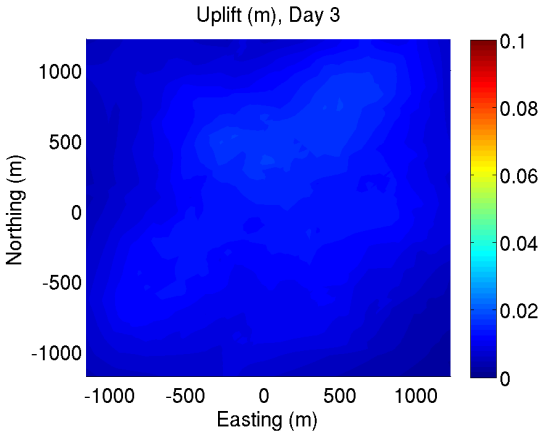

True pressure, noisy surface uplift measurements

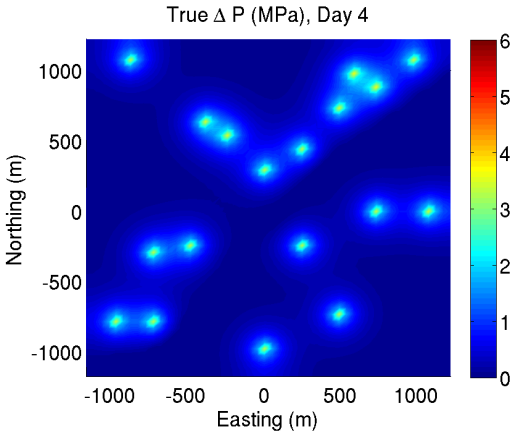

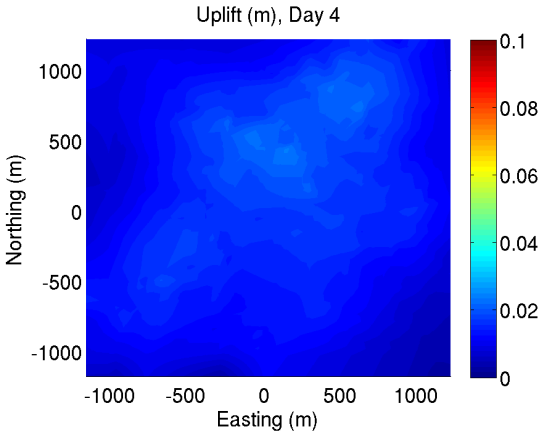

True pressure, noisy surface uplift measurements

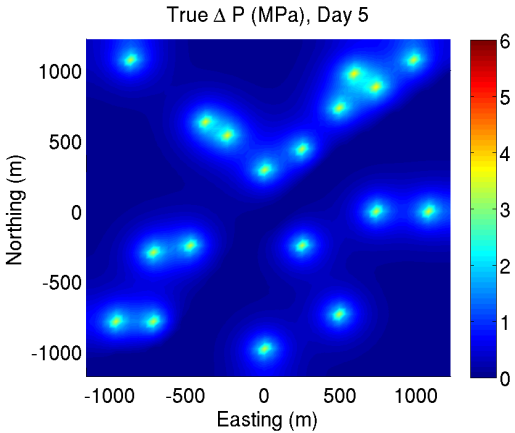

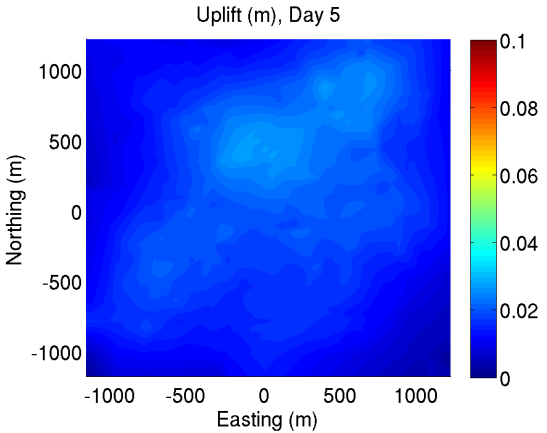

True pressure, noisy surface uplift measurements

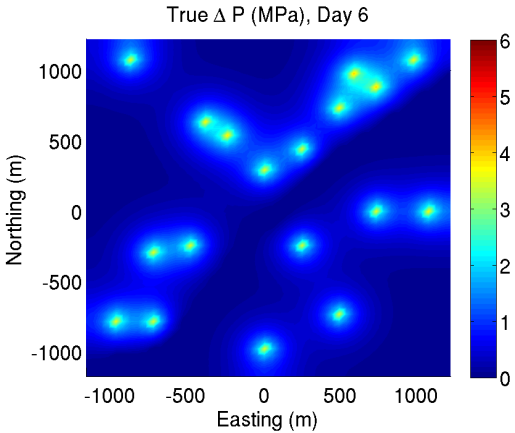

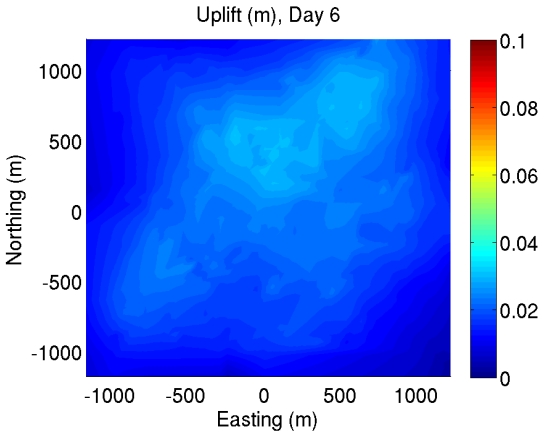

True pressure, noisy surface uplift measurements

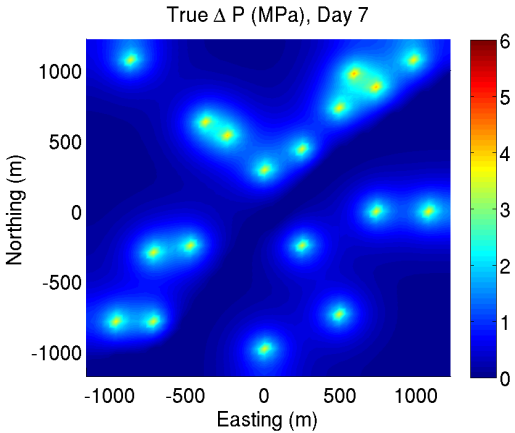

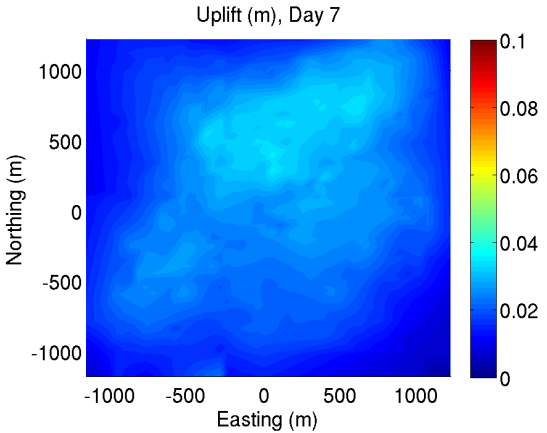

True pressure, noisy surface uplift measurements

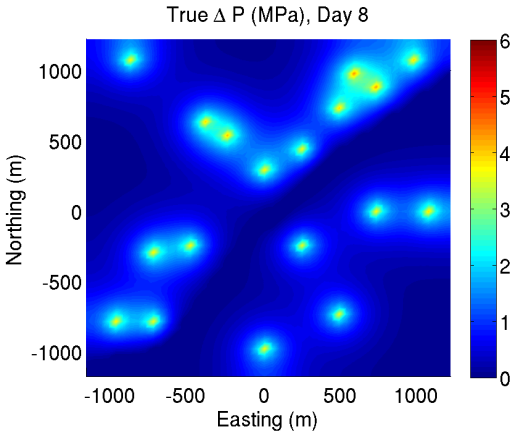

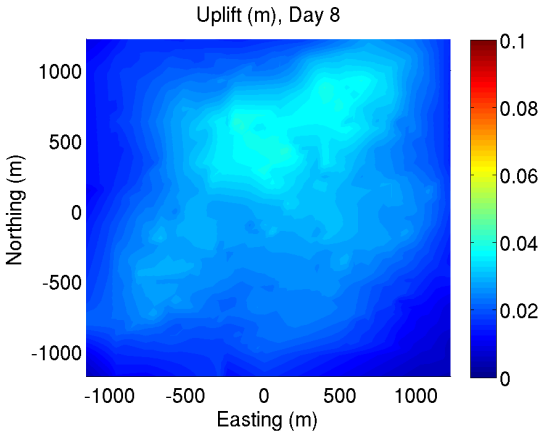

True pressure, noisy surface uplift measurements

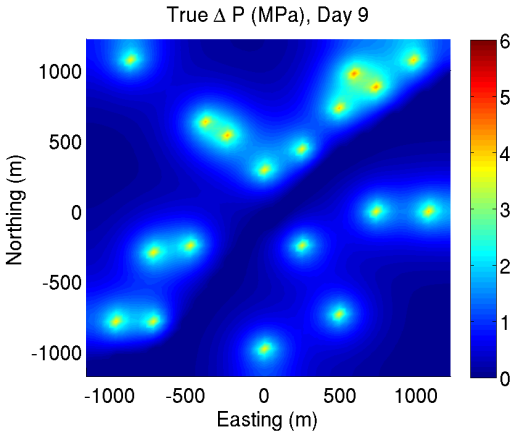

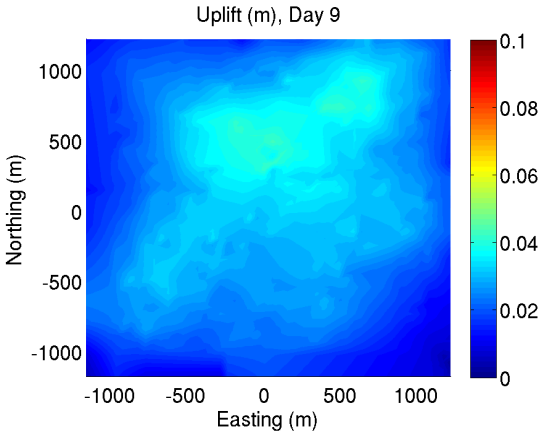

True pressure, noisy surface uplift measurements

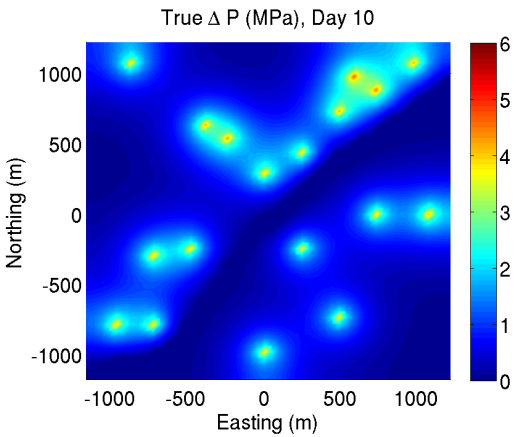

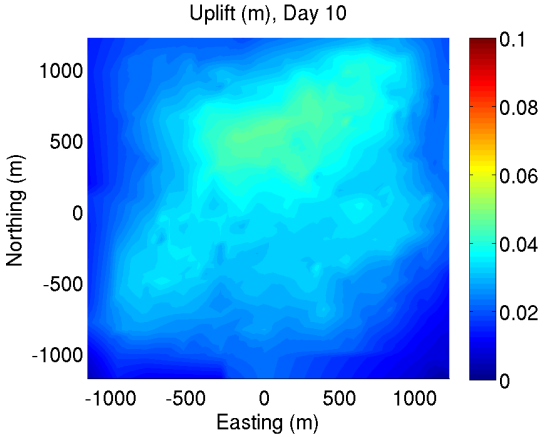

True pressure, noisy surface uplift measurements

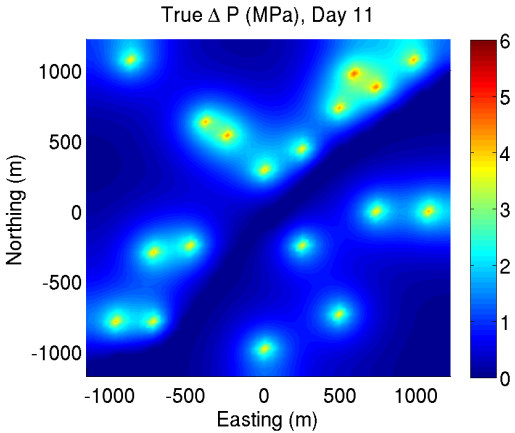

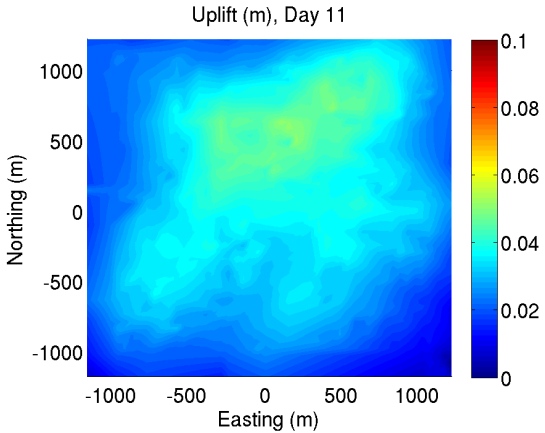

True pressure, noisy surface uplift measurements

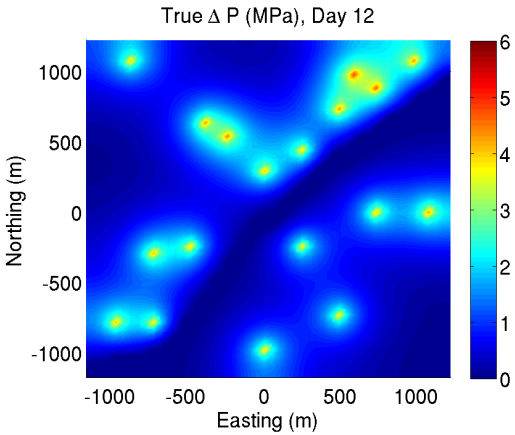

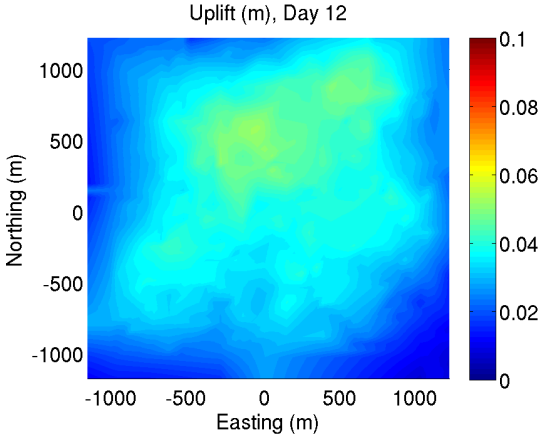

True pressure, noisy surface uplift measurements

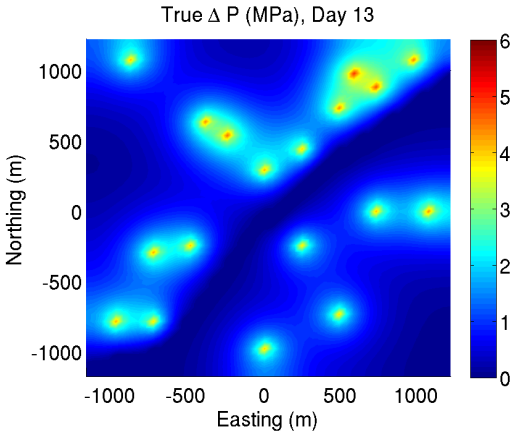

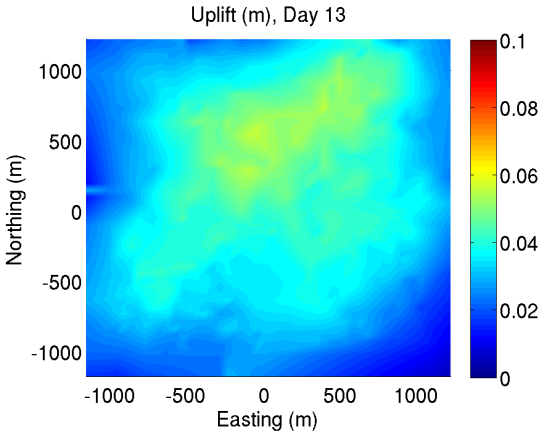

True pressure, noisy surface uplift measurements

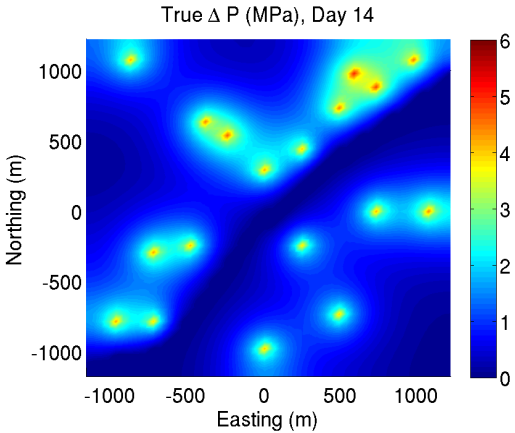

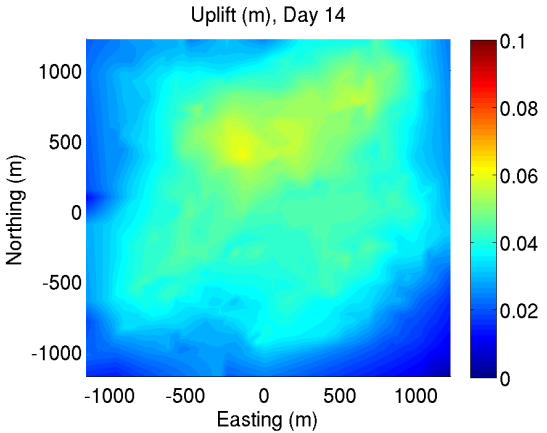

True pressure, noisy surface uplift measurements

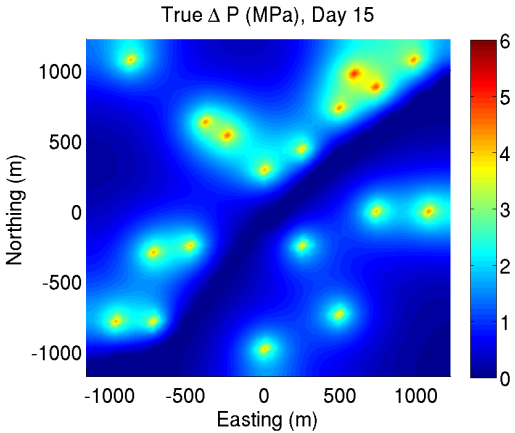

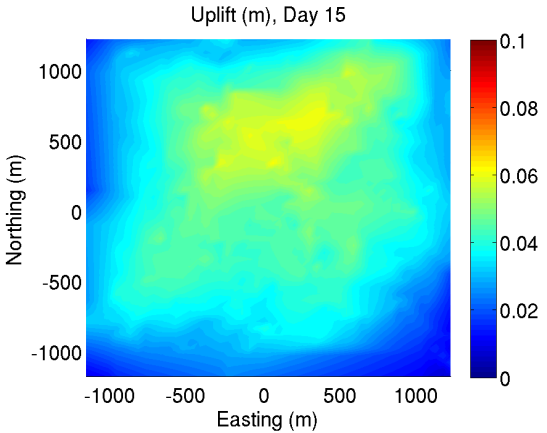

True pressure, noisy surface uplift measurements

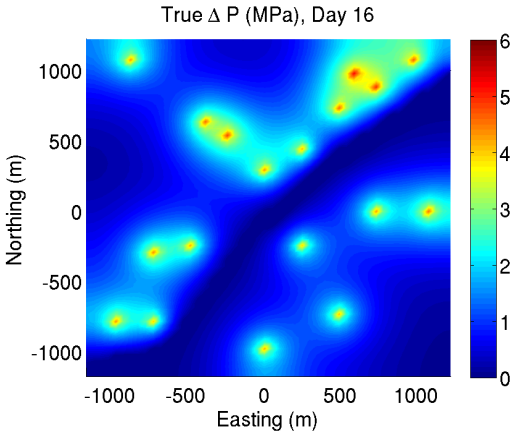

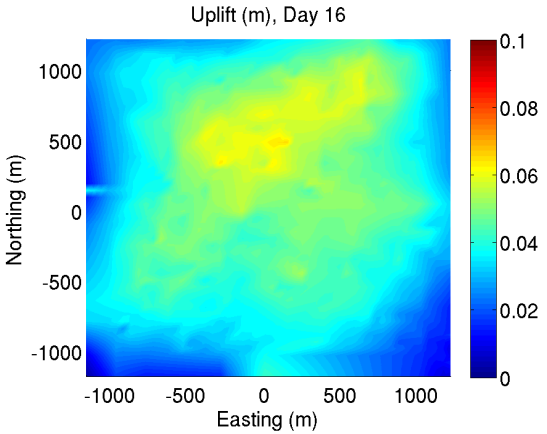

True pressure, noisy surface uplift measurements

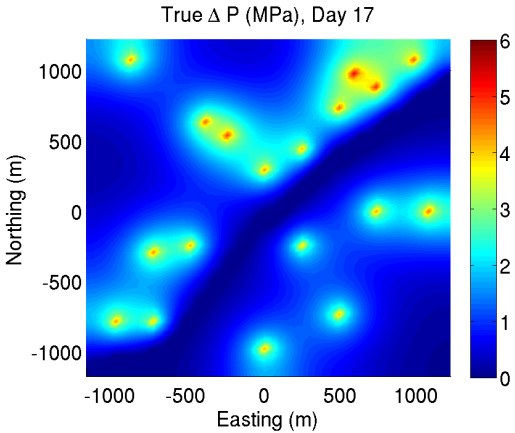

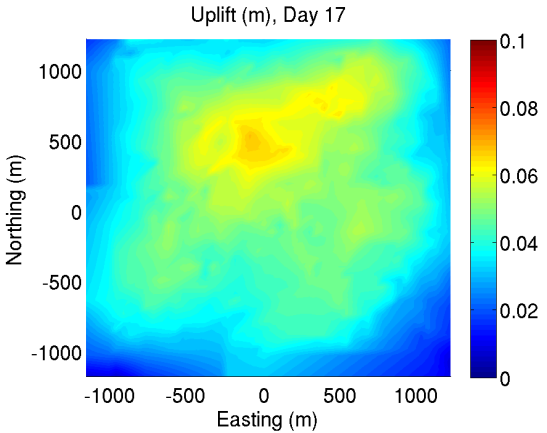

True pressure, noisy surface uplift measurements

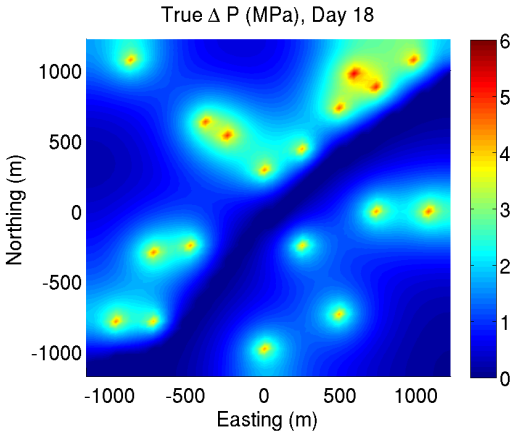

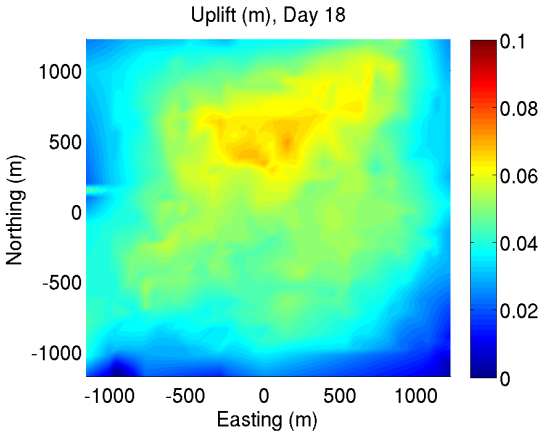

True pressure, noisy surface uplift measurements

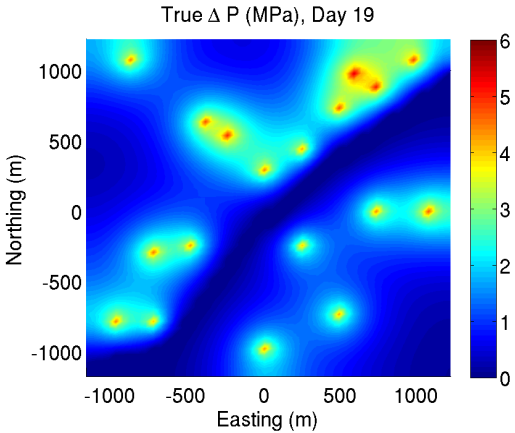

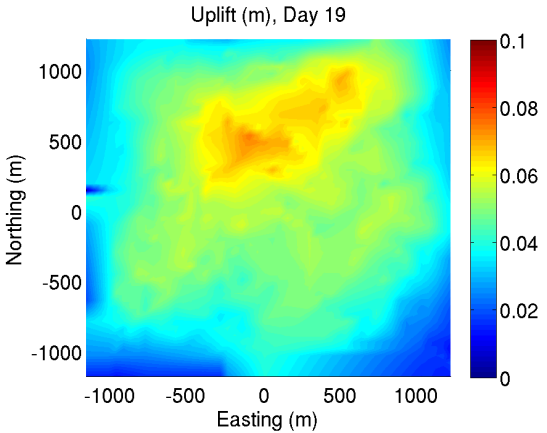

True pressure, noisy surface uplift measurements

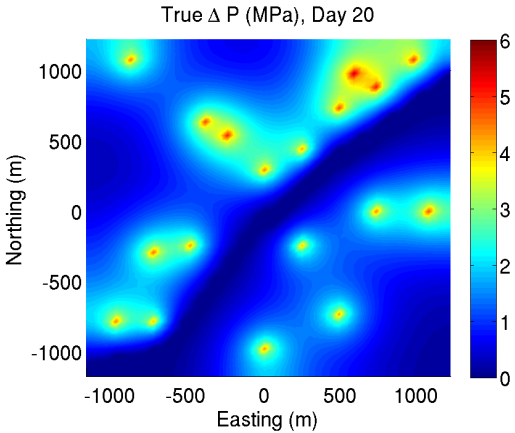

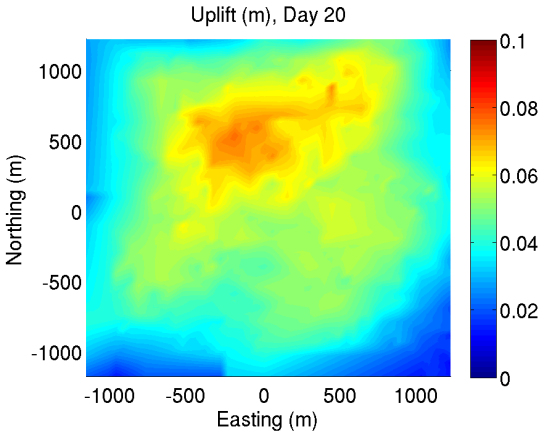

True pressure, noisy surface uplift measurements

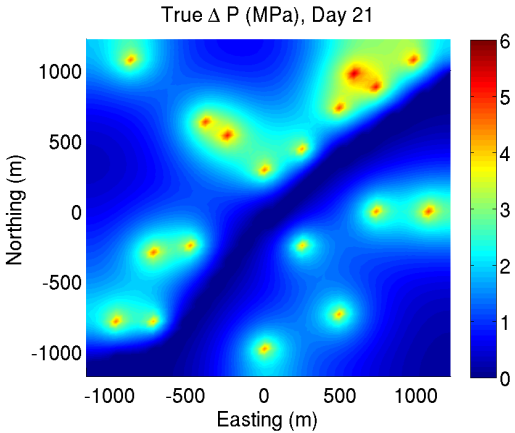

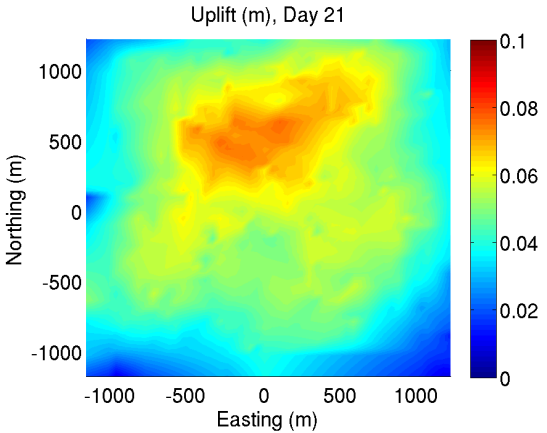

True pressure, noisy surface uplift measurements

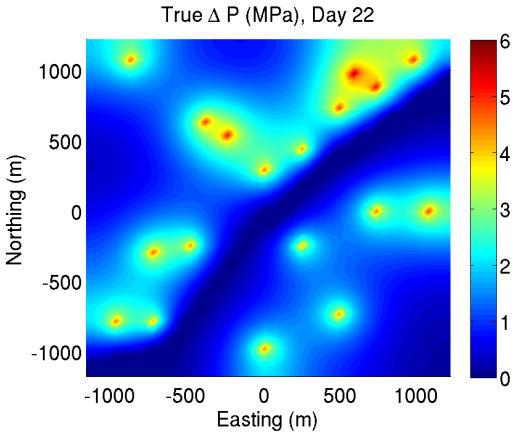

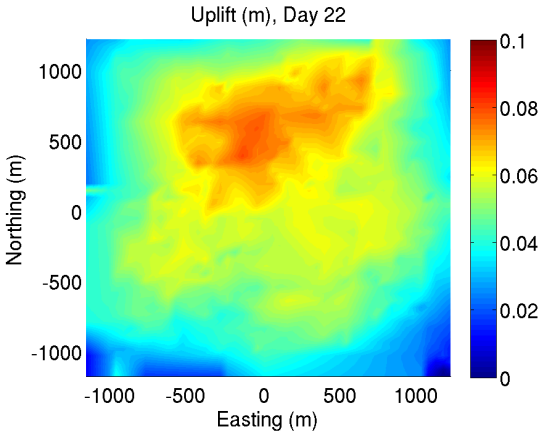

True pressure, noisy surface uplift measurements

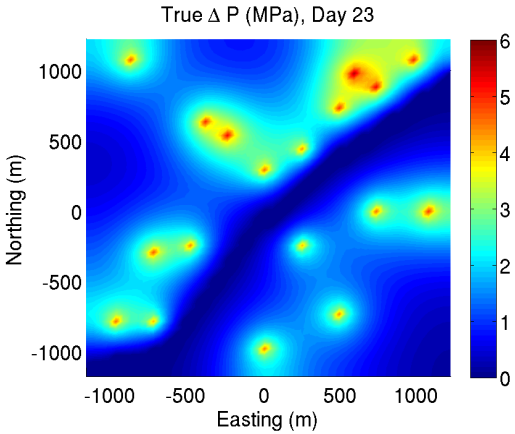

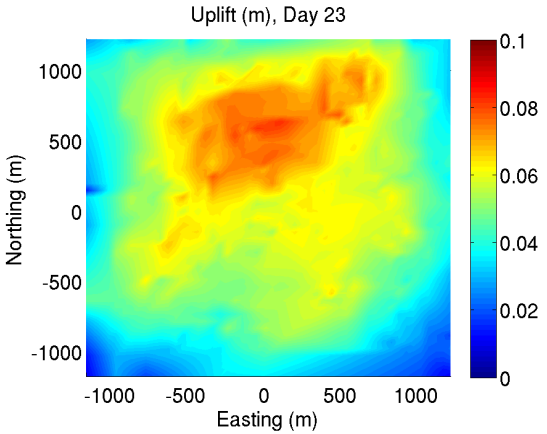

True pressure, noisy surface uplift measurements

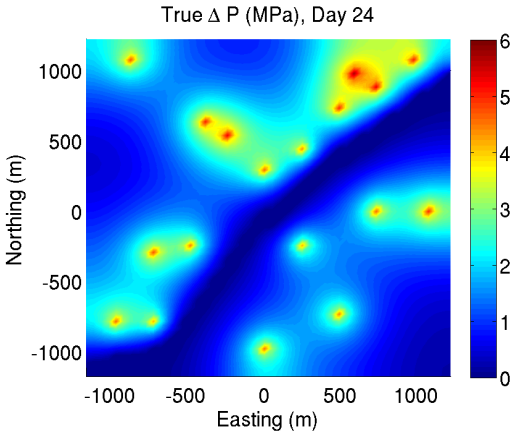

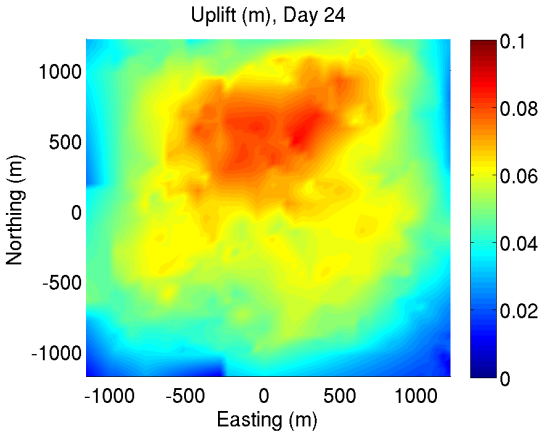

True pressure, noisy surface uplift measurements

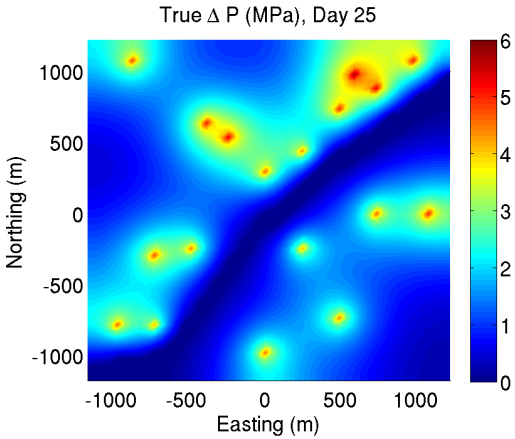

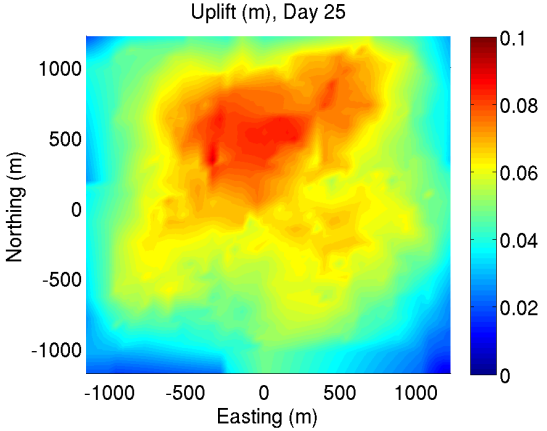

True pressure, noisy surface uplift measurements

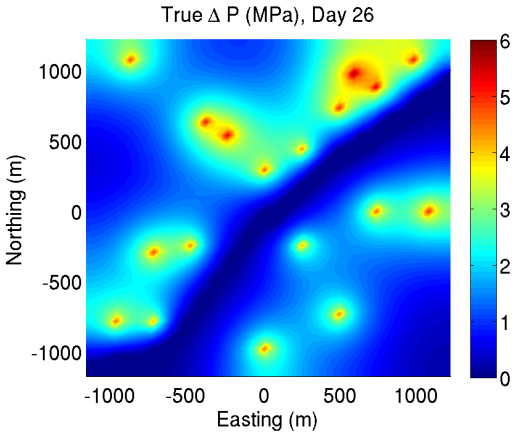

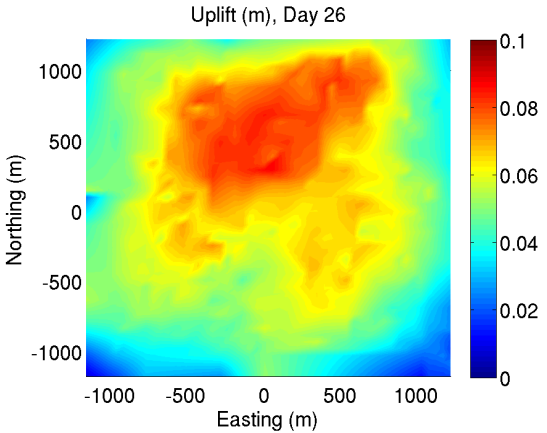

True pressure, noisy surface uplift measurements

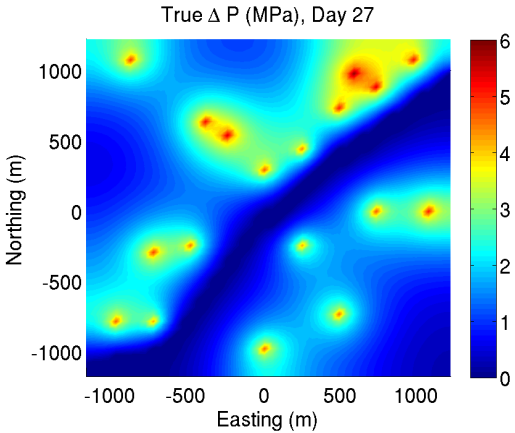

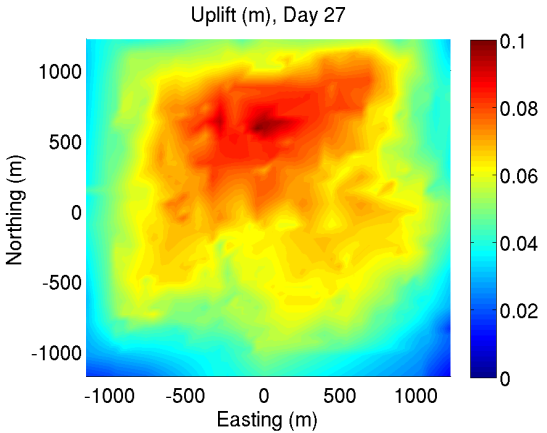

True pressure, noisy surface uplift measurements

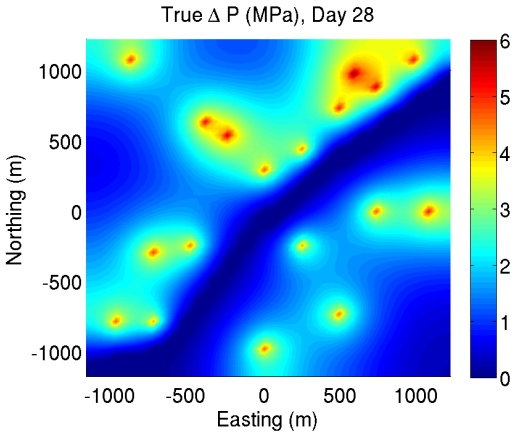

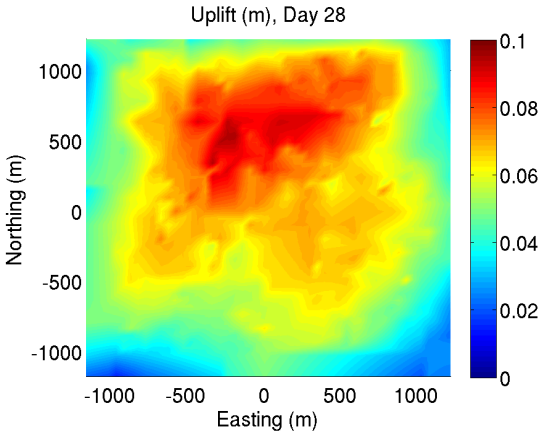

True pressure, noisy surface uplift measurements

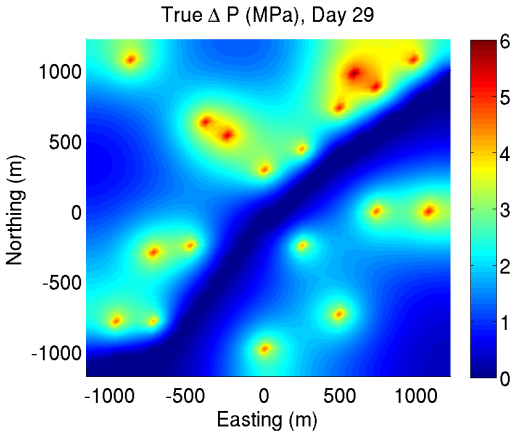

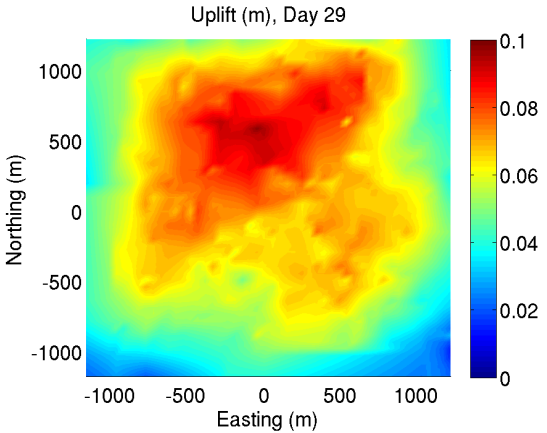

True pressure, noisy surface uplift measurements

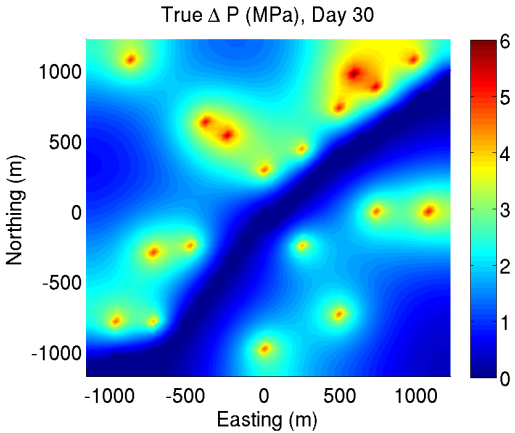

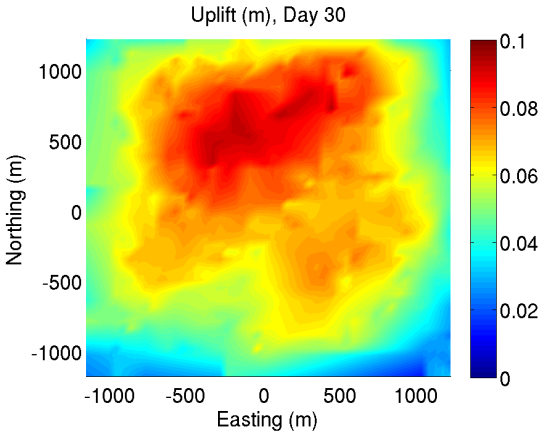

True pressure, noisy surface uplift measurements

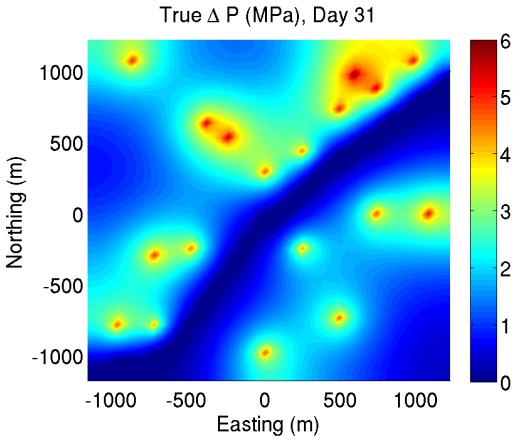

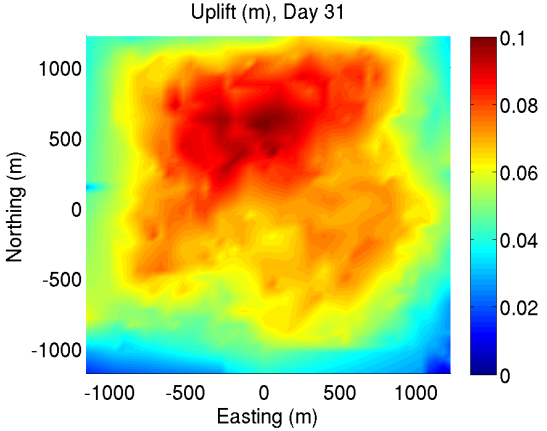

True pressure, noisy surface uplift measurements

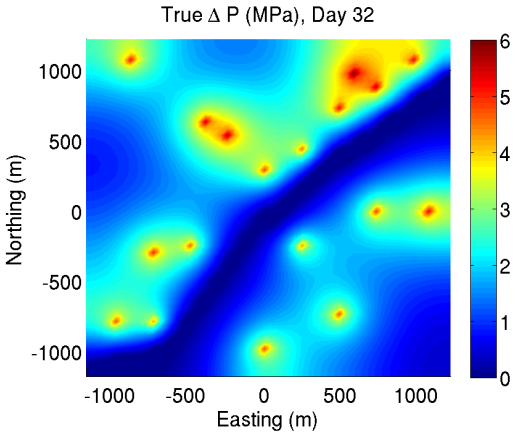

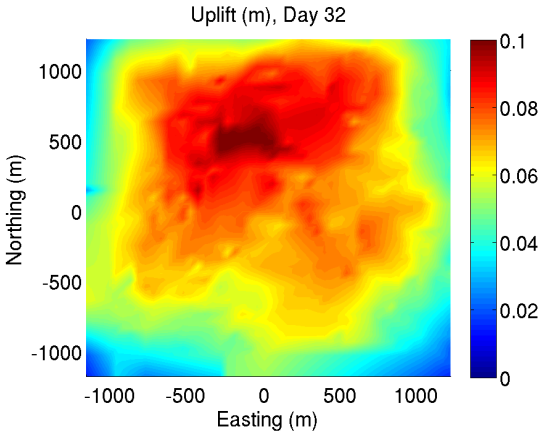

True pressure, noisy surface uplift measurements

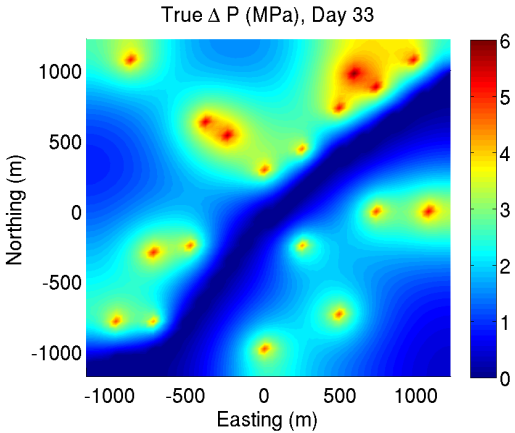

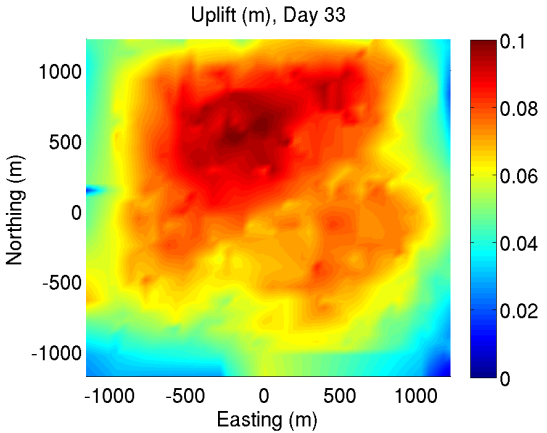

True pressure, noisy surface uplift measurements

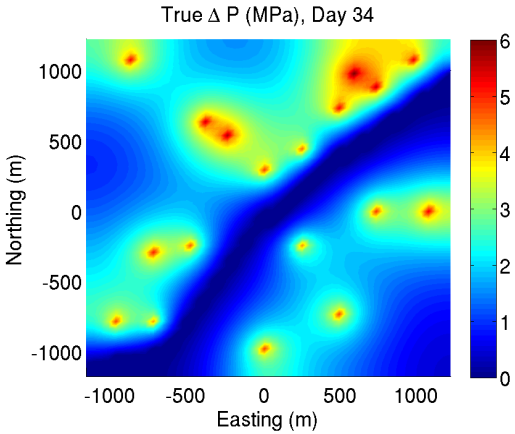

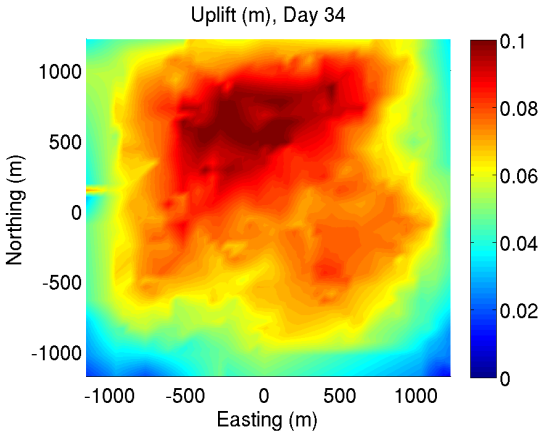

True pressure, noisy surface uplift measurements

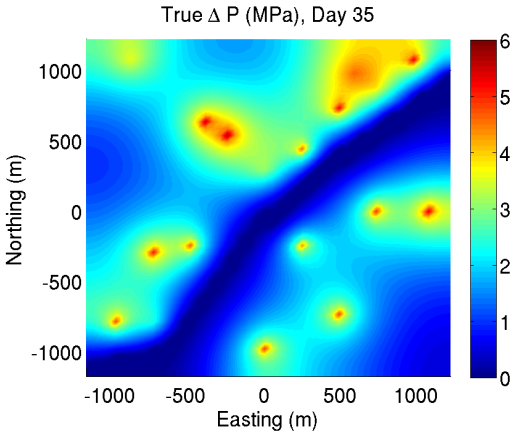

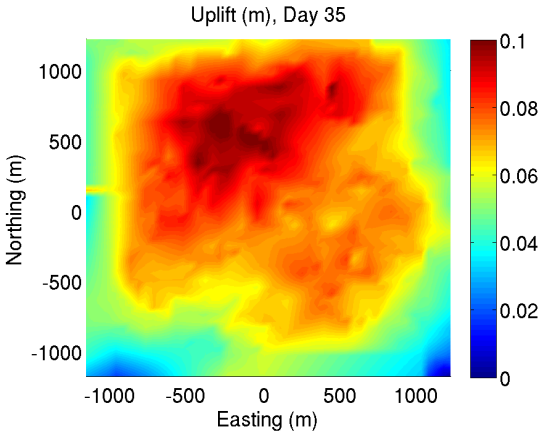

True pressure, noisy surface uplift measurements

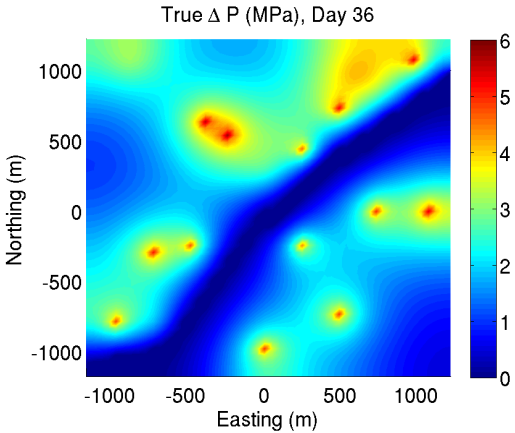

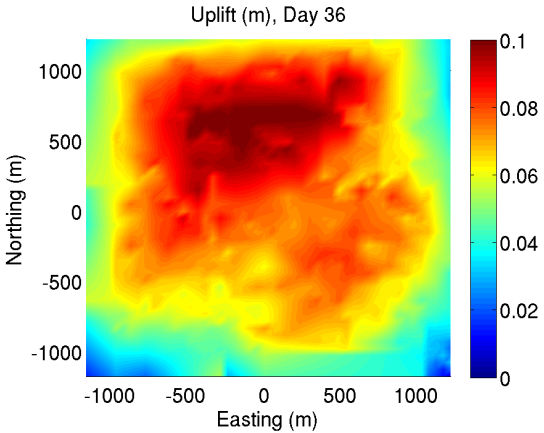

True pressure, noisy surface uplift measurements

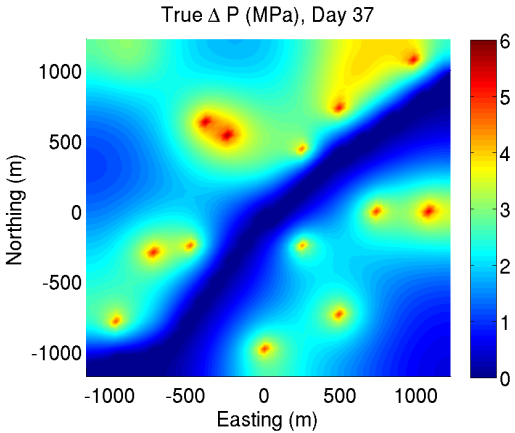

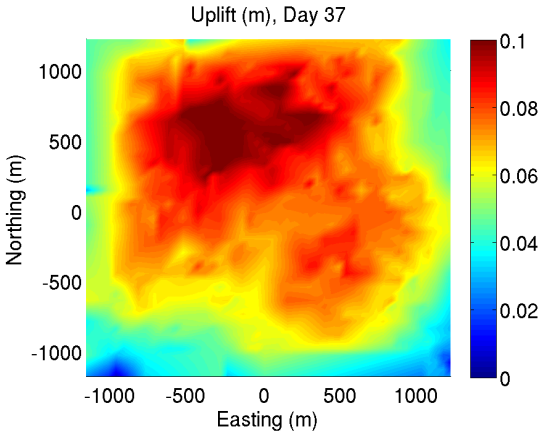

True pressure, noisy surface uplift measurements

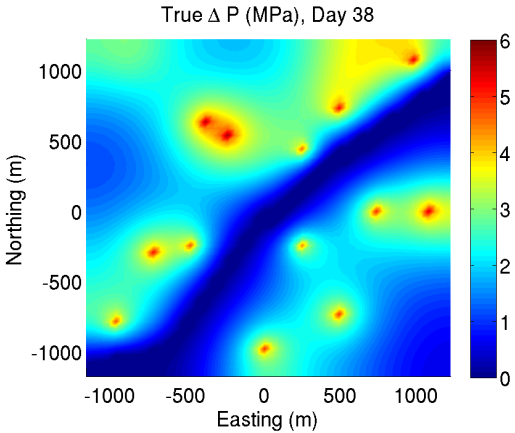

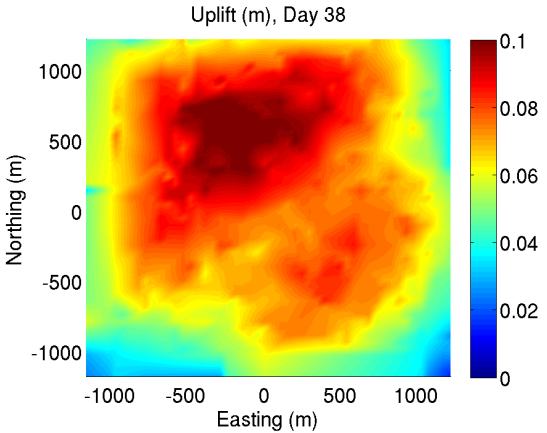

True pressure, noisy surface uplift measurements

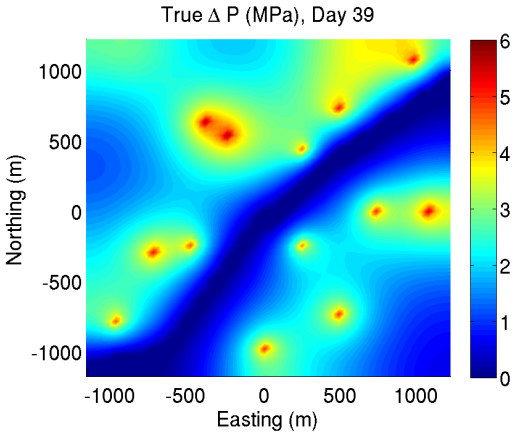

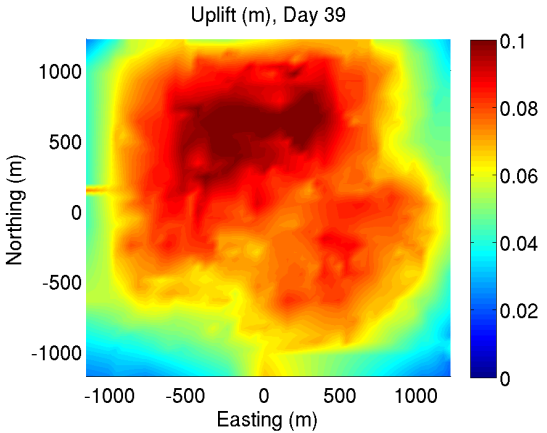

True pressure, noisy surface uplift measurements

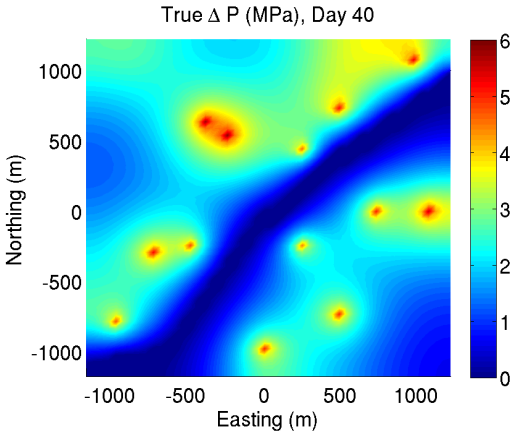

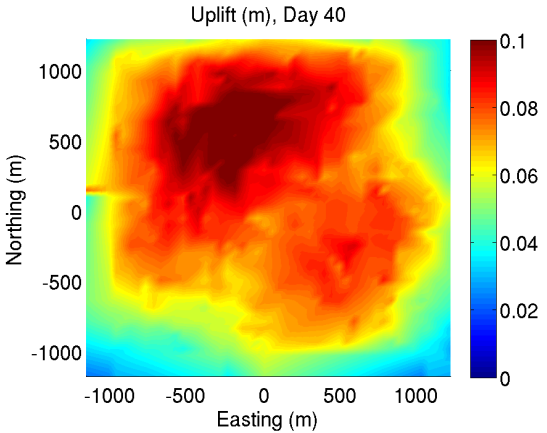

True pressure, noisy surface uplift measurements

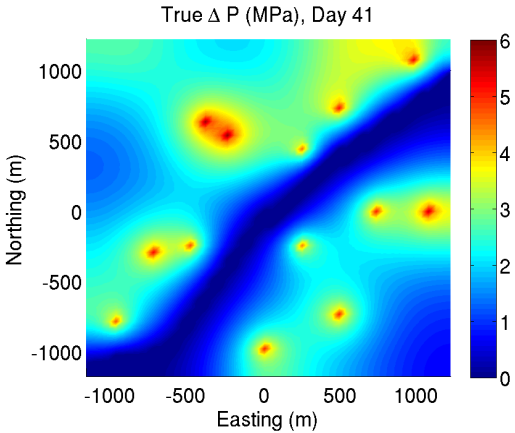

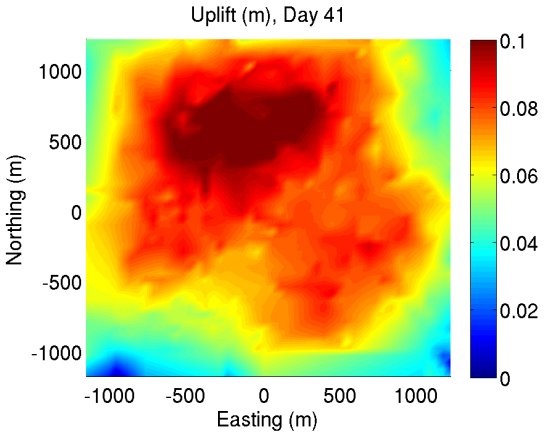

True pressure, noisy surface uplift measurements

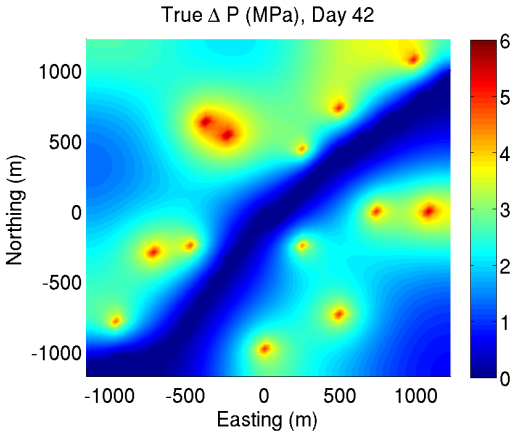

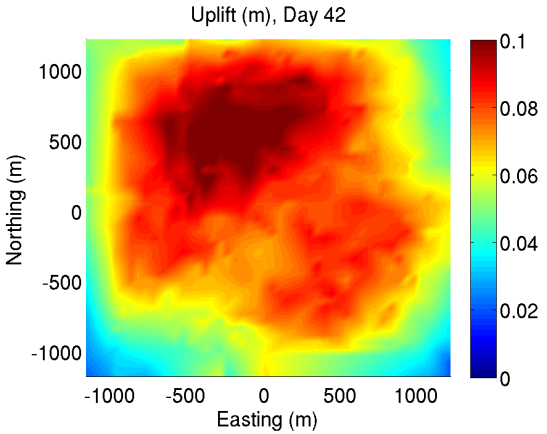

True pressure, noisy surface uplift measurements

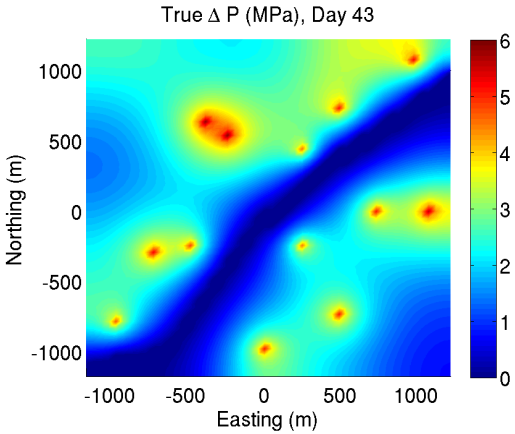

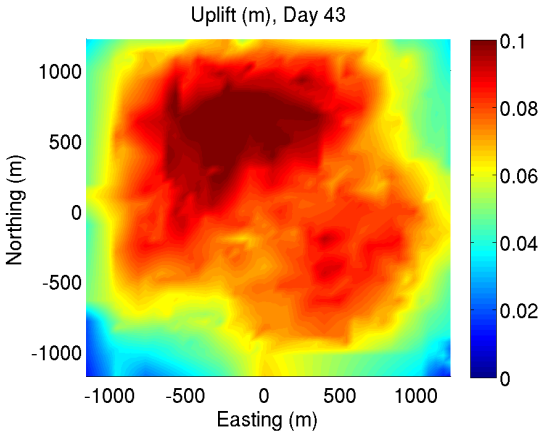

True pressure, noisy surface uplift measurements

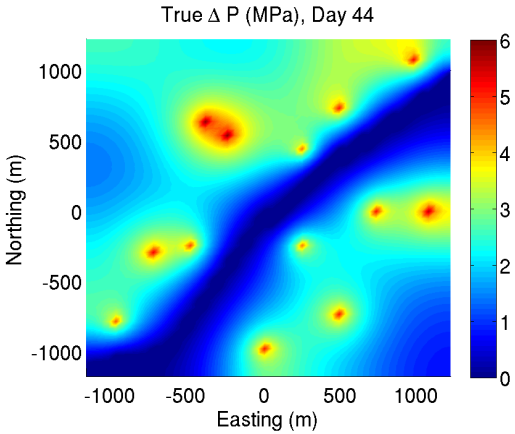

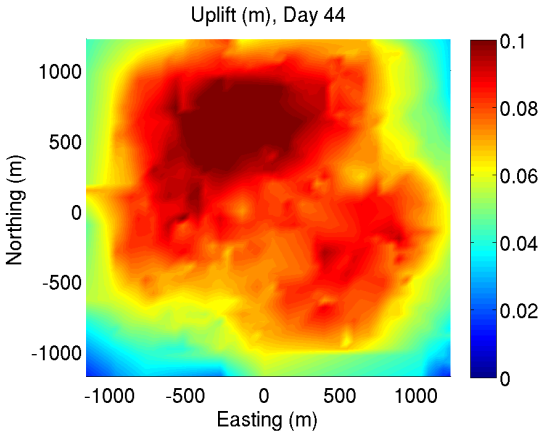

True pressure, noisy surface uplift measurements

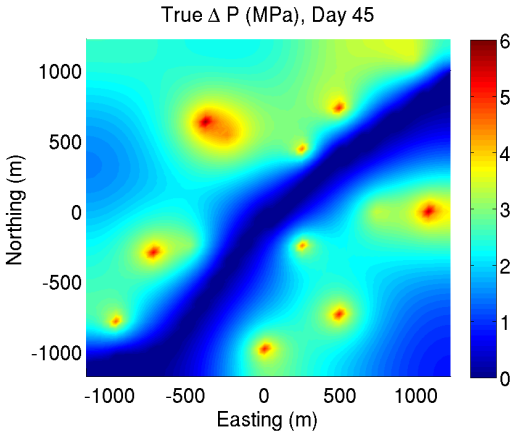

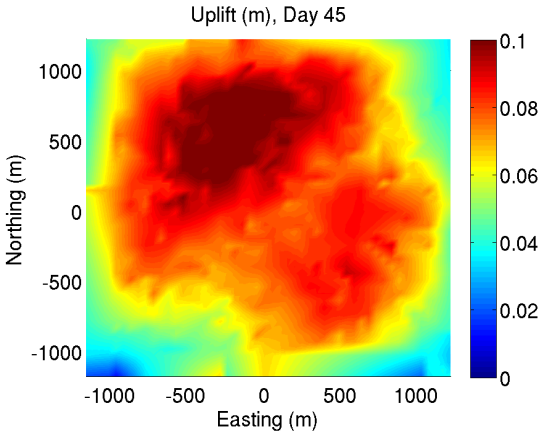

True pressure, noisy surface uplift measurements

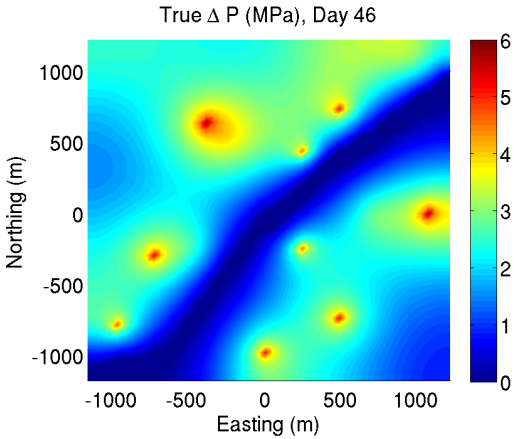

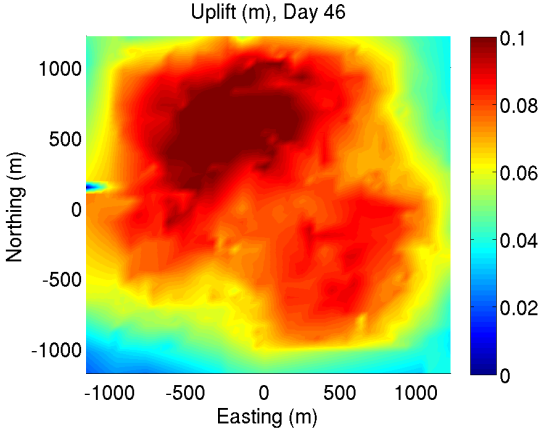

True pressure, noisy surface uplift measurements

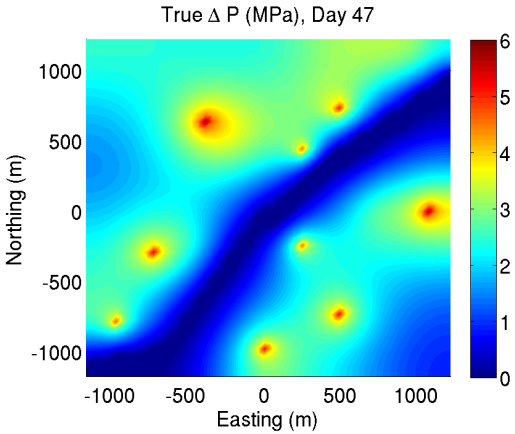

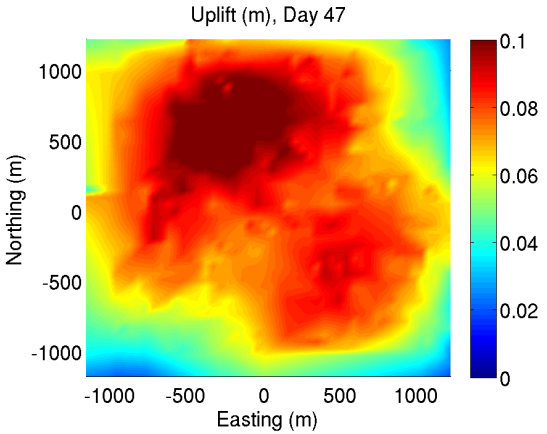

True pressure, noisy surface uplift measurements

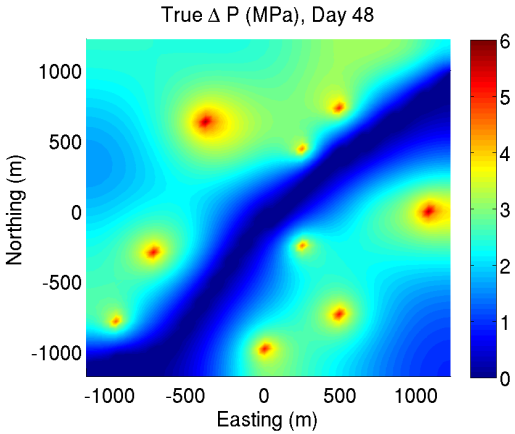

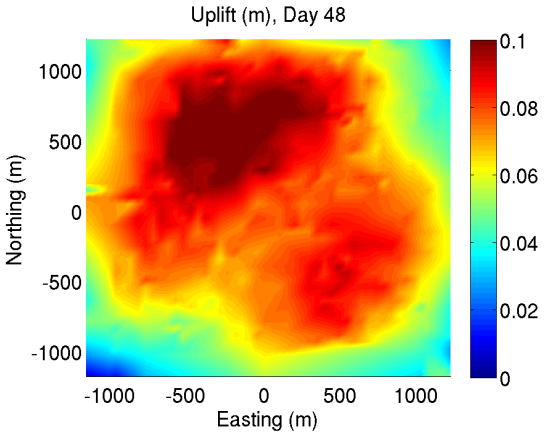

True pressure, noisy surface uplift measurements

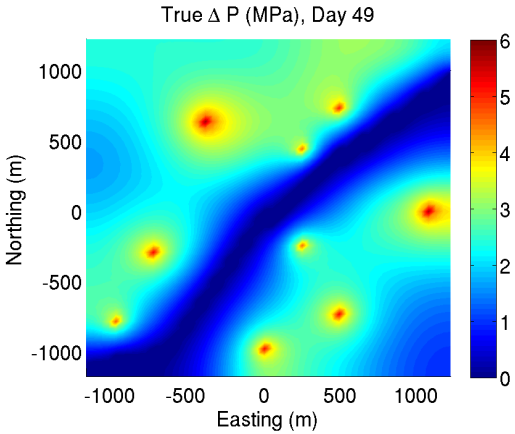

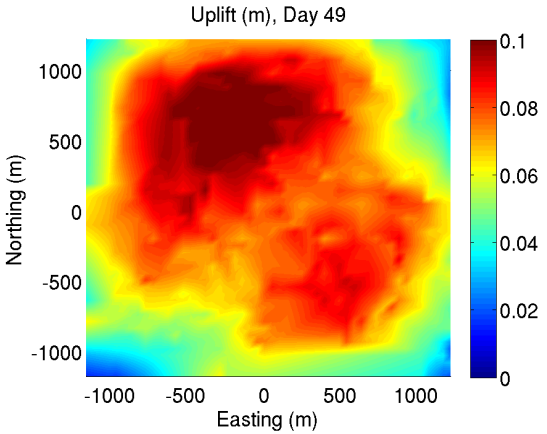

True pressure, noisy surface uplift measurements

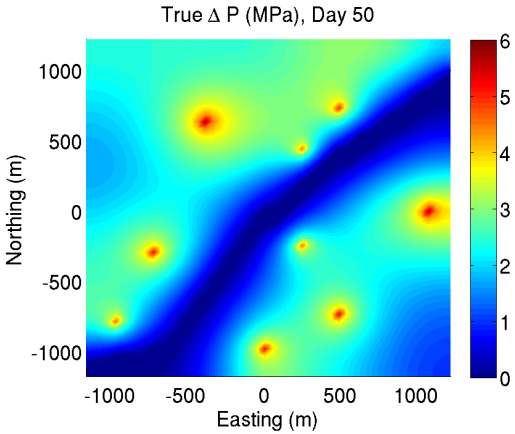

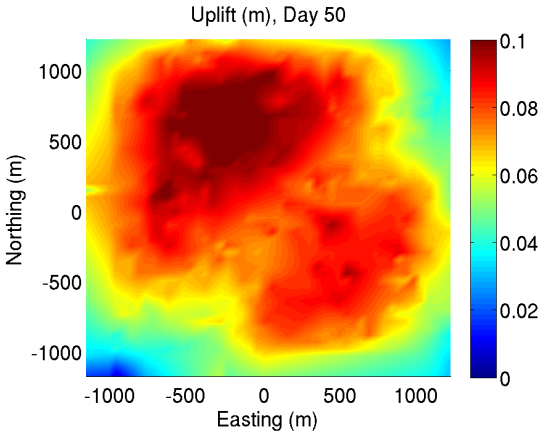

True pressure, noisy surface uplift measurements

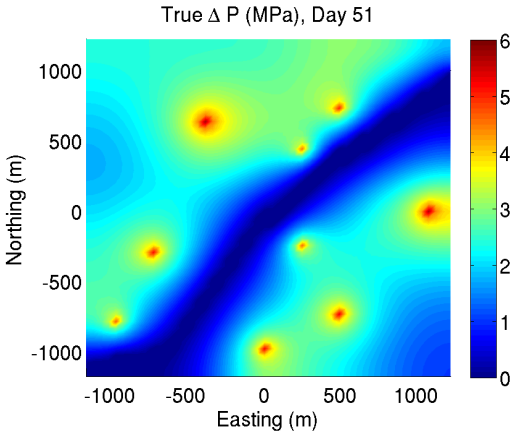

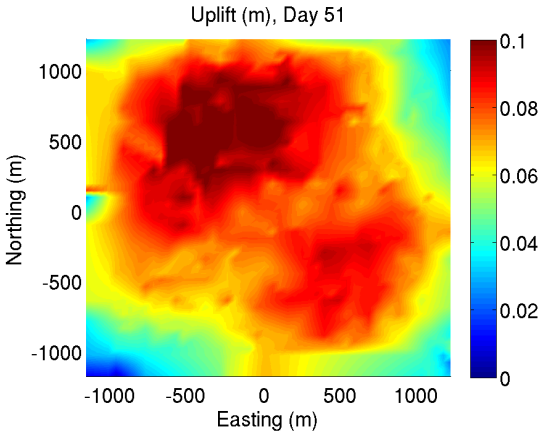

True pressure, noisy surface uplift measurements

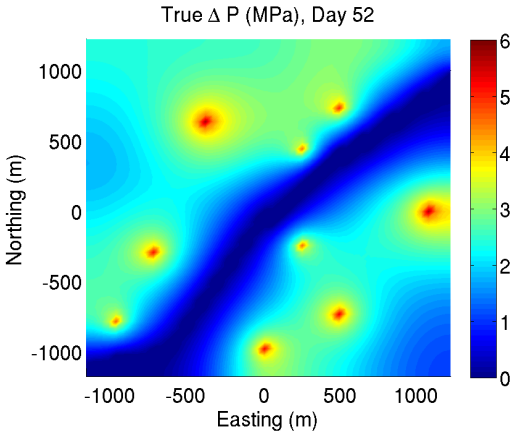

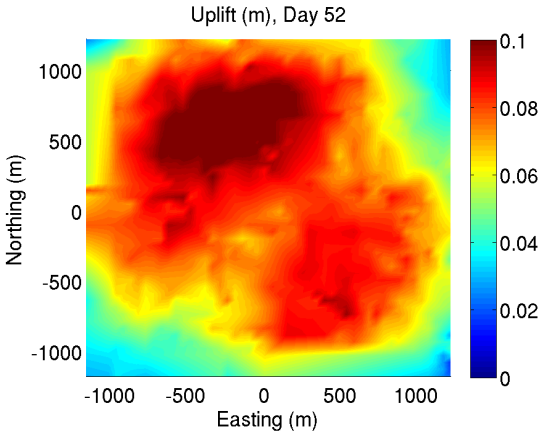

True pressure, noisy surface uplift measurements

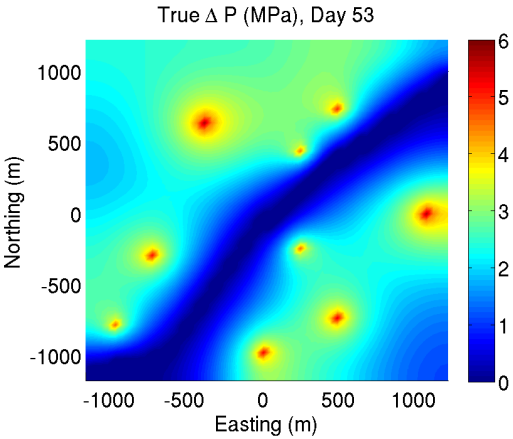

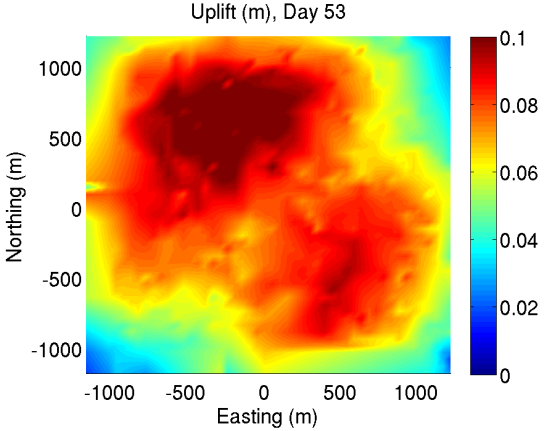

True pressure, noisy surface uplift measurements

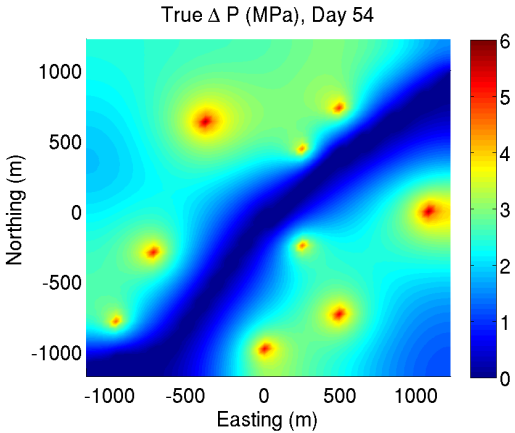

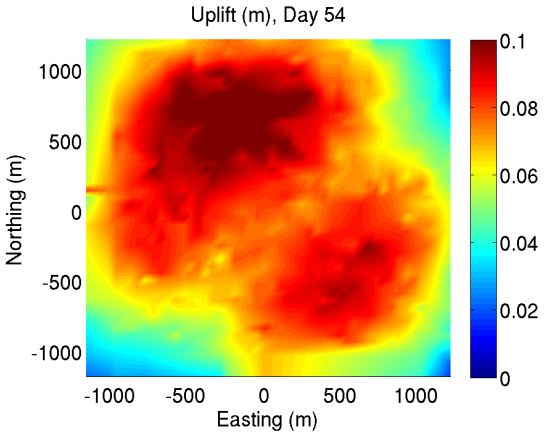

True pressure, noisy surface uplift measurements

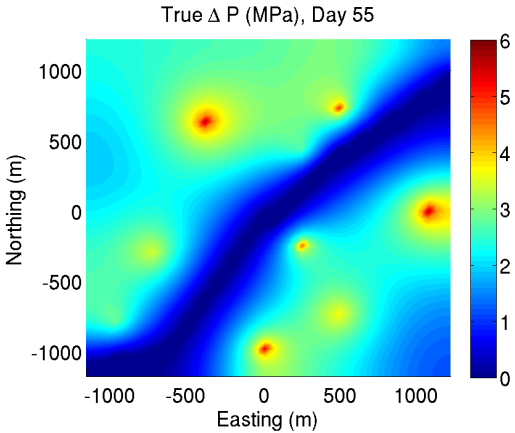

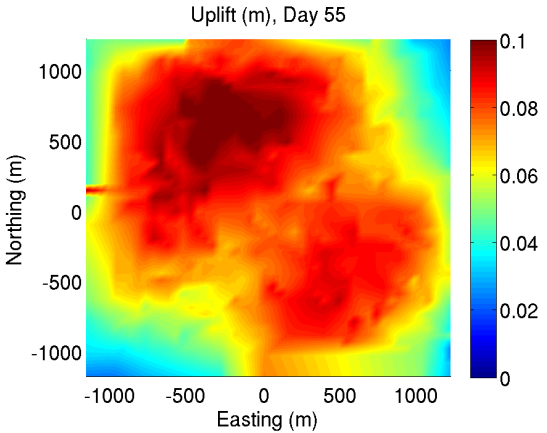

True pressure, noisy surface uplift measurements

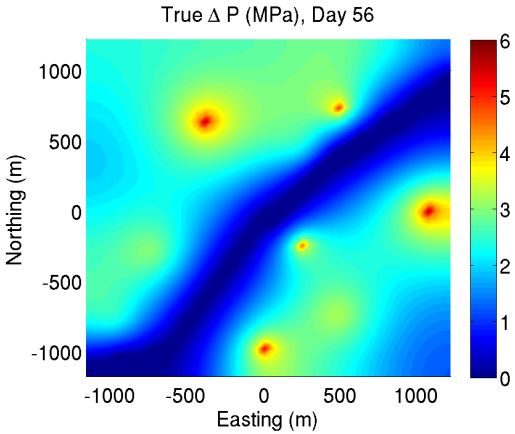

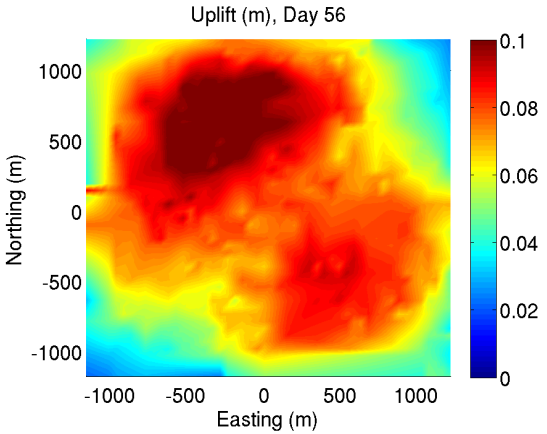

True pressure, noisy surface uplift measurements

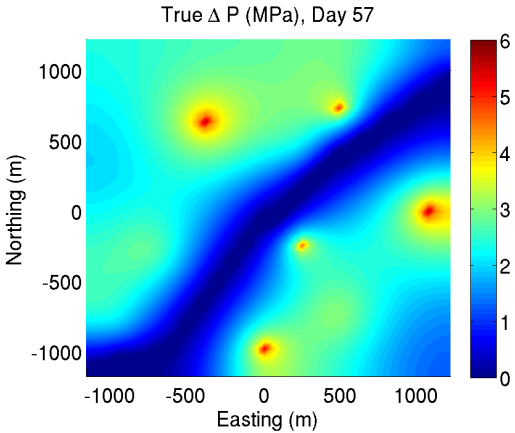

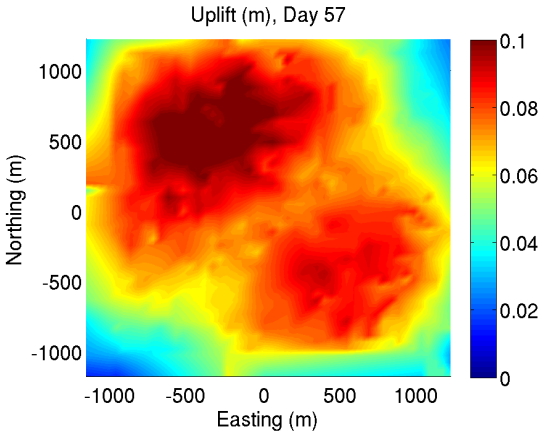

True pressure, noisy surface uplift measurements

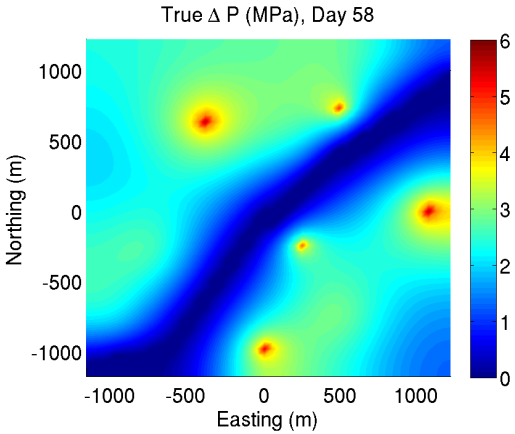

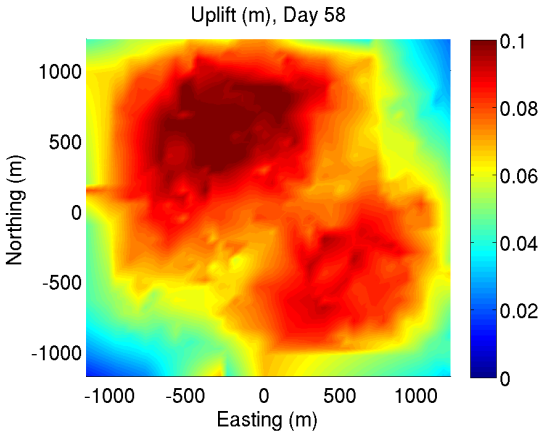

True pressure, noisy surface uplift measurements

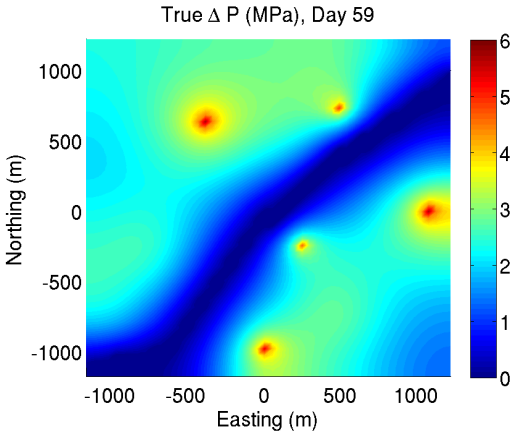

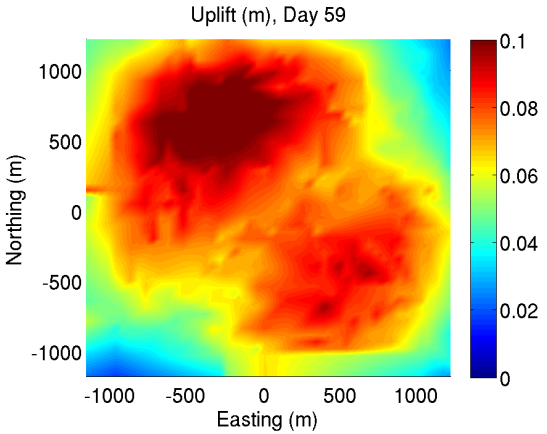

True pressure, noisy surface uplift measurements

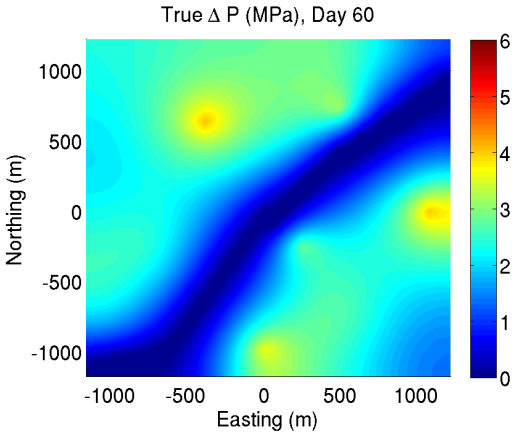

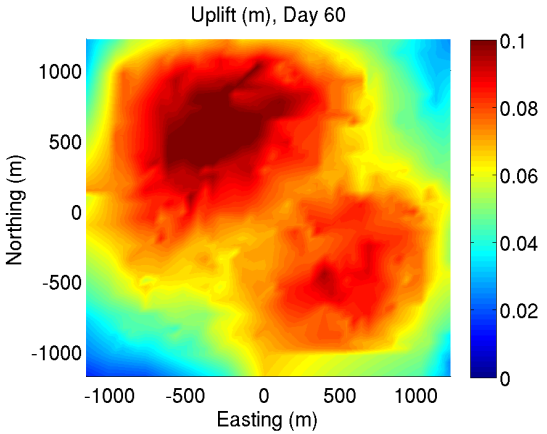

True pressure, inverted pressure using (LS) and (TV)

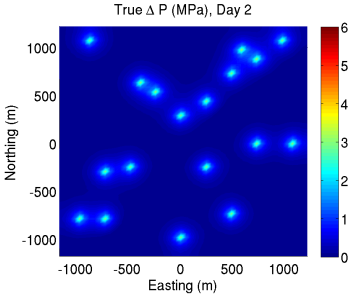

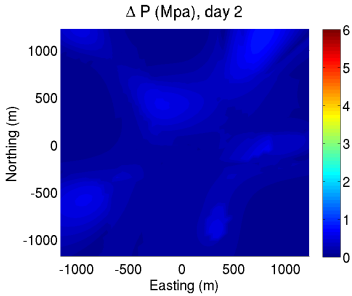

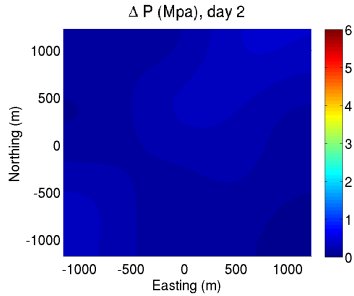

True pressure, inverted pressure using (LS) and (TV)

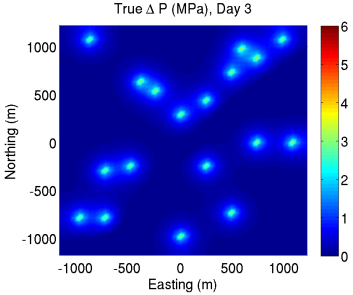

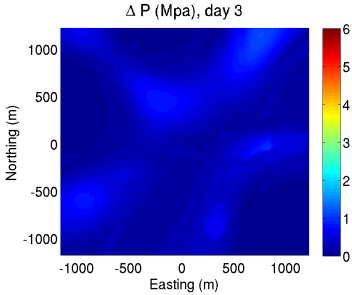

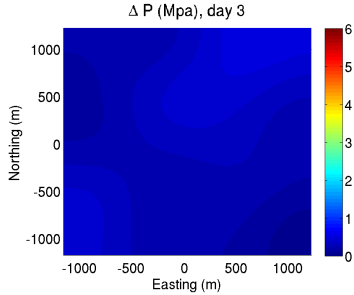

True pressure, inverted pressure using (LS) and (TV)

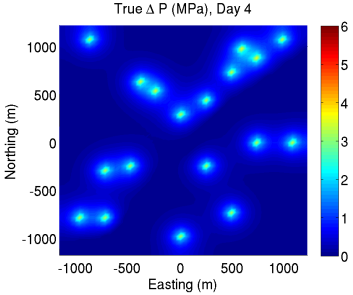

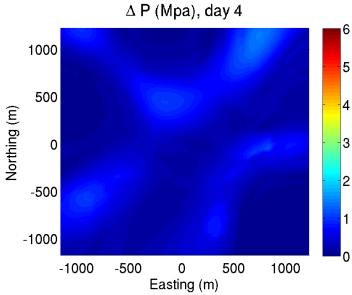

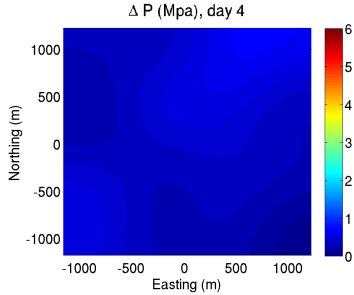

True pressure, inverted pressure using (LS) and (TV)

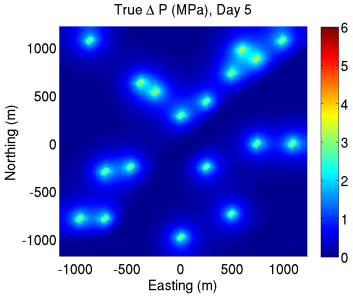

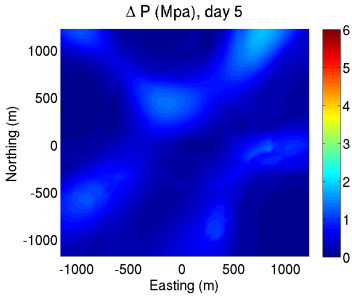

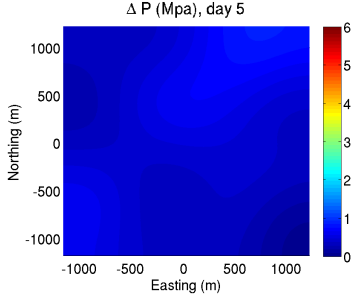

True pressure, inverted pressure using (LS) and (TV)

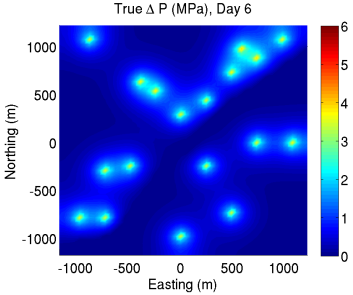

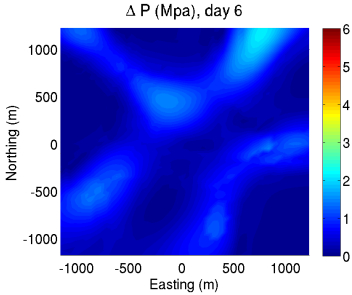

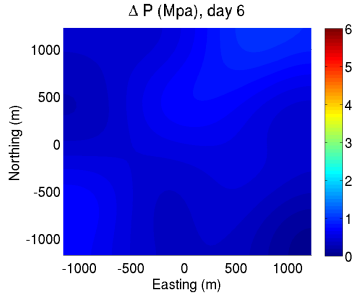

True pressure, inverted pressure using (LS) and (TV)

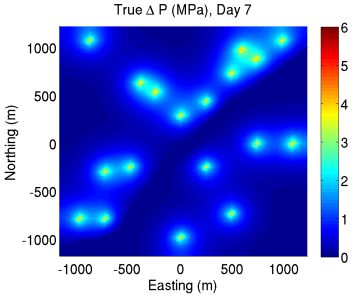

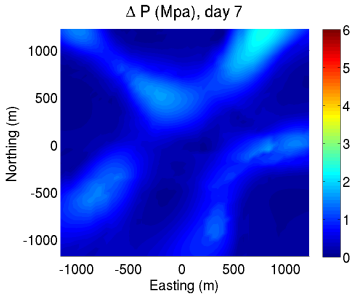

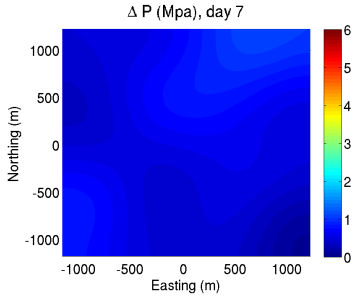

True pressure, inverted pressure using (LS) and (TV)

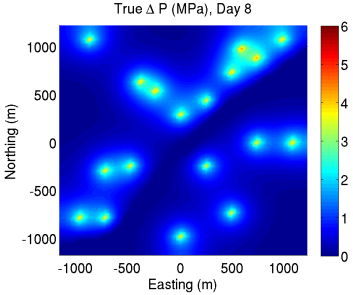

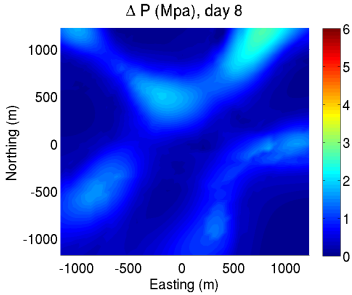

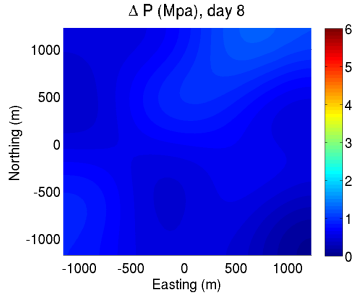

True pressure, inverted pressure using (LS) and (TV)

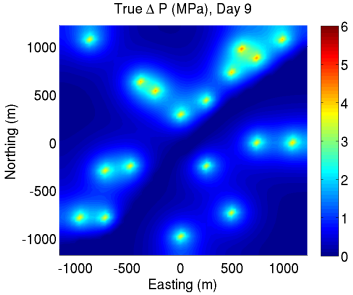

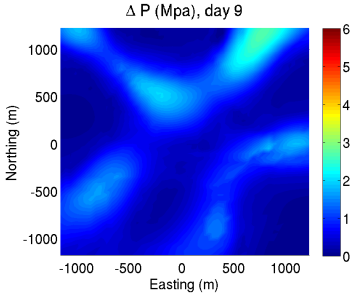

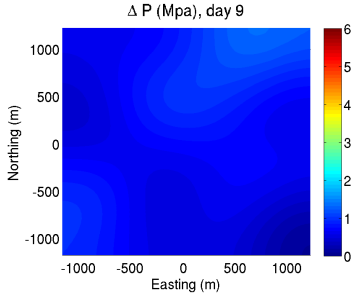

True pressure, inverted pressure using (LS) and (TV)

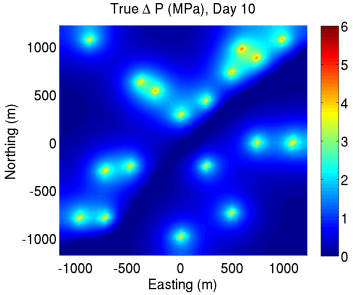

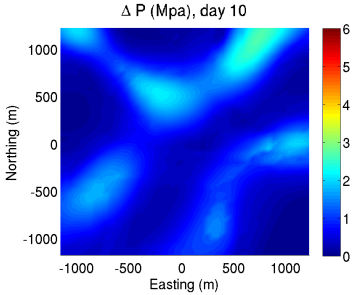

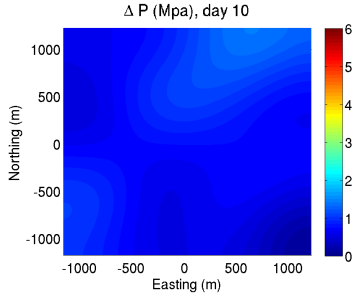

True pressure, inverted pressure using (LS) and (TV)

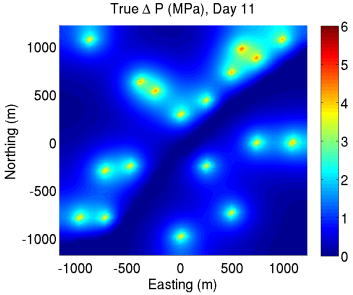

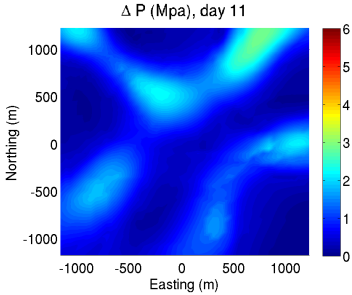

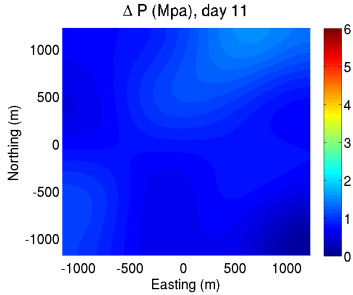

True pressure, inverted pressure using (LS) and (TV)

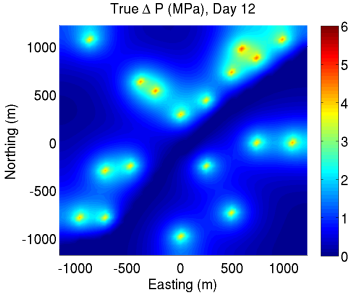

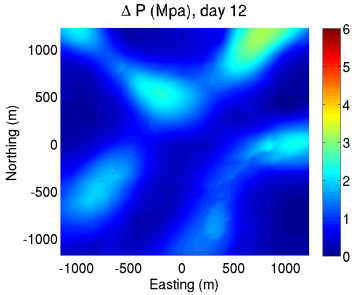

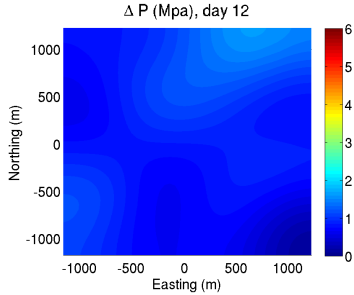

True pressure, inverted pressure using (LS) and (TV)

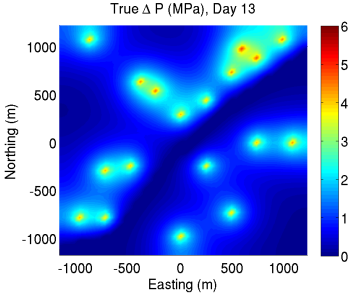

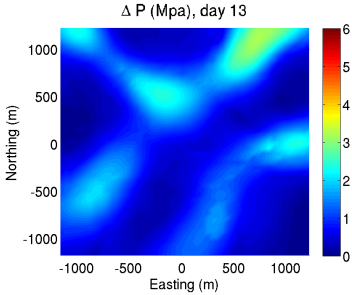

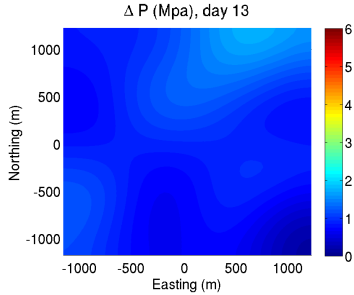

True pressure, inverted pressure using (LS) and (TV)

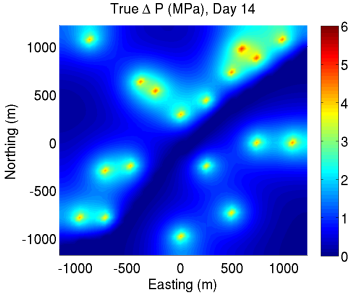

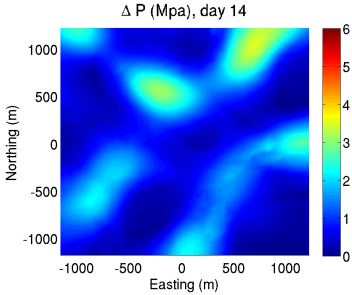

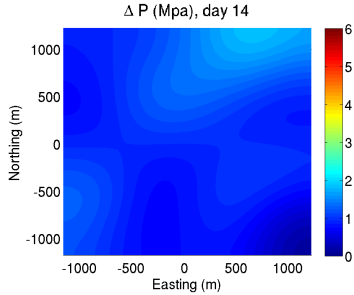

True pressure, inverted pressure using (LS) and (TV)

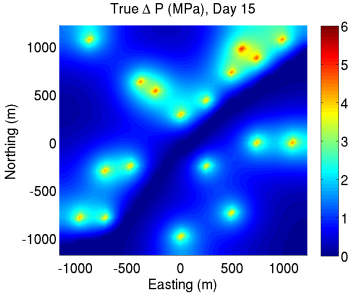

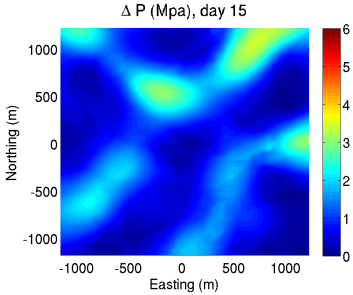

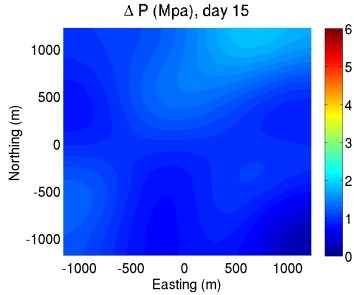

True pressure, inverted pressure using (LS) and (TV)

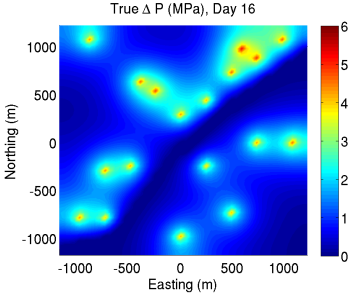

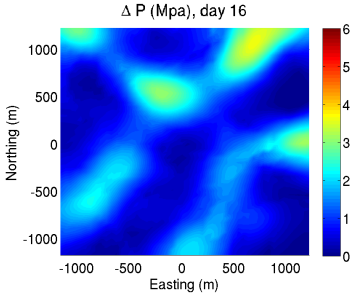

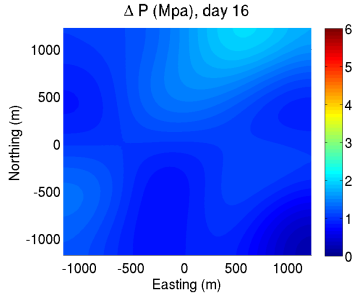

True pressure, inverted pressure using (LS) and (TV)

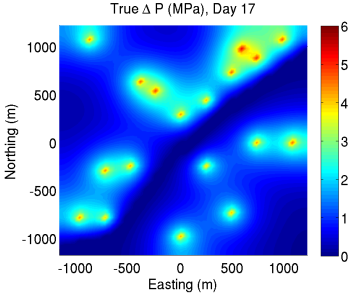

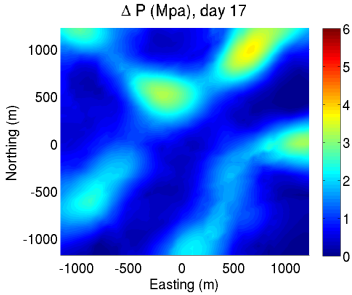

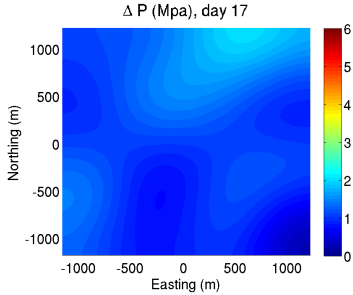

True pressure, inverted pressure using (LS) and (TV)

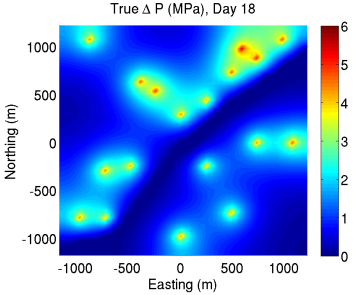

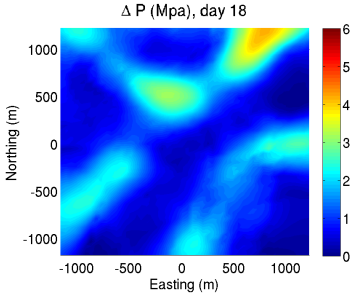

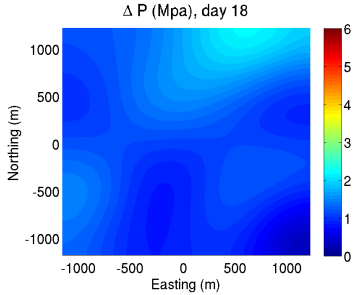

True pressure, inverted pressure using (LS) and (TV)

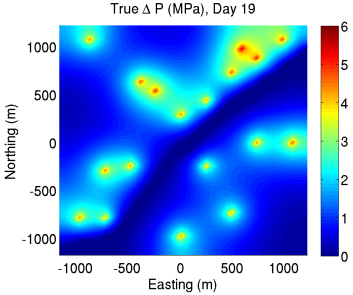

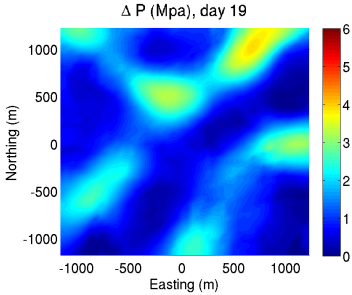

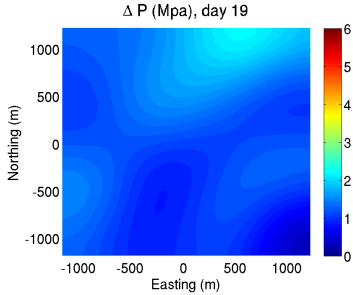

True pressure, inverted pressure using (LS) and (TV)

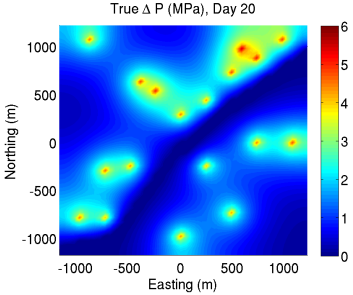

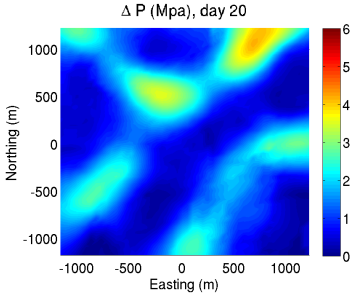

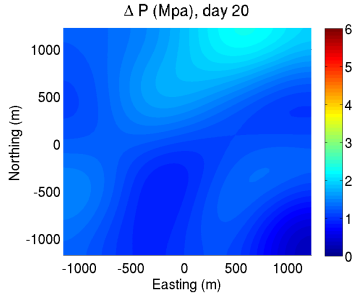

True pressure, inverted pressure using (LS) and (TV)

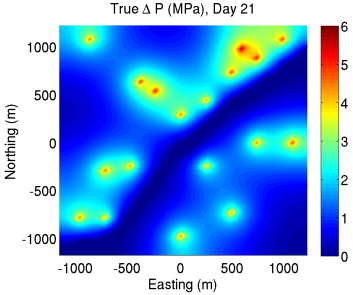

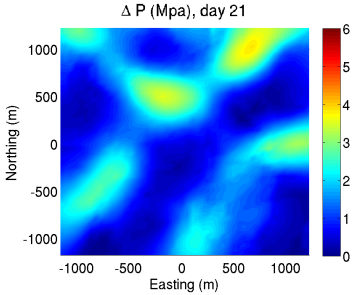

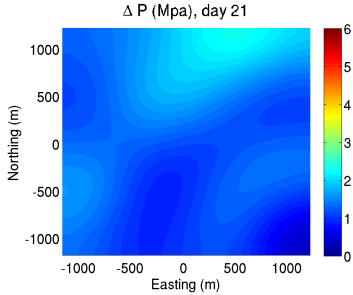

True pressure, inverted pressure using (LS) and (TV)

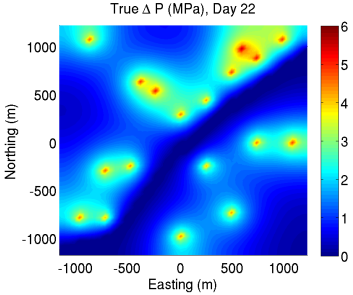

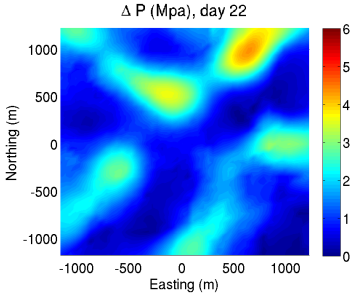

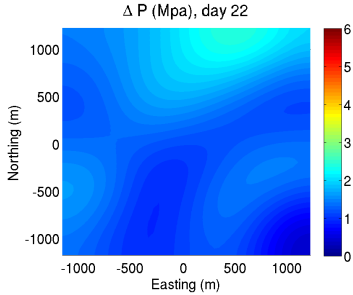

True pressure, inverted pressure using (LS) and (TV)

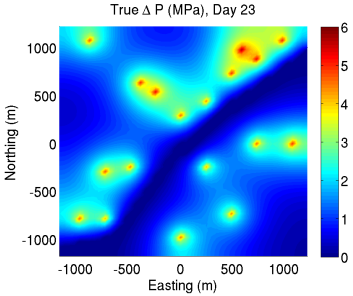

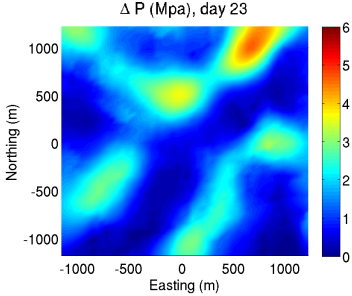

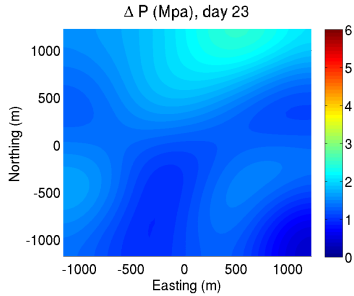

True pressure, inverted pressure using (LS) and (TV)

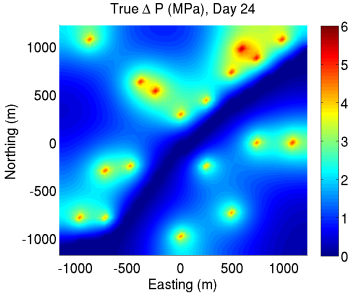

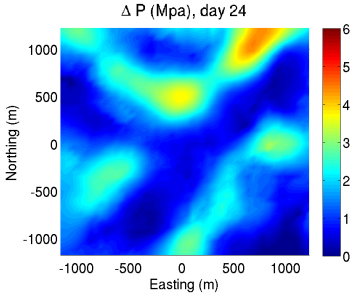

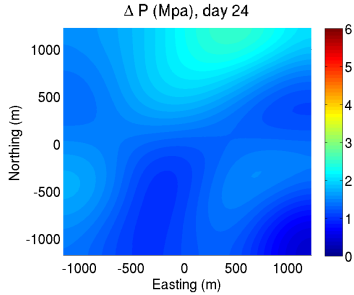

True pressure, inverted pressure using (LS) and (TV)

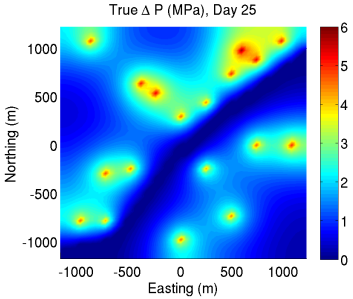

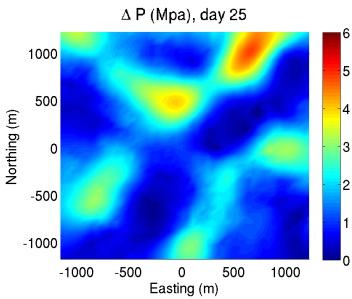

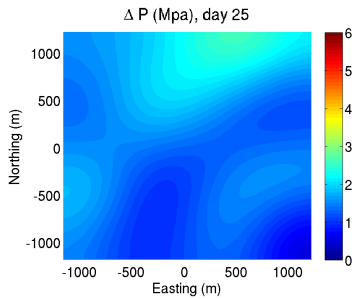

True pressure, inverted pressure using (LS) and (TV)

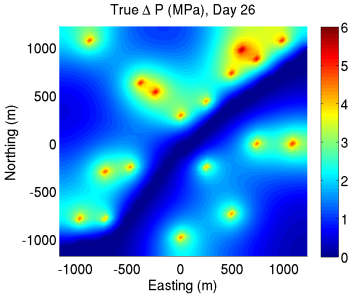

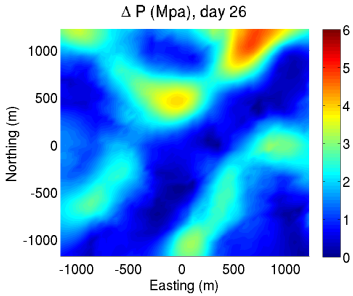

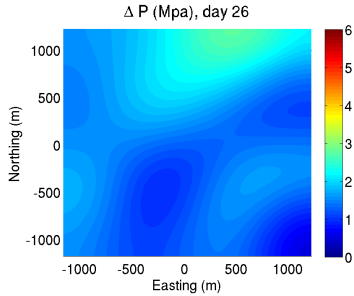

True pressure, inverted pressure using (LS) and (TV)

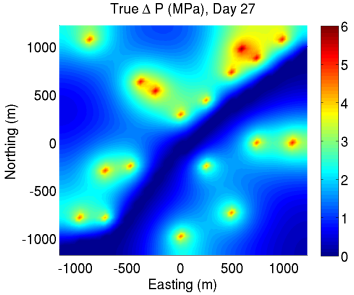

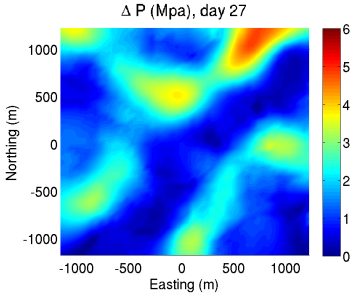

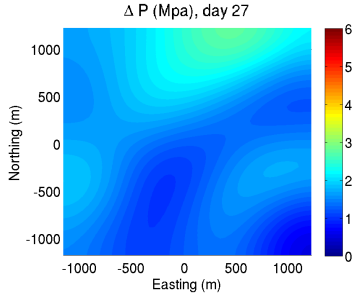

True pressure, inverted pressure using (LS) and (TV)

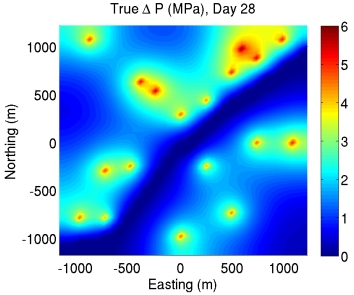

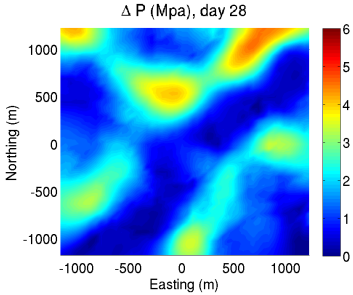

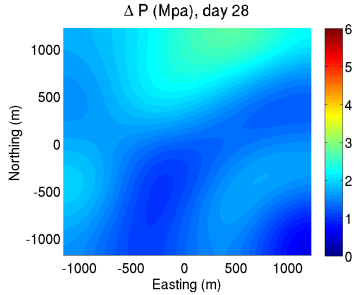

True pressure, inverted pressure using (LS) and (TV)

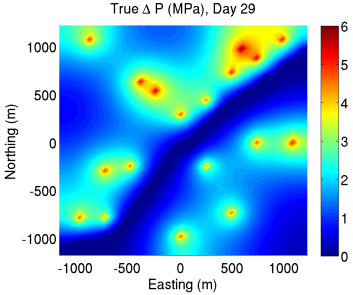

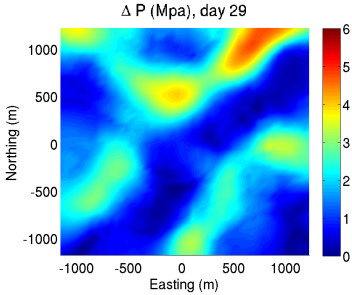

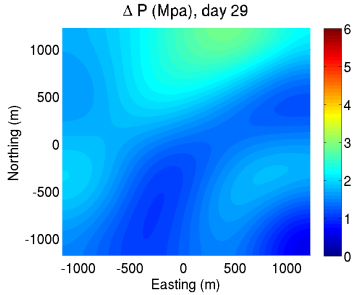

True pressure, inverted pressure using (LS) and (TV)

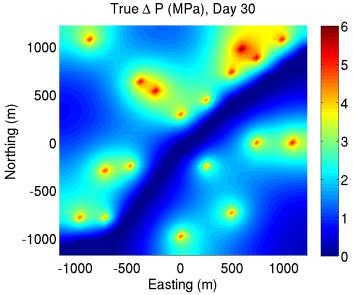

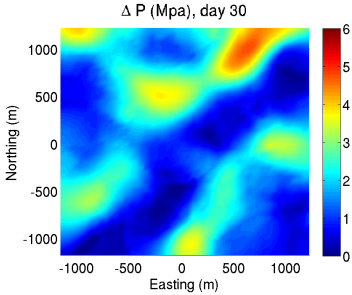

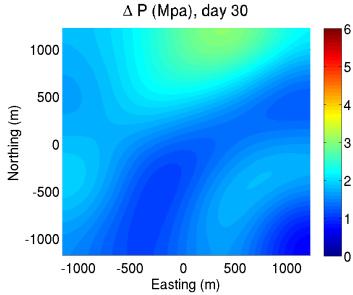

True pressure, inverted pressure using (LS) and (TV)

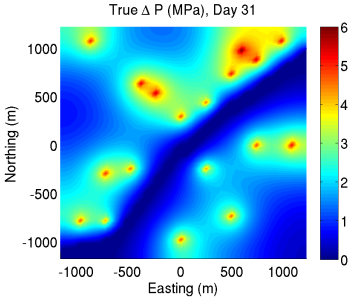

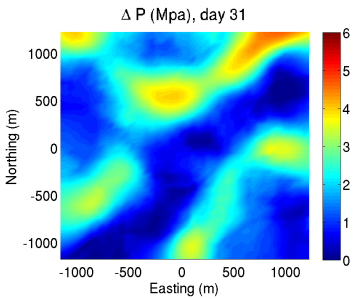

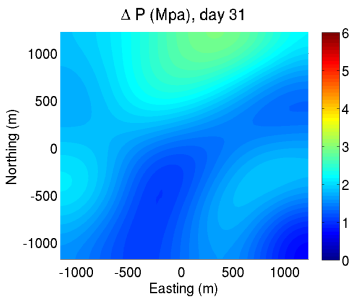

True pressure, inverted pressure using (LS) and (TV)

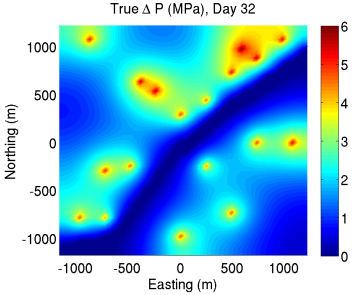

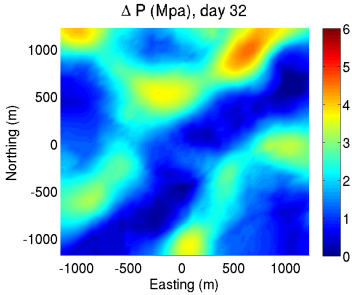

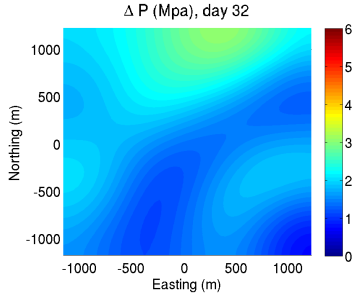

True pressure, inverted pressure using (LS) and (TV)

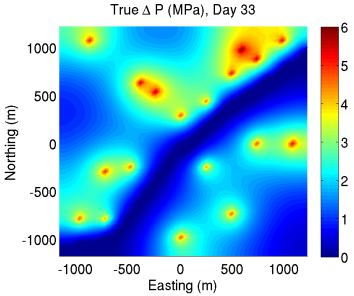

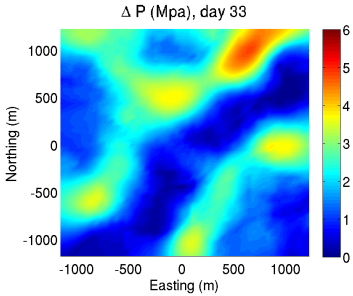

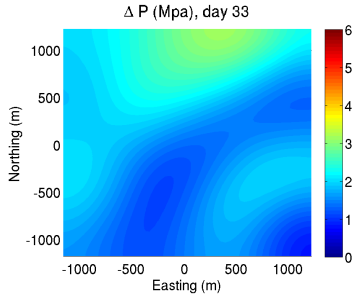

True pressure, inverted pressure using (LS) and (TV)

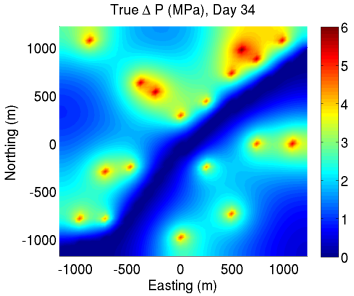

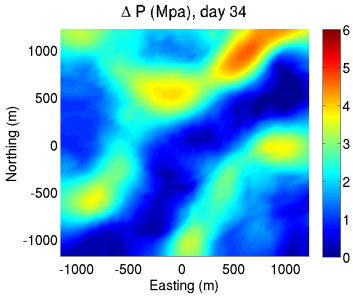

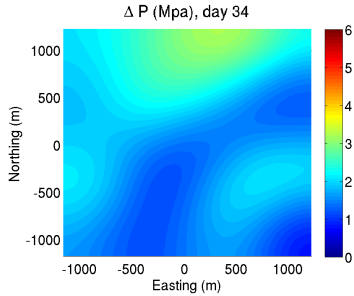

True pressure, inverted pressure using (LS) and (TV)

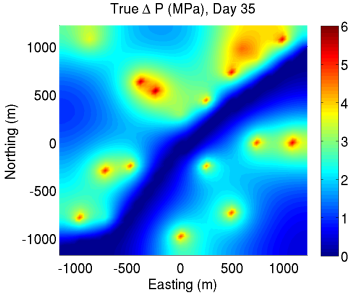

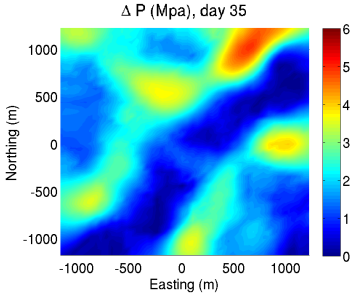

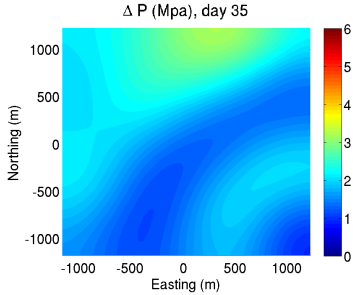

True pressure, inverted pressure using (LS) and (TV)

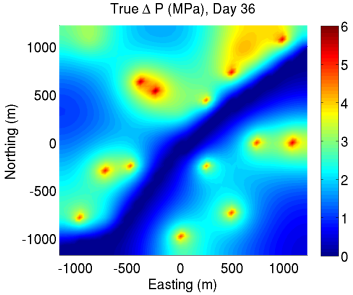

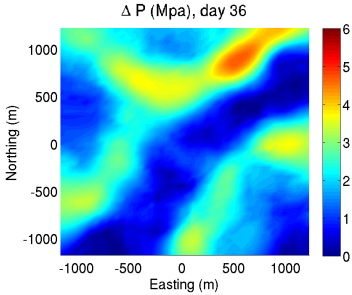

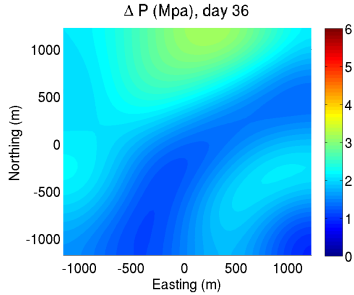

True pressure, inverted pressure using (LS) and (TV)

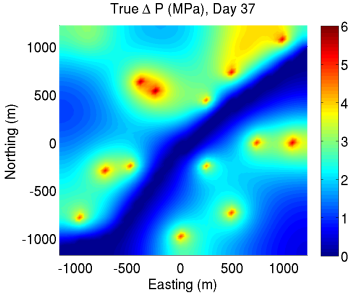

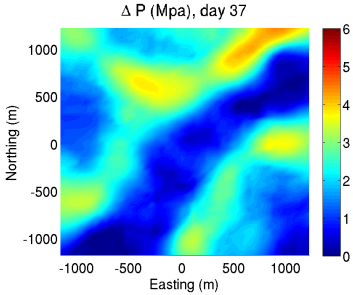

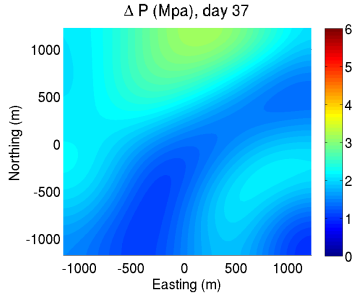

True pressure, inverted pressure using (LS) and (TV)

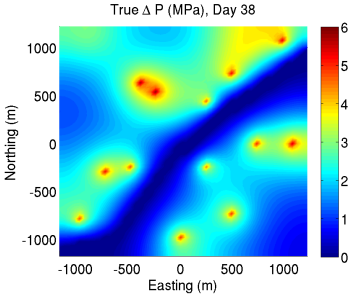

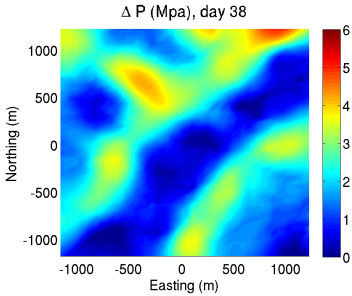

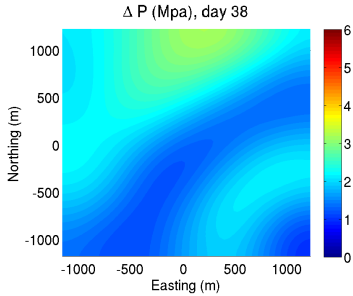

True pressure, inverted pressure using (LS) and (TV)

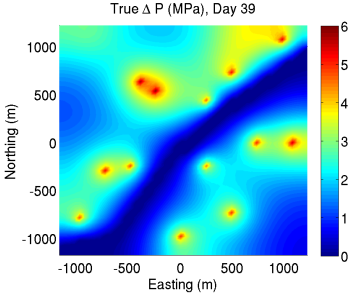

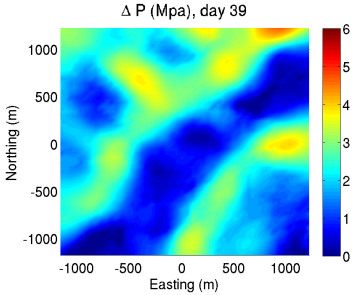

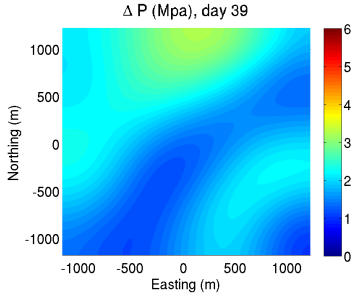

True pressure, inverted pressure using (LS) and (TV)

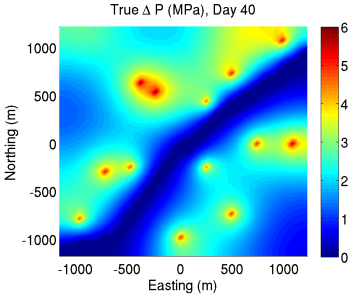

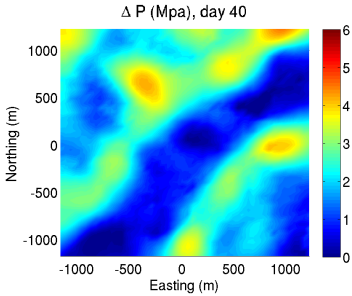

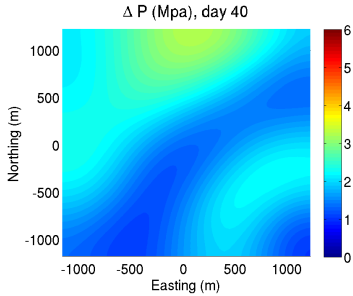

True pressure, inverted pressure using (LS) and (TV)

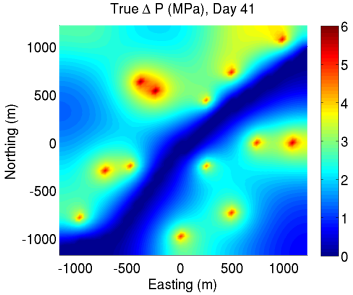

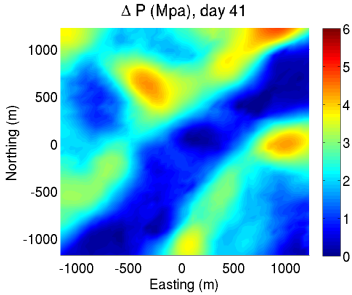

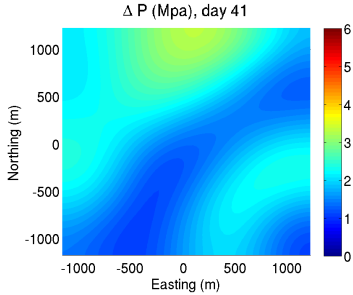

True pressure, inverted pressure using (LS) and (TV)

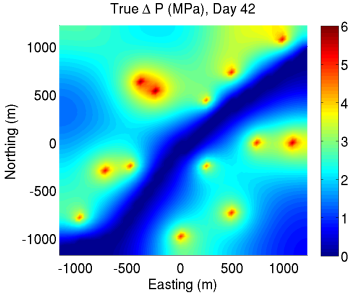

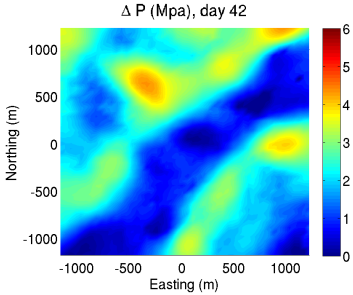

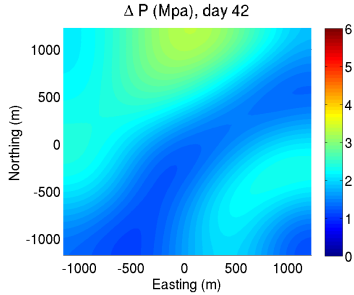

True pressure, inverted pressure using (LS) and (TV)

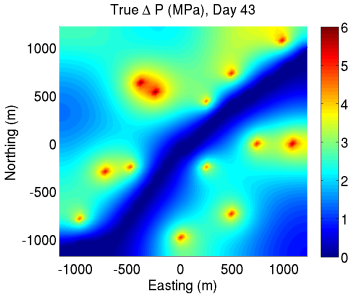

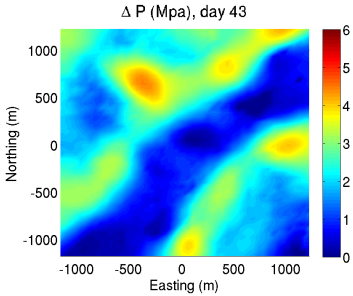

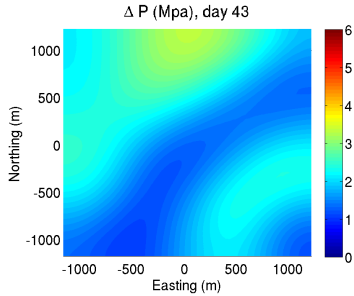

True pressure, inverted pressure using (LS) and (TV)

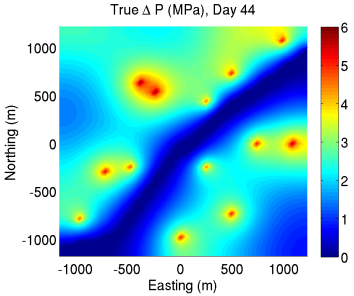

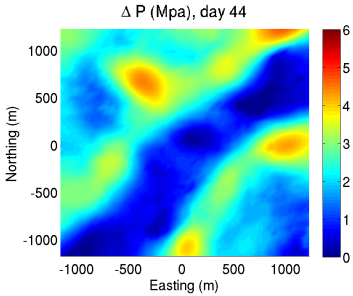

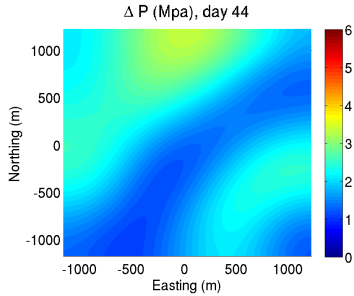

True pressure, inverted pressure using (LS) and (TV)

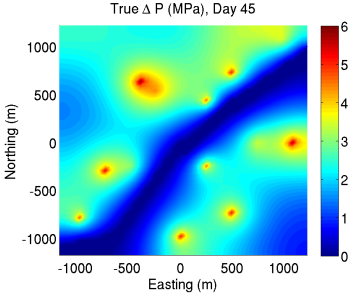

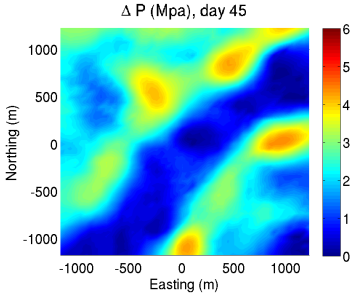

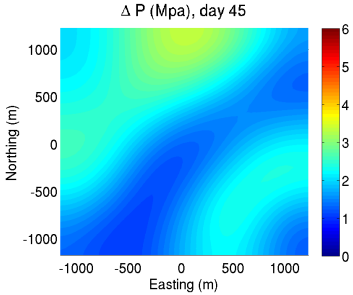

True pressure, inverted pressure using (LS) and (TV)

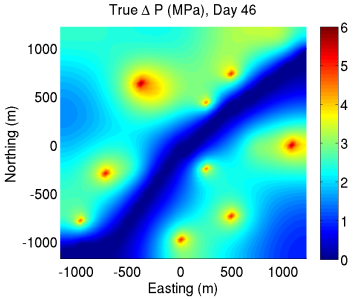

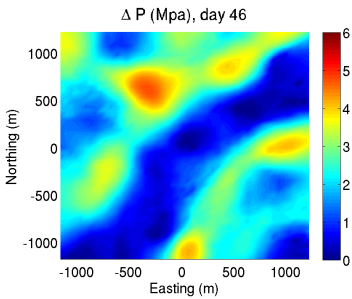

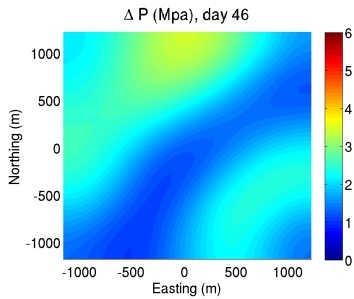

True pressure, inverted pressure using (LS) and (TV)

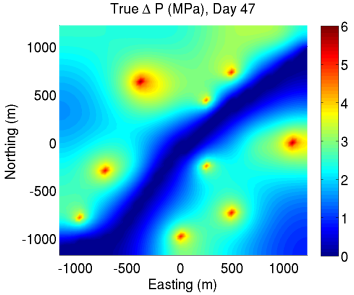

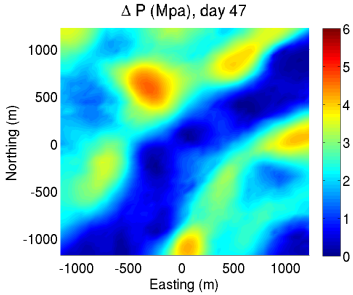

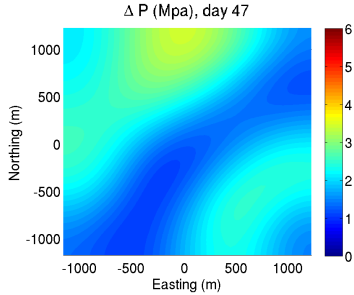

True pressure, inverted pressure using (LS) and (TV)

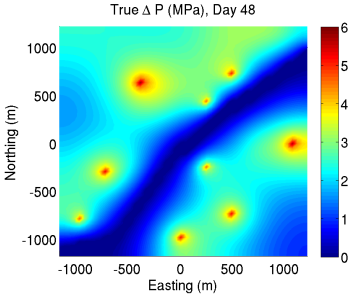

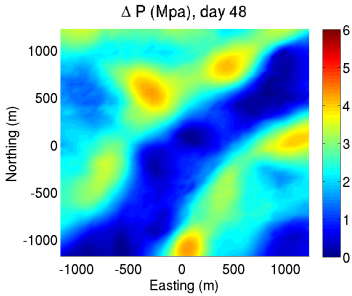

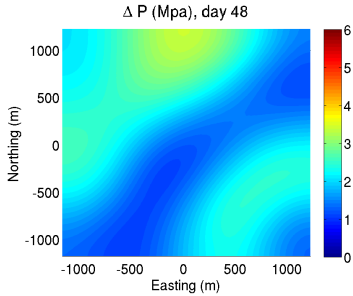

True pressure, inverted pressure using (LS) and (TV)

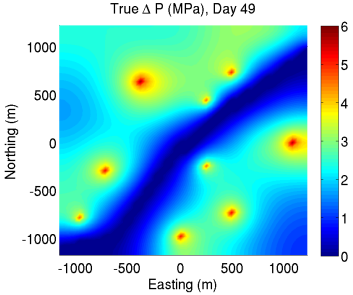

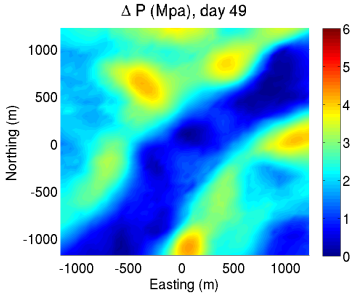

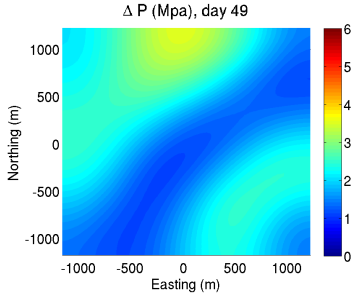

True pressure, inverted pressure using (LS) and (TV)

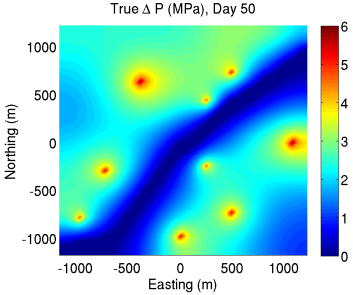

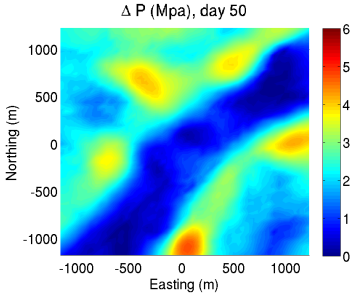

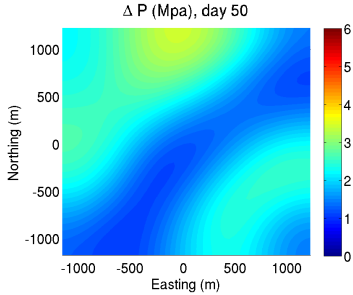

True pressure, inverted pressure using (LS) and (TV)

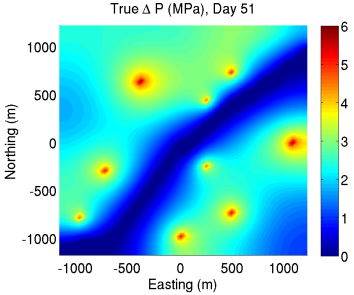

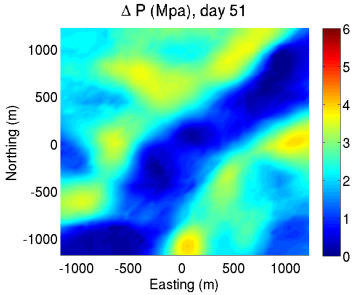

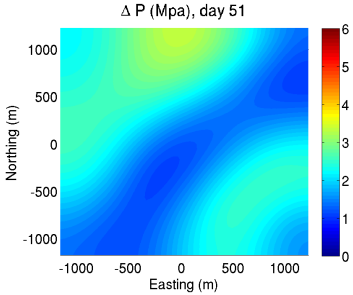

True pressure, inverted pressure using (LS) and (TV)

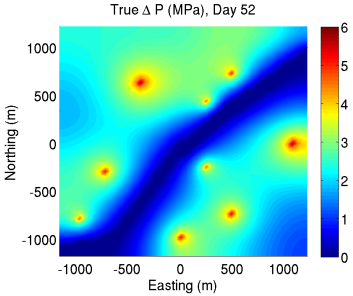

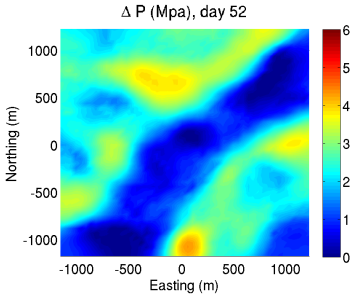

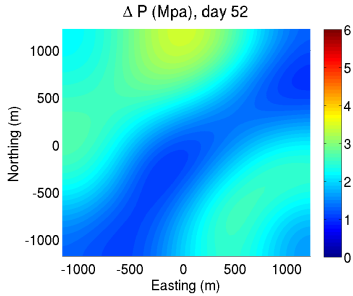

True pressure, inverted pressure using (LS) and (TV)

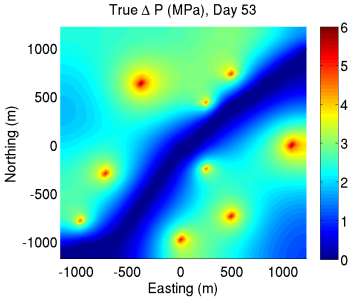

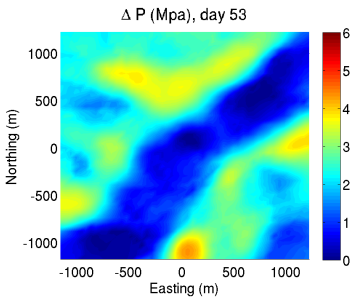

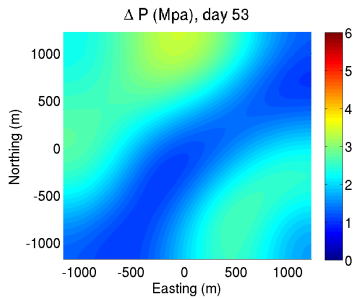

True pressure, inverted pressure using (LS) and (TV)

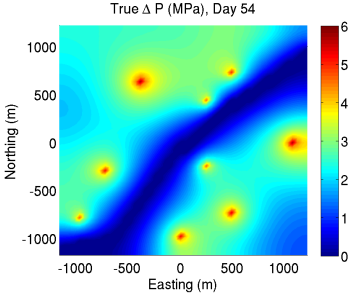

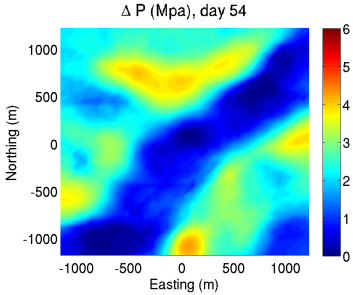

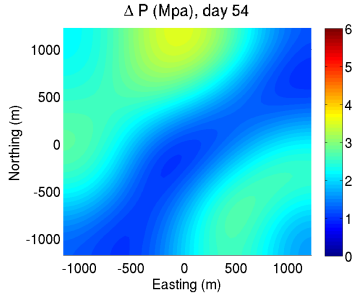

True pressure, inverted pressure using (LS) and (TV)

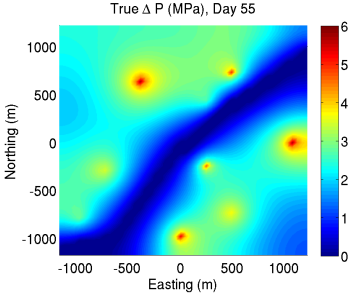

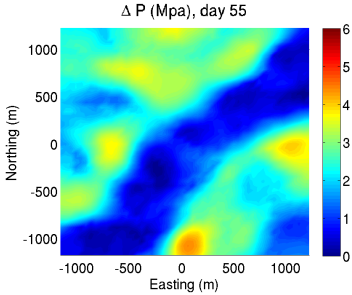

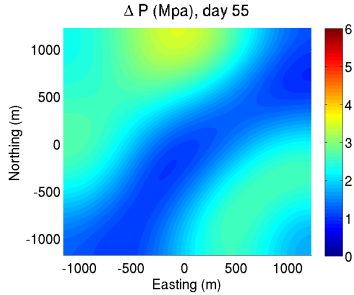

True pressure, inverted pressure using (LS) and (TV)

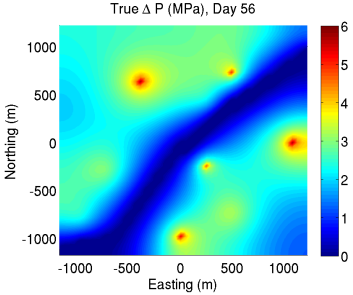

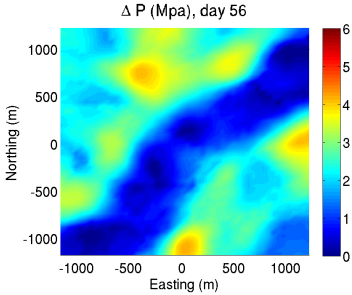

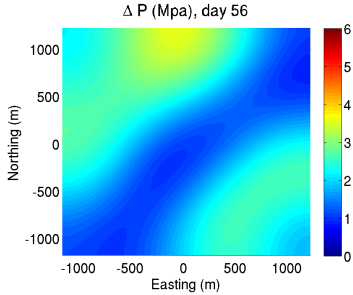

True pressure, inverted pressure using (LS) and (TV)

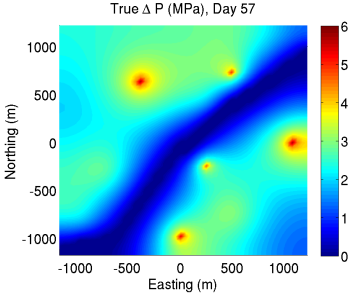

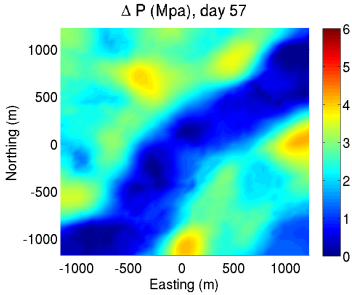

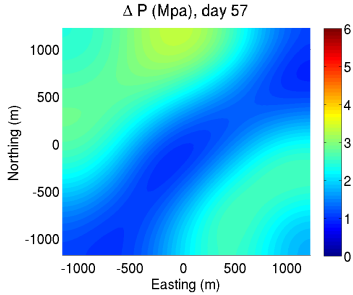

True pressure, inverted pressure using (LS) and (TV)

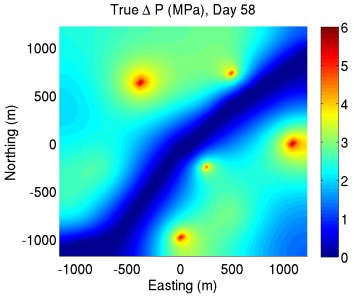

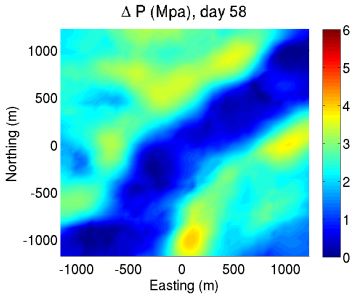

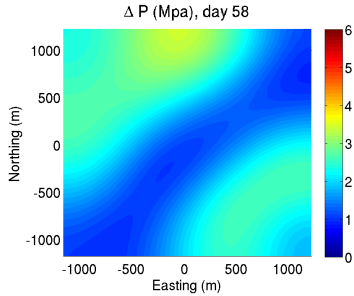

True pressure, inverted pressure using (LS) and (TV)

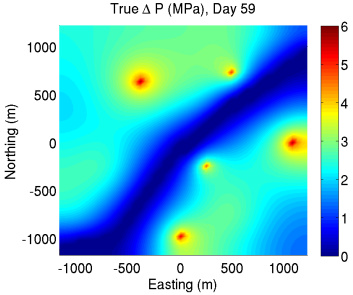

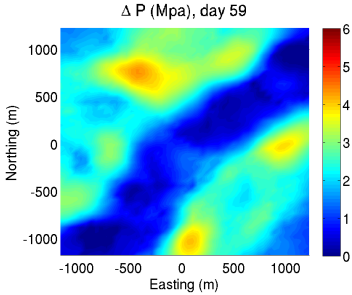

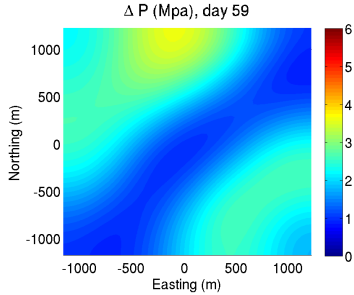

True pressure, inverted pressure using (LS) and (TV)

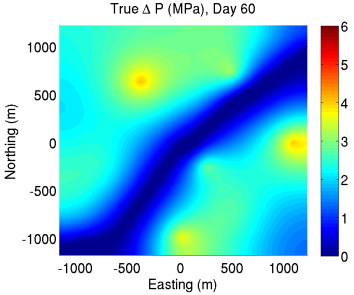

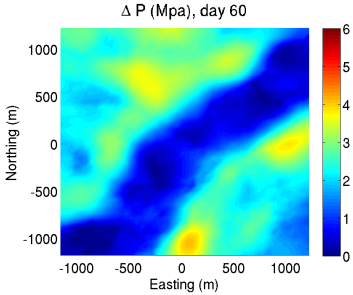

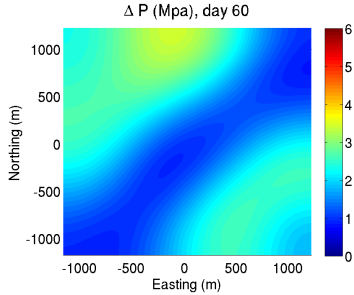

Level curves of (TV) inversion approximate the barrier

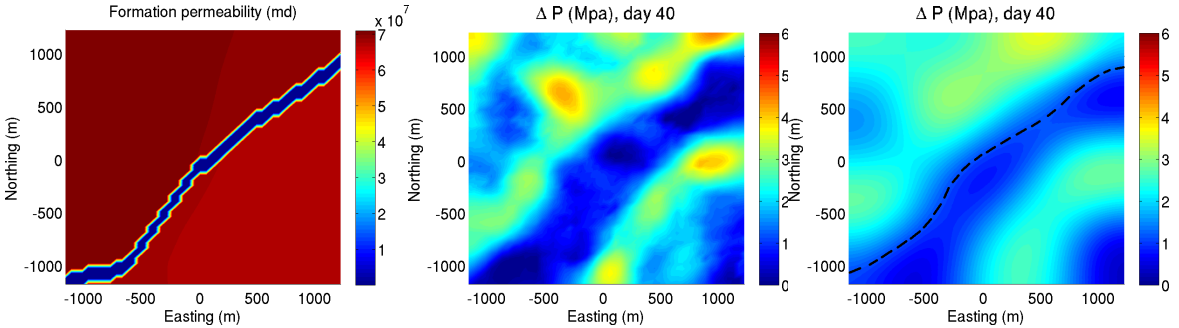

Level curves of (TV) inversion approximate the barrier

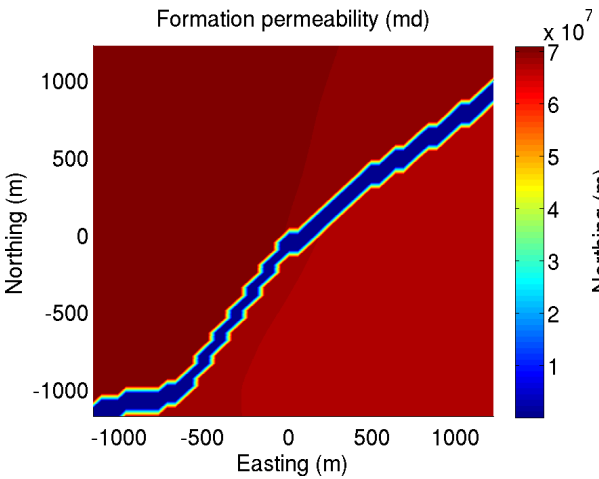

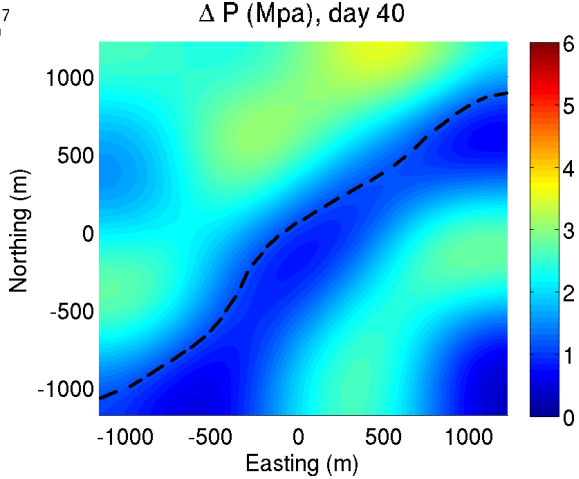

Conclusions and perspectives

1. TV-regularization with bound constraints $\Rightarrow$ location of **sharp** pressure contrasts.

2. Combine linear poroelastostatic deformation model with a "fluid-filled chamber" model to simulate **fluid-conducting faults**.

3. Not limited to directly measurable deformation; e.g., can estimate induced deformation from time-lapse (Hodgson, 2007).

4. Application to **InSAR** field data.

Acknowledgements

- **My family**
- Principal advisor, Professor **Biondo Biondi**
- Second project advisor, Professor **Mark Zoback**
- Professor **Jon Claerbout**

Acknowledgements—Part I, seismic imaging

- **Stewart Levin**, **Mark Meadows**, and **Paul Segall**

- **Shuki Ronen**, **Robert Clapp**, **Clement Kostov**, **Joseph Stefani**, **Dimitri Bevc**, **John Etgen**, **Matthew Karazincir**, **Phuong Vu**, **Min Zhou**, **Jean Paul Gestel**, **Joseph Dellinger**, **Jean Virieux**, **Jack Dvorkin**, **Gary Mavko**, **James Mika**, **Olav Barkved**, and **David Nichols**

- My SEP colleagues for our dynamic and stimulting work environment

- Special thanks to **Chevron**, **ExxonMobil**, and **BHP Billiton** for providing Genesis field seismic data and permission to publish my work

- Affiliate members of **Stanford Exploration Project** for their support

Acknowledgements—Part I, seismic imaging

- **Stewart Levin**, **Mark Meadows**, and **Paul Segall**
- **Shuki Ronen**, **Robert Clapp**, **Clement Kostov**, **Joseph Stefani**, **Dimitri Bevc**, **John Etgen**, **Matthew Karazincir**, **Phuong Vu**, **Min Zhou**, **Jean Paul Gestel**, **Joseph Dellinger**, **Jean Virieux**, **Jack Dvorkin**, **Gary Mavko**, **James Mika**, **Olav Barkved**, and **David Nichols**
- My SEP colleagues for our dynamic and stimulting work environment
- Special thanks to **Chevron**, **ExxonMobil**, and **BHP Billiton** for providing Genesis field seismic data and permission to publish my work
- Affiliate members of **Stanford Exploration Project** for their support

Acknowledgements—Part I, seismic imaging

- **Stewart Levin**, **Mark Meadows**, and **Paul Segall**
- **Shuki Ronen**, **Robert Clapp**, **Clement Kostov**, **Joseph Stefani**, **Dimitri Bevc**, **John Etgen**, **Matthew Karazincir**, **Phuong Vu**, **Min Zhou**, **Jean Paul Gestel**, **Joseph Dellinger**, **Jean Virieux**, **Jack Dvorkin**, **Gary Mavko**, **James Mika**, **Olav Barkved**, and **David Nichols**
- My SEP colleagues for our dynamic and stimulting work environment
- Special thanks to **Chevron**, **ExxonMobil**, and **BHP Billiton** for providing Genesis field seismic data and permission to publish my work
- Affiliate members of **Stanford Exploration Project** for their support

Acknowledgements—Part I, seismic imaging

- **Stewart Levin**, **Mark Meadows**, and **Paul Segall**
- **Shuki Ronen**, **Robert Clapp**, **Clement Kostov**, **Joseph Stefani**, **Dimitri Bevc**, **John Etgen**, **Matthew Karazincir**, **Phuong Vu**, **Min Zhou**, **Jean Paul Gestel**, **Joseph Dellinger**, **Jean Virieux**, **Jack Dvorkin**, **Gary Mavko**, **James Mika**, **Olav Barkved**, and **David Nichols**
- My SEP colleagues for our dynamic and stimulting work environment
- Special thanks to **Chevron**, **ExxonMobil**, and **BHP Billiton** for providing Genesis field seismic data and permission to publish my work
- Affiliate members of **Stanford Exploration Project** for their support

Acknowledgements—Part I, seismic imaging

- **Stewart Levin**, **Mark Meadows**, and **Paul Segall**
- **Shuki Ronen**, **Robert Clapp**, **Clement Kostov**, **Joseph Stefani**, **Dimitri Bevc**, **John Etgen**, **Matthew Karazincir**, **Phuong Vu**, **Min Zhou**, **Jean Paul Gestel**, **Joseph Dellinger**, **Jean Virieux**, **Jack Dvorkin**, **Gary Mavko**, **James Mika**, **Olav Barkved**, and **David Nichols**
- My SEP colleagues for our dynamic and stimulting work environment
- Special thanks to **Chevron**, **ExxonMobil**, and **BHP Billiton** for providing Genesis field seismic data and permission to publish my work
- Affiliate members of **Stanford Exploration Project** for their support

Acknowledgements—Part II, geomechanics

- **Stewart Levin**, **Mark Meadows**, and **Paul Segall**
- **Ran Bachrach**, **Joseph Stefani**, **Jean Paul Gestel**, **Jack Dvorkin**, **Gary Mavko**, **Amos Nur**, **Olav Barkved**, **David Nichols**, and **Randi Walters**
- Affiliate members of **Stanford Exploration Project** and **Stanford Rock Physics and Borehole Geophysics** for their support

Acknowledgements—Part II, geomechanics

- **Stewart Levin**, **Mark Meadows**, and **Paul Segall**
- **Ran Bachrach**, **Joseph Stefani**, **Jean Paul Gestel**, **Jack Dvorkin**, **Gary Mavko**, **Amos Nur**, **Olav Barkved**, **David Nichols**, and **Randi Walters**
- Affiliate members of **Stanford Exploration Project** and **Stanford Rock Physics and Borehole Geophysics** for their support

Acknowledgements—Part II, geomechanics

- **Stewart Levin**, **Mark Meadows**, and **Paul Segall**
- **Ran Bachrach**, **Joseph Stefani**, **Jean Paul Gestel**, **Jack Dvorkin**, **Gary Mavko**, **Amos Nur**, **Olav Barkved**, **David Nichols**, and **Randi Walters**
- Affiliate members of **Stanford Exploration Project** and **Stanford Rock Physics and Borehole Geophysics** for their support

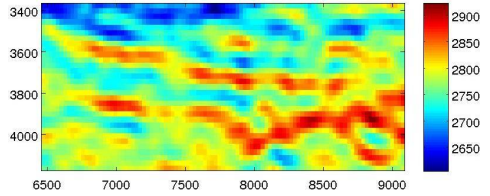
3400
3600
3800
4000
6500
7000
7500
8000
8500
9000
2900
2850
2800
2750
2700
2650

Q&A

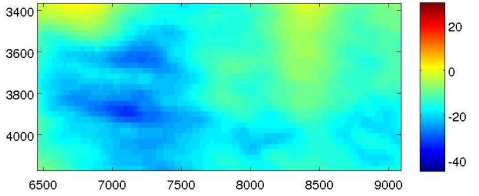
3400
3600
3800
4000
6500
7000
7500
8000
8500
9000
20
0
-20
-40

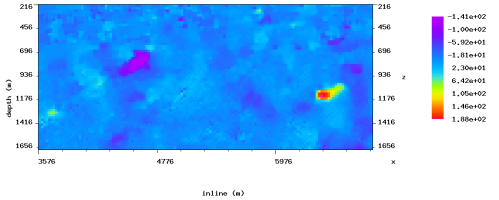
216
456
696
936
1176
1416
1656
depth (m)
3576
4776
5976
inline (m)
z
x
-1.41e+02
-1.00e+02
-5.92e+01
-1.81e+01
2.30e+01
6.42e+01
1.05e+02
1.46e+02
1.88e+02

Appendices – discussion slides

Model decomposition into "blocky" and "wiggly" components = cartoon+texture decomposition (Meyer, 2001):

$$\min_{\mathbf{m},\mathbf{m}_b} \|\mathbf{F}(\mathbf{m}) - \mathbf{d}\|_2^2 + \alpha\||\nabla \mathbf{m}_b|\|_1 + \beta\|\mathbf{R}\mathbf{m}_w\|_2^2, \mathbf{m} = \mathbf{m}_b + \mathbf{m}_w, \quad (7)$$

where

$$\mathbf{R} = \mathbf{I} \text{ or } \mathbf{\Delta}.$$

$$\frac{d\tau}{dt} \approx \frac{\Delta t}{t} = \frac{\Delta z}{z} - \frac{\Delta v}{v}, \tag{8}$$

$$\frac{\Delta v}{v} = -R\frac{\Delta z}{z}, \tag{9}$$

$$\frac{\Delta v}{v} = -\frac{R}{R+1}\frac{\Delta t}{t} \approx -\frac{\Delta t}{t} \approx -\frac{d\tau}{dt}. \tag{10}$$

$$\Delta v \approx -.02 \times 2,800 \text{ m/s} = -56 \text{ m/s}. \tag{11}$$

Model difference, small TV regularization

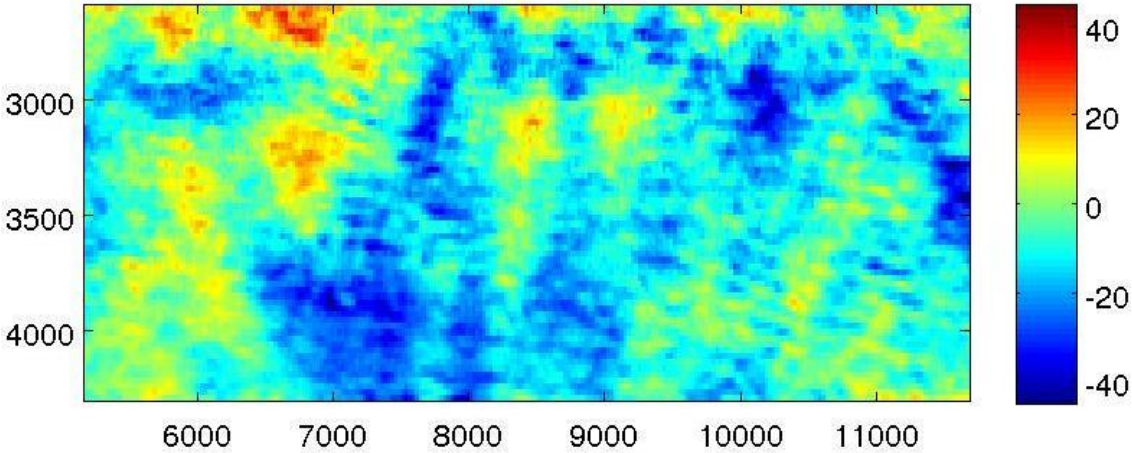

Model difference, medium TV regularization

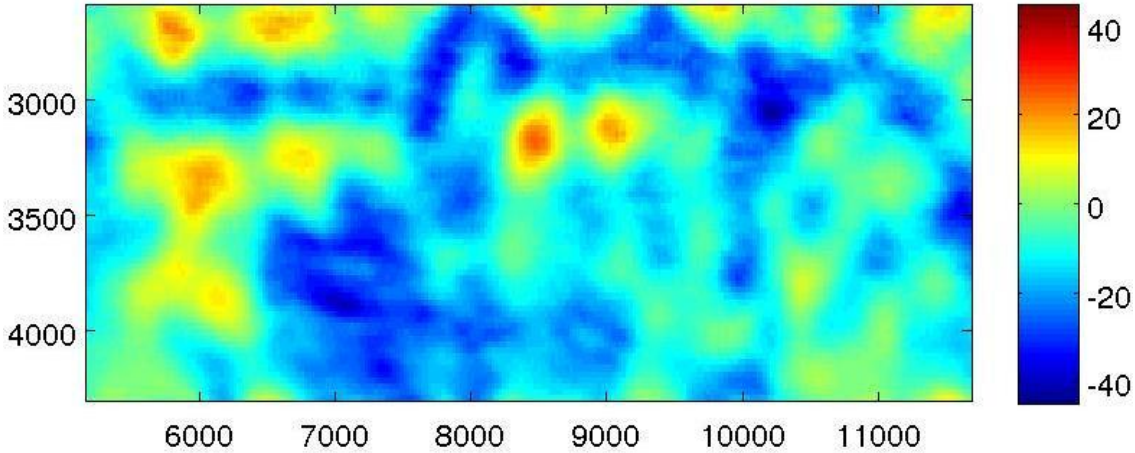

Model difference, strong TV regularization

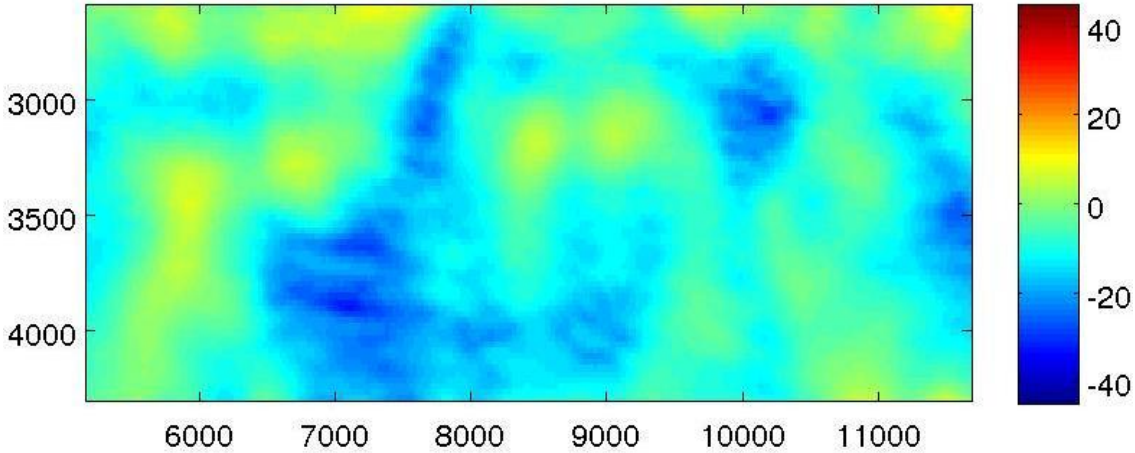

Local inversion vs Genesis wells

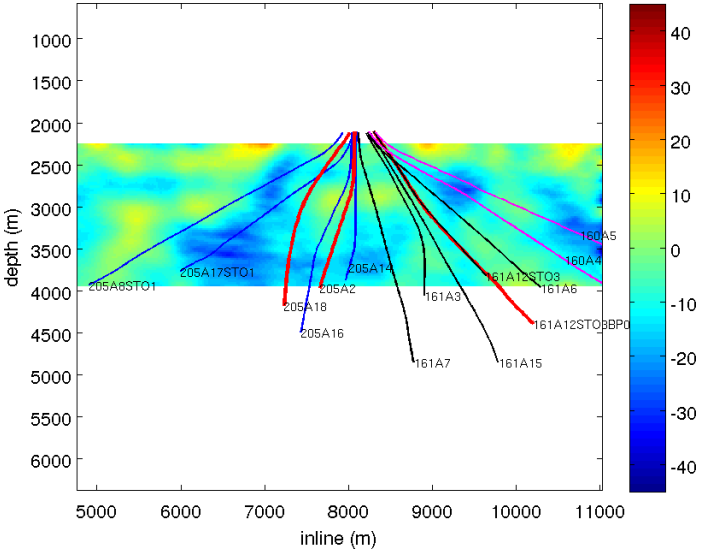

Global inversion vs Genesis wells

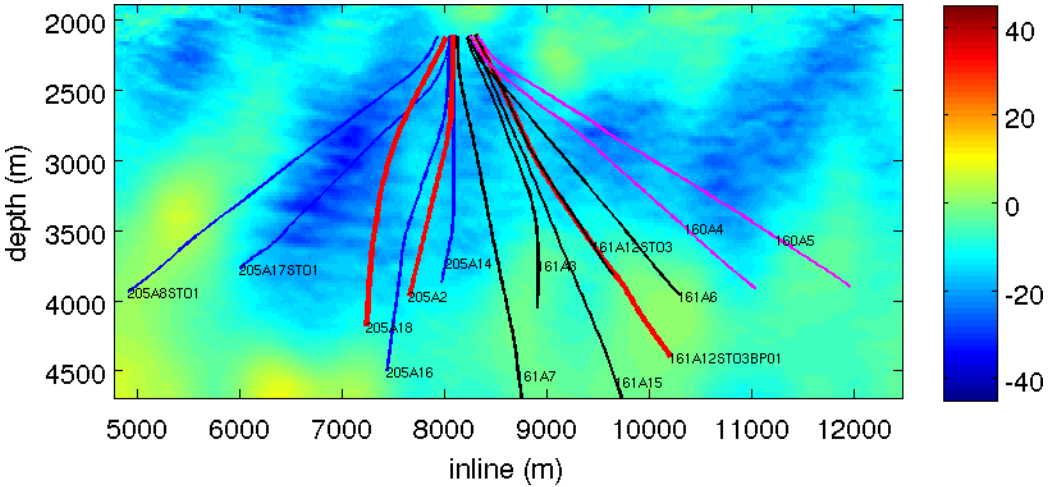

Efficient solution of L_1-TV regularized problems

True ΔP

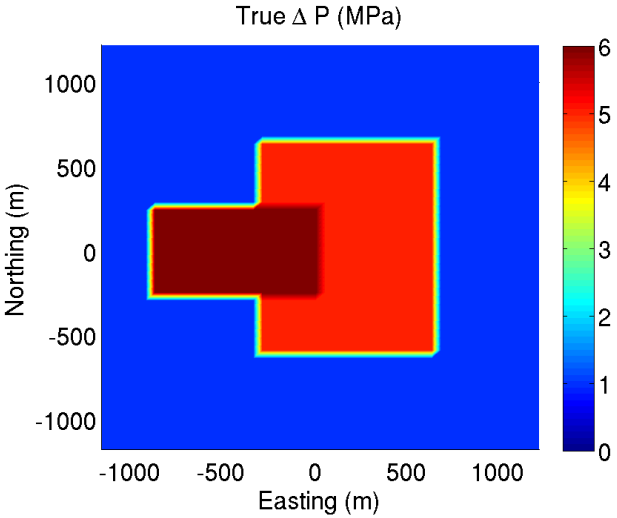
True Δ P (MPa)
1000
500
0
-500
-1000
Northing (m)
-1000
-500
0
500
1000
Easting (m)
6
5
4
3
2
1
0

Noisy uplift, $\sigma = .15\%$

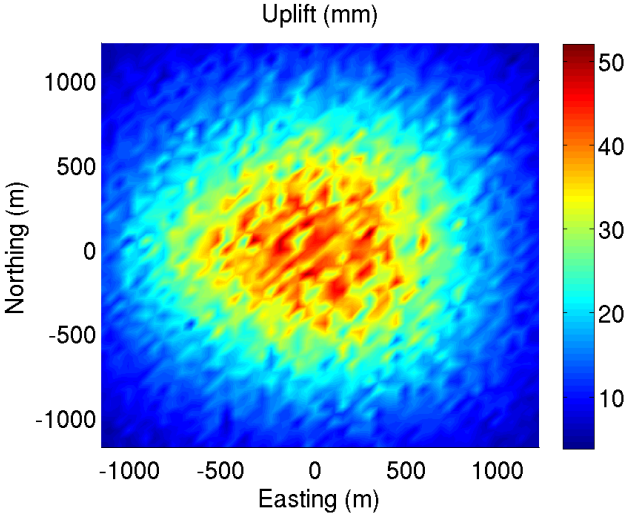

Tikhonov-regularized Inversion

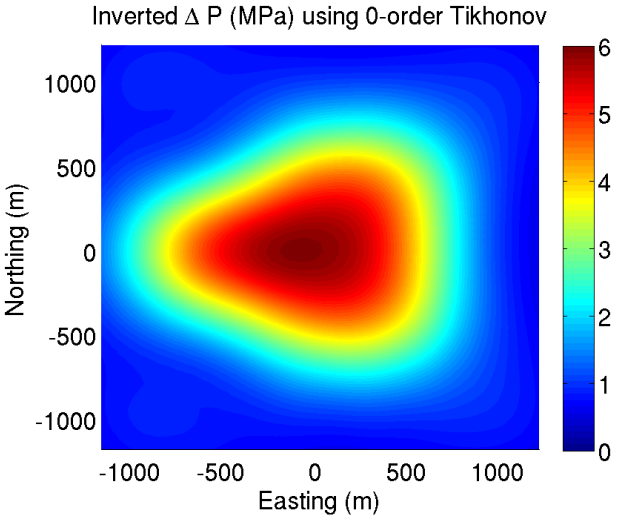

ADMM + Restarted CG, 100 $\mathbf{A}, \mathbf{A}^T$ applications

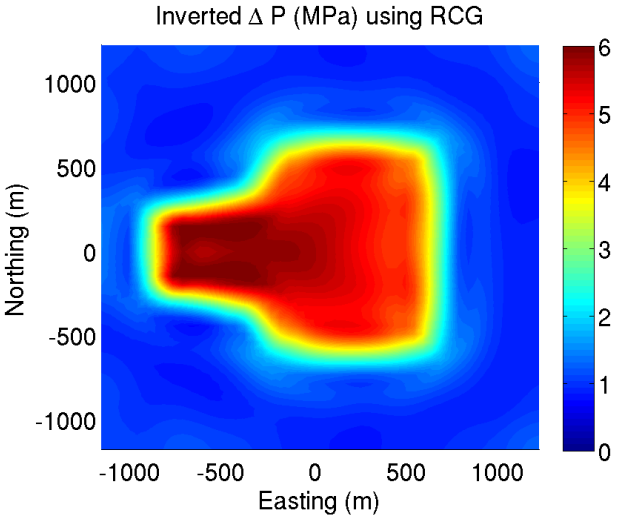

ADMM + Restarted CG, 5000 $\mathbf{A}, \mathbf{A}^T$ applications

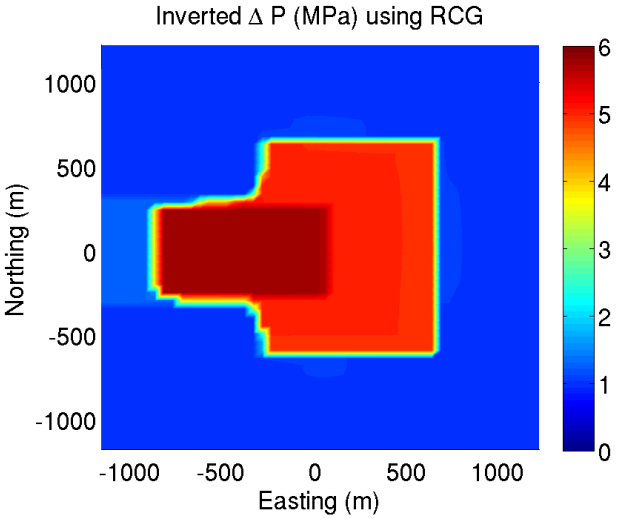

True ΔP

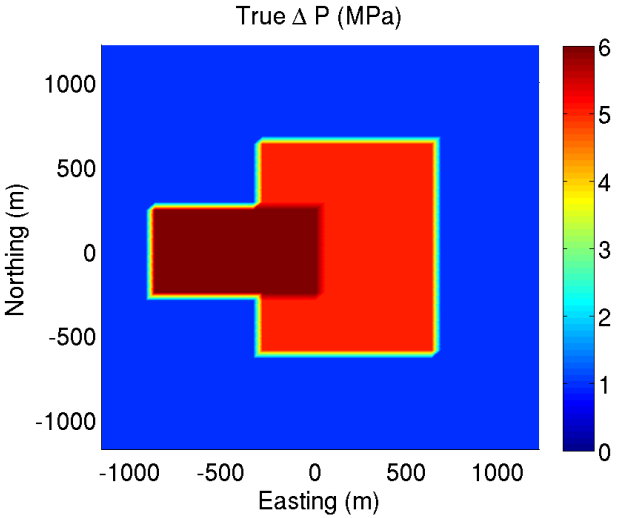
True Δ P (MPa)
1000
500
0
-500
-1000
Northing (m)
-1000
-500
0
500
1000
Easting (m)
6
5
4
3
2
1
0

ADMM + CCD, 100 $\mathbf{A}, \mathbf{A}^T$ applications

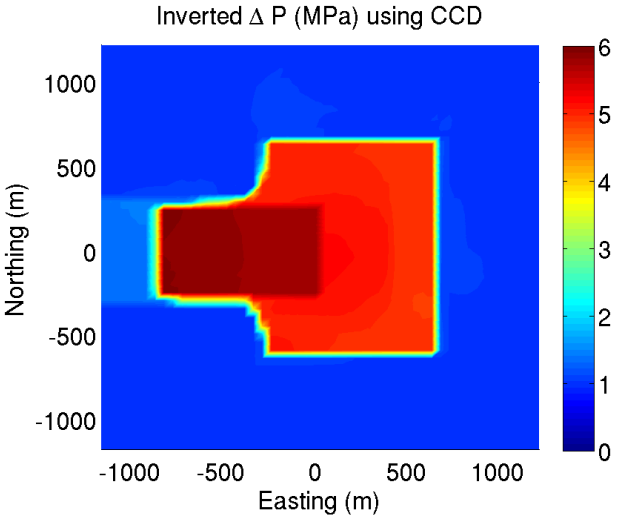

ADMM + CCD vs ADMM + Restarted CG

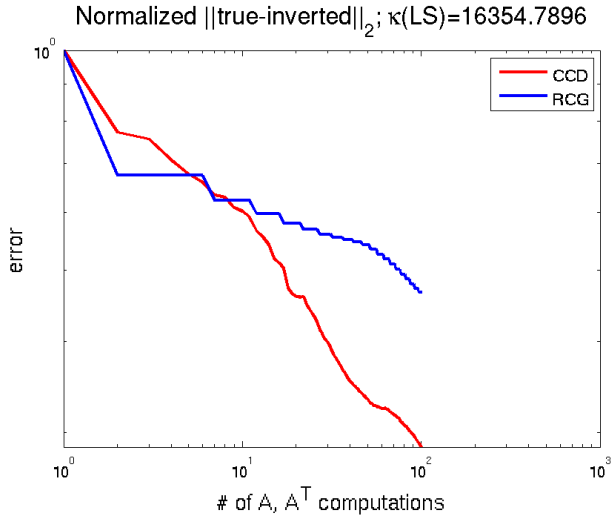

Appendix: shortcuts